12-1-2012

The Contribution of Poly(ADP-ribose)polymerase-1 Activity in the Nucleotide Excision Repair Pathway

Brenee S. King

Brenee S. King
Candidate

Biomedical Sciences
Department

This dissertation is approved, and it is acceptable in quality and form for publication:

Approved by the Dissertation Committee:

Laurie G. Hudson, PhD , Chairperson

Ke Jian "Jim" Liu, PhD

Andrea Allan, PhD

Graham Timmins, PhD

Wenlan Liu, PhD

THE CONTRIBUTION OF POLY(ADP-RIBOSE)POLYMERASE-1 ACTIVITY IN THE NUCLEOTIDE EXCISION REPAIR PATHWAY

by

BRENEE S. KING

B.S. Chemistry, University of California, Santa Barbara, 2005

DISSERTATION

Submitted in Partial Fulfillment of the
Requirements for the Degree of

Doctor of Philosophy
Biomedical Sciences

The University of New Mexico
Albuquerque, New Mexico

December 2012

DEDICATION

This dissertation is dedicated to my husband, Dr. Matthew Kirk, for believing in me during times when I did not have enough strength to believe in myself. Thank you for your continued love and support.

I also dedicate this dissertation to my family and their continued support throughout this process.

ACKNOWLEDGEMENTS

I gratefully acknowledge Dr. Laurie G. Hudson, my advisor and dissertation chair, for her continued support and encouragement throughout my entire PhD experience. Her training and guidance will surely benefit me throughout the remainder of my career and for that I am truly thankful.

I would also like to thank my committee members, Drs. Jim Liu, Andrea Allan, Graham Timmins, and Wenlan Liu for their help and insight during my committee meetings and overall professional development.

To my lab members, past and present, thank you so much for your help, support and love throughout my duration at the University of New Mexico. You are my second family and without all of you this experience would not have been as fruitful.

THE CONTIBUTION OF POLY(ADP-RIBOSE)POLYMERASE-1 ACTIVITY IN THE NUCELOTIDE EXCISION REPAIR PATHWAY

By

Brenee S. King

B.S. Chemistry, University of California, Santa Barbara

PhD, Biomedical Sciences, University of New Mexico

ABSTRACT

Exposure to ultraviolet radiation (UVR) promotes the formation of UVR-induced, DNA helix distorting photolesions such as (6-4) pyrimidine-pyrimidone photoproducts (6-4 PPs) and cyclobutane pyrimidine dimers (CPDs). Effective repair of such lesions by the nucleotide excision repair (NER) pathway is required to prevent DNA mutations and chromosome aberrations. Poly(ADP-ribose)polymerase-1 (PARP-1) is a zinc-finger protein with well documented involvement in base excision repair (BER). PARP-1 is activated in response to DNA damage and catalyzes the formation of poly(ADP-ribose) subunits (PAR) that assist in the assembly of DNA repair complexes at sites of damage. In this dissertation, I present evidence for PARP-1 contributions to NER, extending the knowledge of PARP-1 function in DNA repair beyond the established role in BER. Silencing the PARP-1 protein or inhibiting PARP activity leads to retention of UVR-induced photolesions *in vitro* and *in vivo*. PARP activation following UVR exposure promotes association between PARP-1 and XPC, a central protein in lesion recognition in

the global genomic arm of NER. Additionally, PARP activation following UVR promotes association with XPA, an essential protein in NER that is involved in DNA damage verification and stability of the preincision complex. Both proteins are predicted to contain the well defined 25 amino acid PAR binding sequence. Administration of PARP inhibitors confirms that PAR facilitates PARP-1 association with XPA and XPC in whole cell extracts as well as in isolated chromatin complexes; and illustrates the importance of the PAR binding sequence in PARP-1's interaction with NER proteins. Furthermore, inhibition of PARP activity decreases UVR-stimulated XPA and XPC chromatin association. These data not only illustrate that these relationships occur in the meaningful context for NER, but they also demonstrate a novel role for PAR as a potential modulator of NER proteins. Overall, these results provide a mechanistic link for PARP activity in the repair of UVR-induced photoproducts which could potentially be useful in the development of new combinations of cancer chemotherapy drugs.

Table of Contents

List of Figures

List of Tables

Table of Abbreviations

3,4-dihydro-5-[4-(1-piperidinyl)butoxyl]-1(2H)-isoquinolinone	DPQ
4',6-diamidino-2-phenylindole	DAPI
Basal cell carcinoma	BCC
Base Excision Repair	BER
Cockayne Syndrome	CS
Cyclobutane pyrimidine dimers	CPDs
DNA binding domain	DBD
DNA-damage binding protein 1	DDB1
Global Genomic Repair	GG-NER
Immortalized human keratinocyte cell line	HaCaT
Immunoblot	IB
Immunohistochemistry	IHC
Immunoprecipitation	IP
Nucleotide Excision Repair	NER
Poly(ADP-ribose)	PAR
Poly(ADP-ribose)polymerase	PARP
Pyrimidine (6-4) pyrimidone photoproducts	6-4 PPs
Reactive oxygen species	ROS
Squamous cell carcinoma	SCC
Standard error of the mean	SEM
Transcription Coupled Repair	TC-NER
Trichothiodystrophy	TTD
Ultraviolet Radiation	UVR
Xeroderma pigmentosum complementation groups A-G	XPA-XPG
X-ray repair cross-complementation protein 1	XRCC1

CHAPTER 1

Introduction

1.1. Structures of the skin

The skin is our first line of defense from environmental insults. It has evolved to perform an array of protective functions such as preventing water loss, resisting mechanical stress and participating in immunological responses (Simpson *et al.*, 2011). The skin is the largest organ in the body and consists of three layers: the epidermis, dermis and hypodermis. The dermis consists of connective tissue, and is the location of hair follicles, sweat glands and blood vessels (Fuchs and Raghavan, 2002) . Located within the dermis, there are several appendages that contain niches of stem cells, including the bulge region of the hair follicle, and sebaceous glands. The dermis and the epidermis are separated by a basement membrane, which is composed of extracellular matrix proteins such as collagen and laminin. Keratinocytes are squamous epithelial cells and constitute approximately 95% of the cells found in the epidermis. The remainder of epidermal cells includes melanocytes, Langerhans cells and Merkel cells.

The epidermis is a stratified epithelium comprised of several layers. The outermost layer is the stratum corneum (SC), followed by the stratum granulosum (SG) and stratum spinosum (SS) and the inner most layer of the epidermis is the stratum basale (SB) layer (Fuchs and Raghavan, 2002). Keratinocytes differentiate and migrate outwards, from the stratum basale, to replace cells that are shed from the body's surface. A subset of basal cells meet the universal definition of a stem cell, a cell that can divide to produce both daughter stem cells and cells that go on to differentiate. Those cells that are not

considered to be stem cells are rapidly dividing progenitor cells, referred to as transit amplifying cells, that undergo a limited number of divisions before they withdraw from the cell cycle (Fuchs and Raghavan, 2002). Initially it was believed that intrafollicular stem cells were progenitor cells of transit amplifying cells (Watt *et al.*, 2006). Current studies support a model of the committed progenitor cell, that proliferates like a stem cell but is committed to terminal differentiation similar to a transit amplifying cell (Clayton *et al.*, 2007; Jones and Simons, 2008). Once cells commit to terminal differentiation they detach from the basement membrane and migrate upwards toward the surface of the skin.

Cells within the stratum spinosum exit the cell cycle, grow larger and establish additional intercellular connections. As cells move further upward into the stratum granulosum they become flattened and assemble a water-impermeable cornified envelope underlying their plasma membranes (Fig. 1.1) (Simpson *et al.*, 2011).

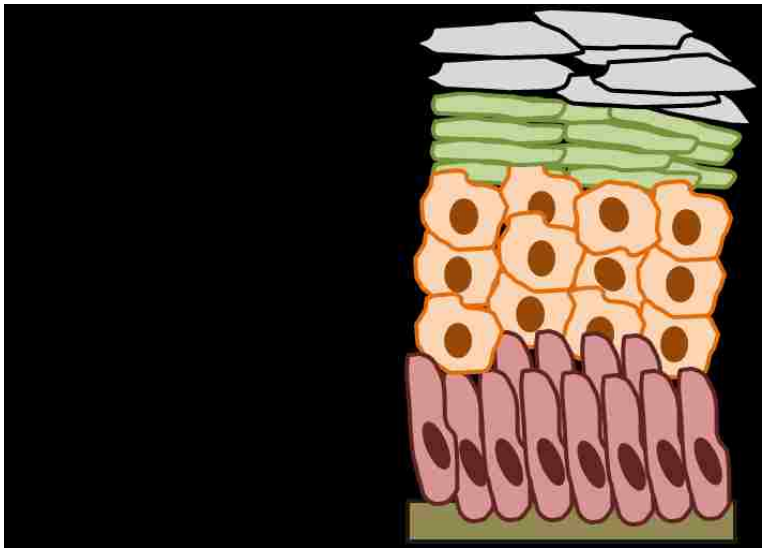

FIGURE 1.1. **Layers of the epidermis**. The outermost layer of the epidermis is the stratum cornea (SC), followed by the stratum granulosum (SG), stratum spinosum (SS), and lastly the stratum basale (BL) which is layered upon the basement membrane.

Lastly, the stratum corneum forms a physical barrier made of a continuous sheet of protein-enriched cells known as corneocytes. At this stage, keratinocytes have completed their differentiation program and lack nuclei and cytoplasmic organelles (Koster, 2009; Proksch *et al.*, 2008). Once constructed, the epidermis is maintained through continual stratification and differentiation of keratinocytes. This constant state of equilibrium allows the epidermis to replenish itself every two weeks throughout life (Fuchs and Raghavan, 2002).

1.2. Skin Cancer

Sunlight is essential to life on earth. What reaches the earth's surface is a frequency spectrum of electromagnetic radiation composed of visible and ultraviolet light (von Thaler *et al.*, 2010). Ultraviolet radiation (UVR) is divided into long wavelength UVA (315-400 nm), medium wavelength UVB (280-315 nm) and short wavelength UVC (<280 nm). As UVR enters the earth's atmosphere, the entire UVC spectrum is absorbed by the ozone layer, in addition to the majority of UVB. Of the UVR that reaches the earth's surface about 90-99 % is UVA (Narayanan *et al.*, 2010), depending on cloud coverage and atmospheric conditions. Energy from UV radiation can be absorbed by cellular proteins and DNA and can cause mutagenic lesions. If these lesions are not repaired properly they may contribute to the formation of cancer.

Skin cancer is the most common type of cancer in humans, and exposure to UVR radiation is thought to be the main etiological factor (Narayanan *et al.*, 2010; Zhang *et al.*, 2011). Skin cancers are broadly divided into melanoma and nonmelanoma skin cancers (NMSC). Nonmelanoma skin cancers are further categorized into squamous cell carcinoma (SCC) and basal cell carcinoma (BCC).

1.2.1. Nonmelanoma skin cancers

It is estimated that 2-3 million cases of NMSC occur world-wide each year (Narayanan *et al.*, 2010). BCC account for 80-85% of NMSC and have been associated with intense acute sun exposure and sunburns before the age of 20 and development of tumors 10 to 50 years after sun damage (Roewert-Huber *et al.*, 2007). In about 80% of cases it is located on the face and neck (Chinem and Miot, 2011). No precursor lesions have been described for BCC and the source cells remain controversial. Even though the tumor cells resemble those in the basal layer of the epidermis, there is evidence that they are derived from immature pluripotent cells of interfollicular epidermis and those in the outer sheath of the hair follicle (Youssef *et al.*, 2010). BCC is locally invasive and has a low metastatic potential.

SCC accounts for about 10-15% of all NMSC and may invade other tissues and cause death. Similar to BCC, SCC is more frequent on sun-exposed areas of the skin such as the head, neck and forehead regions. In contrast to BCC, SCC is often associated with cumulative rather than acute exposure to UVR (Rass and Reichrath, 2008). Interfollicular epidermal basal keratinocytes are the assumed precursor cells for SCC and the recognized precancerous progenitor is actinic keratosis (Alam and Ratner, 2001; Callen *et al.*, 1997). While this precancerous condition can progress to SCC, with one study measuring risk at 1:1000 per year (Marks *et al.*, 1988), it can also be reversible (Frost *et al.*, 2000).

1.2.2. Melanoma

Melanoma, while being the least common form of skin cancer, is the most serious and carries the highest mortality rate. Melanoma represents about 3% of all skin cancers in

the United States but accounts for nearly 75% of all skin cancer deaths (Jerant *et al.*, 2000; Narayanan *et al.*, 2010). Melanoma derives from the malignant transformation of cutaneous melanocytes. These cells reside in the basal layer of the epidermis and are in contact with keratinocytes. Melanocytes represent about 1-2% of epidermal cells (Maddodi and Setaluri, 2008). Melanocytes produce and distribute the photoprotective chromophore melanin which is able to absorb UVR and visible light. The production of melanin varies amongst skin types and is thought to be a contributing factor in melanomagenesis. This is partially revealed in the different incidence rates of various ethnic groups. The incidence rate of melanoma is 16 times greater in Caucasians than African Americans. When compared to Hispanics, the incidence rate is 10 times greater for Caucasians (Gloster and Neal, 2006).

Other factors to consider in the development of skin cancer are disease states due to deficiencies in DNA repair. Xeroderma pigmentosum (XP) is a rare autosomal recessive disorder of DNA repair proteins, XP complementation groups A-G. Some of the clinical traits of this disease are photosensitivity, actinic damage of the skin and cancer of UVR-exposed areas of the skin (DiGiovanna and Kraemer, 2012). XP patients have a higher risk of developing skin cancer. For children less than 20 years of age, there is a 10,000-fold increase in the frequency of NMSC and a 2,000-fold increase in melanoma (Bradford *et al.*, 2011). Patients with cockayne syndrome (CS), a disease associated with mutations in cockayne syndrome A (CKN1/CSA) or cockayne syndrome B (CKN2/ERCC6/CSB) repair proteins, are sun sensitive and deficient in removal of UVR-induced lesions, but compared to individuals with XP, they are not significantly prone to skin cancer. Also, half of trichothiodystrophy (TTD) patients who have mutations in

repair genes XPD, XPB or TTDA are photosensitive (Bergoglio and Magnaldo, 2006). Together, these diseases highlight the importance of DNA repair proteins and their ability to remove damaged DNA.

1.3. DNA damage following UV exposure

Overall, a fundamental commonality to the development of melanoma and non-melanoma skin cancer is exposure, both in duration and intensity, to UVR. Energy from UVR is commonly absorbed by cellular proteins and can induce various forms of DNA damage.

1.3.1. UVA damage

Approximately 90-99% of UVA light reaches the earth's surface. It is long wavelength and low energy light which allows it to penetrate deep into the skin (Timares *et al.*, 2008). This penetration is deep enough to reach regenerative cellular compartments in the basal layer and stem cell niche. UVA is estimated to contribute to 10-20% of sunlight-induced carcinogenesis (Besaratinia *et al.*, 2008). The effects of UVA exposure on DNA damage are largely indirect. UVA is mainly absorbed by chromophores, endogenous or exogenous photosensitizers, as opposed to DNA. The excited sensitizers can undergo either charge transfer to DNA or transfer energy to oxygen, leading to the formation of reactive oxygen species (Douki *et al.*, 1999). Reactive oxygen species (ROS) is a collective term, which includes oxygen radicals (superoxide ($O2^{-}$), hydroxyl (OH), peroxyl (RO_2) and alkoxyl (RO)). ROS also includes nonradicals (HOCl, peroxynitite ($ONOO^{-}$), singlet oxygen ($^{1}O_2$) and H_2O_2) that are oxidizers or easily converted to radicals (Guetens *et al.*, 2002). Guanine is a major target of ROS because it

exhibits a low ionization potential which allows it to behave as a sink for the positive charges that migrate through the DNA double helix (Douki *et al.*, 2003). Following UVA exposure reactive singlet oxygen can react with guanine forming 8-oxo-7,8-dihydro-2'-deoxyguanosine (8-oxo-dG) (Cadet *et al.*, 2005; Pfeifer *et al.*, 2005). Additionally, exposure to UVA can generate single strand breaks (SSBs). These are discontinuities in one strand of the DNA double helix and are usually accompanied by a damaged 5' and/or 3'-end at the site of the break (Caldecott, 2008).

If these SSBs are not repaired during the G1 phase of the cell cycle they can generate double strand breaks (DSBs) during the S-phase which could then result in chromosome aberrations including amplification, deletions or translocations (Wischermann *et al.*, 2008). UVA-induced mutations are commonly G to T transversions and are predominately found at the basal layer of the epidermis, thereby supporting a role for UVA exposure in skin photocarcinogenesis (Besaratinia *et al.*, 2008; Drobetsky *et al.*, 1995; Huang *et al.*, 2009; Pfeifer *et al.*, 2005).

For some time now, studies have demonstrated a role for UVA in the generation of cyclobutane pyrimidine dimers (CPDs) which are traditionally thought to be formed by exposure to UVB (Freeman *et al.*, 1987; Freeman *et al.*, 1989; Young *et al.*, 1998). The initial mechanism by which UVA was thought to produce thymine dimers was through photosensitization. UVA irradiation in the presence of chromophores induced CPDs through triplet energy transfer, but the absorbing chromophore had not been identified, leaving the exact mechanism incomplete (Charlier and Helene, 1972; Douki *et al.*, 2003). Recently, Mouret et al. showed there were no cellular photosensitizers involved in UVA-induced CPDs, but proposed a direct mechanism of action for the formation of these

lesions (Mouret *et al.*, 2010). These results suggest that photoprotection against UVR should include complete blockage of UVA radiation.

1.3.2. UVB damage

While only a small portion (1-10%) of UVB reaches the earth's surface it is by far the most carcinogenic wavelength. One of the major reasons for the carcinogenicity of UVB (280-315nm) is that this wavelength range is near the absorption maximum of DNA (260 nm) (Vink and Roza, 2001). This leads to the formation of several photolesions such as cyclobutane pyrimidine dimers (CPDs) and pyrimidine (6-4) pyrimidone photoproducts (6-4 PPs). The cyclobutane rings of CPDs are formed between the 5,6 bonds of adjacent pyrimidine bases while 6-4 PPs arise from a rearrangement of bases and contain a stable single bond between position 6 and position 4 of two adjacent pyrimidine bases (Batista *et al.*, 2009; Pfeifer and Besaratinia, 2011). 6-4 PPs that absorb around 320 nm are able to photoisomerize into another photolesion known as Dewar valance isomers (Cadet *et al.*, 2005; Perdiz *et al.*, 2000).

The common mutations associated with UVB exposure are C to T or CC to TT tandem base substitutions where C to T transitions can be induced by both CPDs and 6-4 PPs. CPDs are of concern for carcinogenesis due to their relatively high abundance, slow repair and known mutagenicity (You *et al.*, 2001). Less is known regarding the mutagenicity of 6-4 PPs. Studies with plasmids containing site-specific lesions have shown 6-4 PPs to be more mutagenic than CPDs which may be due to the strong helix distorting potential of this lesion. However, this characteristic also results in more efficient repair of 6-4 PPs, thus adding to the uncertainty of its contribution to carcinogenesis (Batista *et al.*, 2009; Ikehata and Ono, 2011).

The presence of CPDs or 6-4 PPs in the DNA double helix can result in physical blockage of proteins which disturbs essential processes such as replication or transcription. If damaged DNA is left unrepaired or misrepaired in the process, mutations can form and promote carcinogenesis. DNA repair mechanisms are a way for cells to counteract the effects of damaged DNA.

1.4. DNA excision repair pathways

Over the course of a given day there are numerous forms of DNA damage that occur in cells. There are an estimated 10^{3}-10^{5} damaging events/mammalian cell/day (Prasad *et al.*, 2011) which reveals the dynamic state of DNA. As such, cells have developed a multitude of repair mechanisms to maintain DNA integrity.

1.4.1. Base excision repair

Single base lesions or strand breaks are the most common form of DNA damage to occur throughout the genome. DNA bases are commonly modified by oxidation (i.e. 8-OHdG), alkylation or deamination by exogenous damaging agents (i.e. arsenic). These types of damages result in small, non-helix distorting lesions which are repaired by the base excision repair pathway (BER). BER is divided into two sub pathways that are differentiated by repair patch size and enzymes involved (Fig. 1.2). Short-patch BER removes a single damaged nucleotide whereas long patch BER replaces two or more damaged nucleotides (Almeida and Sobol, 2007; Prasad *et al.*, 2011). The majority of repair is thought to occur by the short patch repair pathway. Both sub pathways of BER involve an initial step that includes recognition and excision of the altered base by lesion-specific DNA glycosylases (Jacobs and Schar, 2012). The base removal by DNA

glycosylases generates an apurinic/apyrimidinic site (AP site) in the DNA which is further processed by AP endonucleases. The pathway continues with end processing which readies the site for ligation. Next, DNA polymerases participate in gap filling which is followed by the work of flap endonucleases and lastly nick-sealing performed by DNA Ligases (Almeida and Sobol, 2007; Caldecott, 2008).

An additional protein involved in the overall orchestration of BER is X-ray repair cross-complementing protein 1 (XRCC1). XRCC1 has no known enzymatic activity but is essential in DNA repair. XRCC1-deficient mice are embryonic lethal and mutant cells with no functional XRCC1 are hypersensitive to a wide range of DNA damaging agents

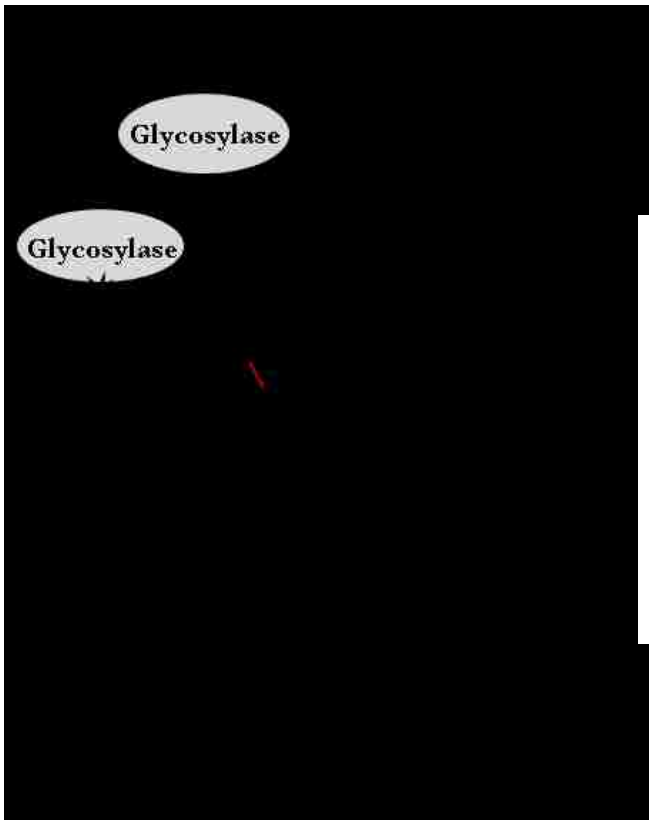

FIGURE 1.2. **Base excision repair pathway (BER)**. Simplified schematic of BER. The pathway begins with initiation by glycoylases followed by entry of AP endonucleases and strand scission. End processing is then followed by entry of DNA polymerase and gap filling. Lastly there is religation by XRCC1 and DNA Ligase III.

including alkylating agents, reactive oxygen species and ionizing radiation, thus showing a role for this protein in DNA repair pathways (Tebbs *et al.*, 1999; Thompson *et al.*, 1982; Thompson *et al.*, 1990). In addition, XRCC1 interacts with most components within the BER short-patch pathway and within this context, acts as a scaffolding protein (Kubota *et al.*, 1996; Marintchev *et al.*, 1999; Rice, 1999). The first XRCC1 partner to be discovered was DNA Ligase III (Caldecott *et al.*, 1994; Caldecott *et al.*, 1995). The two isoforms of DNA Ligase III (α and β) differ in their C-termini and as such, XRCC1 only interacts with DNA Ligase IIIα. These two proteins interact through their respective BRAC1 C-terminus-like motifs (BRCT) located in each of their C-termini (Mackey *et al.*, 1997; Nash *et al.*, 1997; Taylor *et al.*, 1998). Furthermore, this interaction has functional consequences. Cells lacking XRCC1 display a five-fold decrease of DNA Ligase III polypeptide and its activity (Caldecott *et al.*, 1995; Ljungquist *et al.*, 1994; Shen *et al.*, 1998). Another key protein that interacts with XRCC1 is poly(ADP-ribose)polymerase-1 (PARP-1). Masson et al. identified this interaction using the two-hybrid system and further confirmed that this interaction occurred via the BRCT domains within each respective protein (Masson *et al.*, 1998). Additional studies show that XRCC1 interacts with DNA gap tailoring proteins such as APE1, pol β, PNKP and Tdp1 (Almeida and Sobol, 2007; Lan *et al.*, 2004; Plo *et al.*, 2003; Whitehouse *et al.*, 2001).

1.4.2. Nucleotide excision repair

In addition to the small lesions repaired by BER there are also large, bulky, helix-distorting lesions caused by chemical agents (i.e. benzo(a)pyrene), cross-linking agents (i.e. cisplatin) or exposure to UVR that are repaired by the nucleotide excision repair pathway (NER). This is a versatile repair pathway with the ability to remove a multitude

of lesions. There are two sub pathways within NER, transcription coupled repair (TC-NER) and global genomic repair (GG-NER). TC-NER repairs lesions within transcriptionally active regions, while GG-NER repairs lesions over the entire genome. These two pathways differ in their recognition steps (Fig. 1.3). Within TC-NER, lesions are initially recognized when the transcription machinery, RNA pol II, becomes stalled at lesions and is subsequently displaced by cockanye syndrome proteins (CSB) (Fousteri and Mullenders, 2008; Rastogi *et al.*, 2010; Tornaletti, 2009). The current consensus regarding recognition of lesions in GG-NER centers on the xeroderma pigmentosum complementation group C (XPC) protein (Rechkunova *et al.*, 2011). This protein is part of a stable heterotrimeric complex which includes hHR23A or hHR23B (S. *cerevisiae* RAD23p homologs) and centrin 2 (Kamionka and Feigon, 2004; Sugasawa, 2008) and is essential for GG-NER initiation in *in vitro* and in intact cells (Sugasawa *et al.*, 1998; Volker *et al.*, 2001). XPC is able to detect strongly helix-distorting lesions with high affinity toward bubble structures and 6-4 PPs (Hey *et al.*, 2002). Additionally, UV-damaged DNA binding protein (UV-DDB) participates in damage recognition (Nishi *et al.*, 2009; Sugasawa, 2011). UV-DDB is a heterodimer comprised of DDB1/p127 and DDB2/p48 that tightly binds to UV-irradiated DNA (Protic *et al.*, 1989). DDB2 preferentially recruits XPC to CPDs through a direct physical interaction (Fitch *et al.*, 2003; Moser *et al.*, 2005; Rastogi *et al.*, 2010; Sugasawa *et al.*, 2005).

Following lesion recognition, all subsequent steps are common to TC-NER and GG-NER pathways (Fig.1.3).

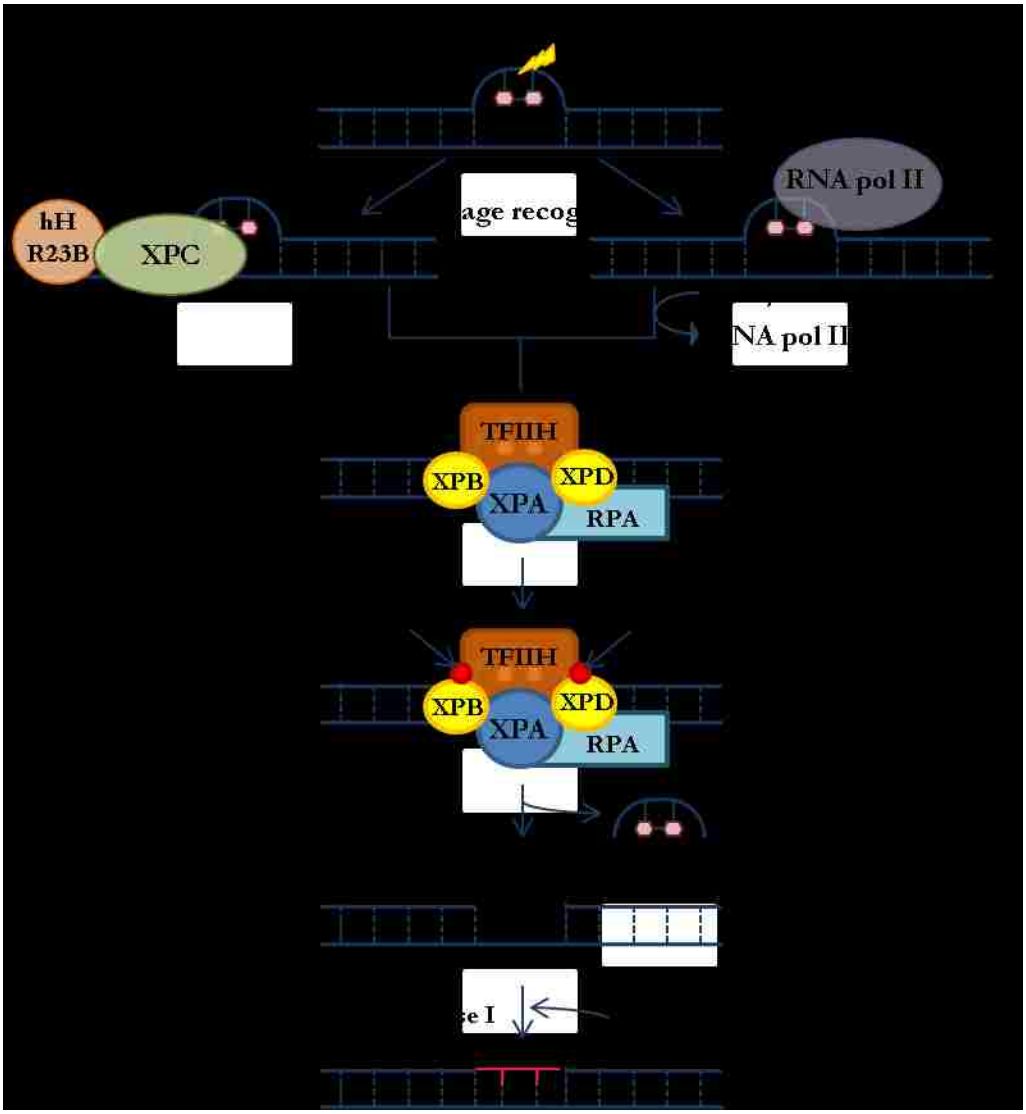

FIGURE 1.3. **Nucleotide excision repair pathway (NER)**. Schematic depicting the molecular mechanisms of the two sub pathways of NER, global genomic repair (GG-NER) and transcription coupled repair (TC-NER) (Rastogi *et al.*, 2010).

The next protein to be recruited is the ten-subunit complex TFIIH. This multiprotein complex contains two ATP-dependent DNA helicases, p89/XPB and p80/XPD, that contain opposite polarities (Schultz *et al.*, 2000; Thomas and Chiang, 2006). XPB unwinds double stranded DNA along the 3' to 5' end while XPD is a 5' to 3' helicase that tracks along the DNA stalling as it encounters lesions, confirming the presence of chemical alterations in the DNA (Fagbemi *et al.*, 2011; Fan *et al.*, 2006; Fan *et al.*, 2008). The combined effect of these proteins leads to an opened DNA structure and the entrance of XPA, replication protein A (RPA) and XPG, and the formation of the preincision complex (Rechkunova *et al.*, 2011). XPA is a small 36 kDa Zn-binding protein that has high affinity for kinked rather than damaged DNA. This observation led to the hypothesis that XPA interacts with intermediate DNA structures subsequent to DNA recognition (Camenisch *et al.*, 2006; Missura *et al.*, 2001). Since XPA binds RPA (Ikegami *et al.*, 1998; Li *et al.*, 1995), TFIIH (Li *et al.*, 1998; Park *et al.*, 1995) and ERCC1, it is thought to assist in the correct positioning of the repair factors and allow for proper dual incision. RPA is a trimeric protein that binds to single-stranded DNA. It is the only preincision factor that is also found with postincision proteins suggesting that it might protect the undamaged strand from nuclease attack (Hermanson-Miller and Turchi, 2002; Overmeer *et al.*, 2011). At its initial entrance, XPG fulfills a structural role. It stabilizes the preincision complex, generating an open-stable complex. At this point in the repair process, XPG has little to no catalytic activity and full activity is only revealed once the ERCC1-XPF complex has made the 5' incision. This allows for the correct polarity required for the incision 3' to the lesion in NER (Fagbemi *et al.*, 2011; Scharer, 2008).

ERCC1-XPF are the last factors to join the preincision complex and are recruited through an interaction with XPA (Croteau *et al.*, 2008; Orelli *et al.*, 2010). Following dual incision an oligonucleotide of 24-32 nucleotides in length, containing the lesion, is released. The resulting gap is filled by DNA polymerase δ, ε or κ (Ogi *et al.*, 2010) and finally the nick is sealed by DNA ligase I or III/XRCC1 , restoring the DNA back to its original form (Moser *et al.*, 2007).

1.5. Aspects of PARP-1 function

Poly(ADP-ribose)polymerases (PARPs) are an ancient family of enzymes. This family of proteins contains 18 family members, the most studied being PARP-1. PARP-1 is a 113 kDa protein and is the most abundant family member, with an average of 10^6 molecules/cell (Ludwig *et al.*, 1988). It is a chromatin associated enzyme that is involved in many cellular processes including DNA repair, cell cycle control, apoptotic signaling, and transcriptional regulation (D'Amours *et al.*, 1999; Schreiber *et al.*, 2006). The PARP-1 protein has three major domains: the DNA binding domain (DBD, residues 1-374), the automodification domain (residues 375-525) and the catalytic domain (residues 526-1014) (Fig. 1.4) (Langelier *et al.*, 2008).

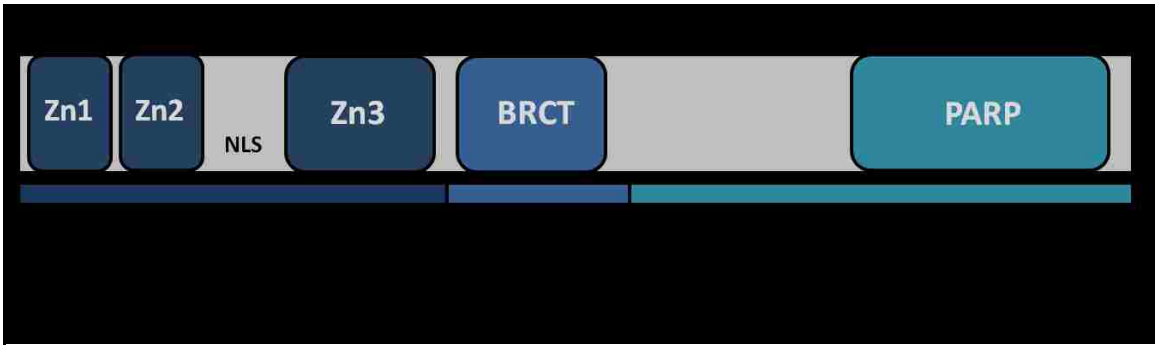

FIGURE 1.4. **Functional domains of human PARP-1**. Schematic depicting the three main segments of PARP-1: DNA binding domain, containing three zinc finger domains, automodification domain and catalytic domain (Langelier *et al.*, 2008).

The DBD is located in the N terminus of the PARP-1 protein. It contains two zinc-fingers that recognize damaged DNA. These zinc fingers are unique in that they recognize altered DNA structures rather than specific sequences (Clark *et al.*, 2012; Eustermann *et al.*, 2011). A recent low-resolution structure of the N-terminal half of PARP-1 revealed structural flexibility in the form of hinges connecting the two zinc fingers with the third zinc finger (Lilyestrom *et al.*, 2010). These data supports the notion of PARP-1's third zinc finger being able to couple the DNA binding and catalytic activities of PARP-1 (Langelier *et al.*, 2010; Langelier *et al.*, 2008; Tao *et al.*, 2008). The automodification domain contains a BRCT domain that is thought to assist in protein: protein interactions. The BRCT domain also contains glutamic acid residues that act as a binding motif for poly(ADP-ribose) (PAR) (Desmarais *et al.*, 1991; Hassa and Hottiger, 2008). Lastly, all PARP members contain a highly conserved 50 amino acid catalytic domain (Ame *et al.*, 2004) which is located at the C-terminus of PARP-1.

1.5.1. Poly(ADP-ribose) (PAR)

Following DNA damage, PARP-1 binds to altered DNA structures which activate its catalytic activity by 500-fold thereby producing poly(ADP-ribose) subunits (PAR) (Gagne *et al.*, 2006; Malanga and Althaus, 2005). PARP-1 uses NAD+ as a substrate to form PAR. NAD^+/NADH is one of the most versatile biomolecules because it can be used as a coenzyme as well as a substrate for ADP-ribosoyl transfer reactions. PAR is covalently transferred onto glutamic acid, aspartic acid, or lysine residues of target proteins ('acceptors') followed by the successive addition of subunits (Burkle, 2005). PARP-1 catalyzes more than 90% of PAR that occurs following DNA damage (Andrabi *et al.*, 2008). The main acceptor of PAR is PARP-1 itself resulting in automodification

(Alvarez-Gonzalez and Jacobson, 1987; Satoh and Lindahl, 1992) and subsequent release from DNA. PAR modifies additional substrates including proteins involved in chromatin structure, DNA synthesis, DNA repair, transcription and the cell cycle (Malanga and Althaus, 2005). PAR subunits undergo elongation at the 2'-OH of the mono(ADP-ribose) and can subsequently branch off at the 2''-OH of the ribose moiety. Chain lengths on acceptor proteins can reach up to 200 ADP-ribose units (Burkle, 2005). The net effect of adding PAR subunits is an overall negative charge and drastic change to the properties of the acceptor protein. Additionally, PAR formation in response to DNA damage has been reported to serve other purposes: (1) modification of histone tails leading to relaxation of chromatin fibers and increased access to breaks (2) signaling the extent of DNA damage which can result in cell death or repair and (3) assistance in the recruitment of DNA repair factors (Schreiber *et al.*, 2006). PAR production is an important signal to determine response to DNA damage. Minimal damage leads to PARP stimulation and nuclear accumulation of PAR which then assists DNA repair pathways and leads to an overall cytoprotective effect. On the other hand, too much damage leads to excessive PARP-1 activation and cellular depletion of NAD^+ stores which can result in cell death through necrotic and apoptotic pathways (Heeres and Hergenrother, 2007; Woodhouse and Dianov, 2008). PARP activation also leads to a unique form of cell death which involves PAR and the nuclear translocation of apoptosis inducing factor (AIF) from the mitochondria. This PARP-1 dependent cell death pathway is called parthanatos and its morphological features include shrunken and condensed nuclei, membrane disintegration, and sensitivity to propidium iodide within a few hours of onset (Andrabi *et al.*, 2008; Wang *et al.*, 2009).

There are three main PAR-binding motifs responsible for mediating associations between PAR and acceptor proteins. One PAR binding motif is a highly conserved domain known as the 'macro domain' of approximately 130-190 amino acid residues. This motif is present in several PARP family members such as PARP-9, PARP-14 and PARP-15 (Han *et al.*, 2010; Karras *et al.*, 2005). Another PAR-binding motif is known as the PBZ domain. This domain is a putative C2H2 zinc-finger and has been identified in the checkpoint protein CHFR (checkpoint protein with forkhead-associated and RING domains) and the DNA damage response protein APLF (aprataxin PNK-like factor) (Ahel *et al.*, 2008; Li *et al.*, 2011). The best characterized PAR-binding motif contains approximately 20-25 amino acids with an N-terminal basic amino acid cluster followed by hydrophobic residues interspersed with basic amino acids. This motif has been identified in several of the core histones, p53, cyclin-dependent kinase inhibitor 1 (p21), XRCC1 and other proteins including XPA (Malanga *et al.*, 1998; Pleschke *et al.*, 2000; Schmitz *et al.*, 1998). The presence of the well characterized PAR-binding motif in various groups of proteins emphasizes the versatility of this modification. In the case of DNA repair pathways, this motif is important in mediating protein interactions (Malanga and Althaus, 2005; Masson *et al.*, 1998).

1.5.2. Poly(ADP-ribose) glycohydrolase (PARG)

Since PARP activity and the formation of PAR are important in numerous cellular processes, it is not surprising that PARP's enzymatic activity is tightly regulated. The primary protein involved in the removal of PAR subunits from modified proteins is poly(ADP-ribose) glycohydrolase (PARG). PARG contains both endo- and exo-glycosidase activity (Bonicalzi *et al.*, 2005). Another protein, ADP-ribosyl protein lyase

removes the proximal ADP-ribosyl subunit bound to the protein (Oka *et al.*, 1984). To date, only one PARG gene has been detected in mammals which encods three cDNAs that generate 3 isoformes, 110 kDa, 102 kDa and 99 kDa, with the major product being the 110 kDa isoform (Koh *et al.*, 2004; Meyer *et al.*, 2003).

The importance of PARG is demonstrated by lethality at the larval stage in *Drosophila parg -/-* embryos suggesting that PARG is essential in the development of the fruit fly (Hanai *et al.*, 2004). *parg-/-* mouse embryonic stem cells survive but display increased sensitivity to methylmethanesulfonate (MMS) and γ irradiation (Fujihara *et al.*, 2009). This supports the view that PARG is involved in the DNA repair response. PARG is predicted to participate in DNA repair by removing PAR from modified proteins and PARP-1 itself, leading to recondensation of chromatin (Rouleau *et al.*, 2004). Also, Maruta et al. suggested that PARG and ADP-ribose pyrophosphate can work together to generate ATP from ADP-ribose (Maruta *et al.*, 1997). As one might expect, this local recycling of ADP-ribose to ATP would be beneficial during the ligation step in DNA repair. These findings support the conclusion that PARG is involved in the DNA repair response.

1.5.3. PARP-1 and Base Excision Repair

There is evidence that PARP-1 participates in BER. Using PARP-$1^{-/-}$ 3T3 cells Dantzer et al. found that long-patch repair was severely affected by the lack of PARP-1 whereas short-patch repair was only slightly diminished (Dantzer *et al.*, 2000). In contrast, when studying the repair of plasmid DNA, Vodenicharov et al. found that following irradiation or treatment with an alkylating agent PARP-$1^{+/+}$ and PARP-$1^{-/-}$ mouse embryonic fibroblasts had the same capacity to repair plasmid DNA. Additionally,

repair occurred independently of NAD^+ in a PARP-1 null background, but the presence of PARP-1 restored the NAD^+ dependency (Vodenicharov *et al.*, 2000). The discrepancies between these groups were partially resolved by Allinson et al. A cell-free system demonstrated that PARP-1 actively slows down the progress of both BER sub-pathways even in the presence of NAD^+ (Allinson *et al.*, 2003). They propose that the discrepancy could be due to differences in the experimental approach. Studies by Dantzer et al. were based on nucleotide incorporation rather than monitoring of actual repair rates. The results presented by Allinson et al. support a theory that the main role for PARP-1 in BER does not lie in direct catalysis of DNA damage processing (Allinson *et al.*, 2003).

This theory is supported by studies demonstrating the direct binding of PARP-1 to essential proteins in BER, such as XRCC1 and DNA Ligase III (Caldecott *et al.*, 1996; Leppard *et al.*, 2003; Masson *et al.*, 1998; Nazarkina Zh *et al.*, 2007). PAR is also important in BER. Parsons et al. reported that PARP-1 binds to AP sites very early on in the BER process. When PARP-1 activity is inhibited by 3-aminobenzamide, this blocks PARP-1 dissociation and completely prevents further repair thus illustrating a role for PAR in the progression of BER (Parsons *et al.*, 2005). PAR formation has also been implicated in recruiting BER proteins to damaged sites. Specifically, PARP activity is required for the assembly and/or stability of XRCC1 nuclear foci after oxidative damage (El-Khamisy *et al.*, 2003). Lastly, DNA Ligase III has been shown to preferentially bind poly(ribosyl)ated PARP-1, again demonstrating the importance of PARP-1 activity and PAR in this DNA repair pathway (Leppard *et al.*, 2003).

1.5.4. PARP-1 and Nucleotide Excision Repair

The role of PARP-1 in NER is less researched. Currently, there are only a handful of reports that discuss a role for PARP-1 in this DNA repair pathway. Flohr et al. used a dominant negative approach to decrease PARP activity by transfecting a hamster cell line with the PARP-1 DBD. Under conditions of PARP inhibition, they showed decreased repair of pyrimidine dimers when compared to control cells. These data were confirmed using the PARP inhibitor, 3,4-dihydro-5-[4-(1-piperidinyl)butoxyl]-1(2H)-isoquinolinone (DPQ). There was no additive effect in the repair rates in csb-/- and DPQ treated cells which suggested possible cooperation between PARP-1 and CSB protein as an underlying mechanism (Flohr *et al.*, 2003). A few years following this initial report, Ghodgaonkar et al. more fully dissected PARP-1's role in NER (Ghodgaonkar *et al.*, 2008). They utilized the host cell reactivation assay (HCR) which offers a simple model where host cells are not irradiated but are required to repair exogenously damaged virus. The cellular capacity for DNA repair is determined by the extent of expression of the reporter gene. Using this approach, Ghodgaonkar et al. demonstrated decreased DNA repair capacity of PARP-depleted NER-competent cells. Further studies to compare repair capacity of XPC and CSB deficient cells revealed a significant decrease in HCR capacity of PARP-depleted CSB cells at late time points (24h-44h) following UVB exposure, again suggesting a cooperative role between PARP-1 and CSB (Ghodgaonkar *et al.*, 2008). Overall, these studies suggest a role for PARP in NER but details relating to its exact mechanism of action have yet to be fully elucidated.

1.6. Other PARP Family Members

As mentioned above, the PARP family consists of 18 members. It was noted that *Arabidopsis thaliana* (a small flowering plant native to Europe) had gene coding for a PARP-related protein that was structurally different than the PAR-related protein found in maize (Ame *et al.*, 1999). When PARP-1 -/- mouse embryonic fibroblasts (MEFs) retained residual DNA-dependent PARP activity it was suggested that similar to plants, mammals may also have other PARP family members. Ame et al. cloned this cDNA and denoted the new protein as PARP-2 (65 kDa) and showed that it was a nuclear PARP family member that catalyzed poly(ADP-ribose) in the presence of DNA damaging agents. PARP-2 binds DNA, but in contrast to PARP-1 it does so through a non-conventional DNA binding domain (Ame *et al.*, 1999). PARP-2 and several of the other PARP family members retain homology to PARP-1 in their C-terminal region, referred to as the catalytic site. This site is a 40 kDa fragment that is sufficient for PARP-1's catalytic activity (Ruf *et al.*, 1996; Simonin *et al.*, 1993). PARP-2 has 60% homology to PARP-1 within this region (Smith, 2001). Schreiber et al. further characterized PARP-2 and found its expression pattern within tissues similar to that of PARP-1. PARP-2 interacted with BER proteins XRCC1, DNA pol β, and DNA Ligase III, all of which also bind PARP-1. PARP-2 was also found to be a functional component of BER, likely through its interaction with PARP-1.(Schreiber *et al.*, 2002). PARP-2, and more recently PARP-3, are the only other PARP family members involved in the DNA damage response. PARP-2 contributes about 5-10% of the total PARP response following DNA damage and PARP-3 contributions are under investigation (Boehler *et al.*, 2011; Yelamos *et al.*, 2008). Several reports have begun to address more specific functions for PARP-2

in areas other than the DNA damage response. Some of these include a possible role for PARP-2 in differentiation, the inflammatory response and its use as a target for therapy [review (Yelamos *et al.*, 2008)]. Despite the number of PARP family members only three appear to actively participate in DNA repair and PARP-1 is the major protein.

Rationale

It is imperative to investigate the underlying mechanisms of DNA repair pathways because unrepaired or misrepaired DNA lesions may lead to mutations and promote cancer. In addition, therapeutic modulation of DNA repair is an emerging strategy for cancer therapy. While there is some evidence to support a possible contribution of PARP to NER, our goal is to further define a mechanism of action for PARP in this repair pathway.

The work described in this dissertation tested the following hypothesis:

Hypothesis

Following UVR exposure PARP-1 activation and subsequent formation of PAR subunits allow PARP-1 to interact with essential proteins in NER, thereby contributing to the repair of ultraviolet induced photoproducts (Fig. 1.5).

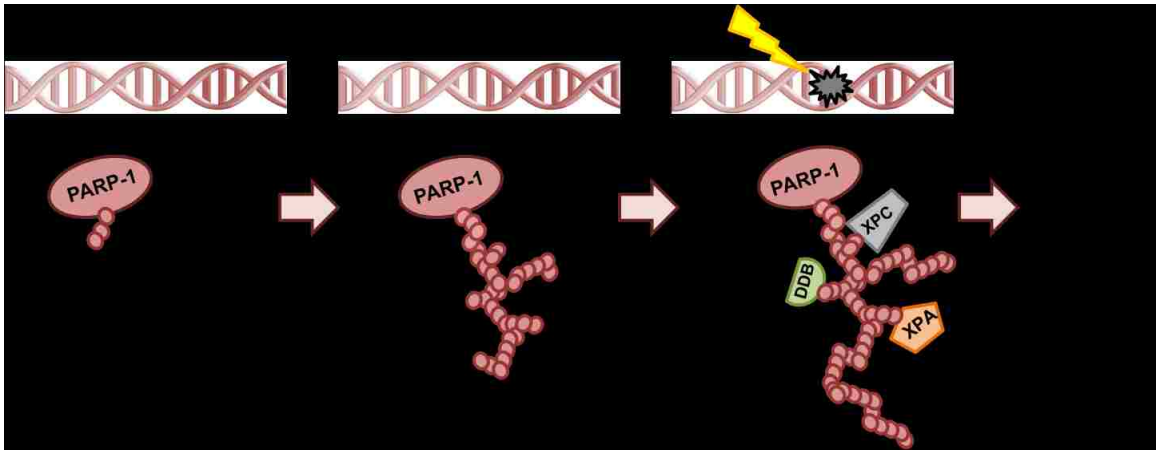

FIGURE 1.5. **Model of PARP-1's role in NER.** *A,* In the resting cell, basal levels of PARP-1 activity are low. *B,* Following UVR exposure, PARP-1 becomes activated and forms poly(ADP-ribose) subunits[PAR] which are placed on PARP-1 itself and other acceptor proteins. *C,* PAR act as a scaffold for NER components which contribute to the repair of UV-induced photoproducts.

The specific aims to test this hypothesis are as follows:

Project Aims

Aim 1: Establish a role for PARP-1 in the repair of ultraviolet induced DNA damage in keratinocytes

Hypothesis: Loss of PARP-1 expression (shRNA) or activity (pharmacologic inhibitors) will lead to increased retention of UV-induced photolesions repaired by NER

Results: Chapter 2 (cellular systems) and Chapter 4 (*in vivo*)

Aim 2: Identify whether the mechanism of PARP-1's involvement requires its catalytic activity thereby promoting PARP-1 interaction with NER proteins

Hypothesis: Following UVR exposure, activation of PARP-1 will lead to the formation of PAR subunits which act as a scaffold for components of the NER pathway

Results: Chapter 2 (XPA) and Chapter 3 (XPC)

Aim 3: Establish the impact of decreased PARP-1 activity on NER proteins

Hypothesis: Modifications to PARP-1 catalytic activity, by pharmaceutical approaches, will reduce PAR formation thereby disrupting the scaffold needed for PARP-1 interaction with NER proteins

Results: Chapter 2 (XPA) and Chapter 3 (XPC)

CHAPTER 2

Data contained within this chapter has been accepted for publication in the *Journal of Biological Chemistry (King et al., 2012).*

Authors include: Brenee S. King, Karen L. Cooper, Ke Jian Liu and Laurie G. Hudson

2. Poly(ADP-ribose) contributes to an association between Poly(ADP-ribose)polymerase-1 and Xeroderma pigmentosum complementation group A in nucleotide excision repair

2.1. Introduction

Keratinocytic tumors (basal cell and squamous cell carcinomas) are the most common cancers in the United States and solar ultraviolet radiation (UVR) is the major etiologic factor (Narayanan *et al.*, 2010). Solar UVR exposure forms DNA photoproducts such as cyclobutane pyriminde dimers (CPDs) and (6-4) pyrimidine-pyrimidone photoproducts (6-4 PPs) which are helix distorting lesions repaired predominantly by nucleotide excision repair (NER) (Nouspikel, 2009; Park and Choi, 2006). If such lesions are retained, they may lead to mutations, chromosome aberrations and cellular malfunctions including cell death, senescence and cancer (Pfeifer *et al.*, 2005; Sinha and Hader, 2002).

Poly(ADP-ribose)polymerase-1(PARP-1) has numerous functions in cells including orchestration of DNA damage response (Woodhouse and Dianov, 2008). While PARP-1's involvement in single strand break repair and base excision repair (BER) is established, less is known regarding the contributions of PARP-1 to NER. Chemical inhibition of PARP activity or over expression of the PARP-1 DNA binding domain decreased CPD repair rate in a transformed cell line (Flohr *et al.*, 2003) and PARP depletion by RNA interference (RNAi) decreased host cell reactivation of a UVR-

damaged reporter gene in fibroblasts (Ghodgaonkar *et al.*, 2008). While these studies provide evidence that PARP enzymes may modulate NER, little insight exists into a mechanism to account for these observations.

PARP-1 is rapidly activated in response to DNA damage leading to consumption of NAD+ as a substrate to form poly(ADP-ribose) subunits [PAR] and accounts for more than 70% of PAR production by PARP enzymes (Burkle, 2001; Schreiber *et al.*, 2002). PAR residues bind to acceptor proteins including PARP-1, histones and various proteins involved in DNA processing and repair. PAR fosters protein:protein associations (Hassa and Hottiger, 2008; Malanga and Althaus, 2005; Schreiber *et al.*, 2006) and a PAR-binding motif has been identified in certain proteins, including xeroderma pigmentosum complementation group A protein (XPA) (Pleschke *et al.*, 2000). XPA is part of a group of core proteins that are essential for the initial phase of the NER process (Aboussekhra *et al.*, 1995; Mu *et al.*, 1995). Data suggests that loss of this protein, through silencing or chemical suppression, can decrease repair of UVR-induced photoproducts and lead to increased cell sensitivity to DNA damaging agents, therefore, illustrating that loss of the XPA protein is rate-limiting to NER (Kang *et al.*, 2011b; Koberle *et al.*, 2006). Additionally, XPA binding, in conjunction with RPA, is proposed to be important in a secondary recognition step that verifies the presence of DNA lesions. Along these lines, XPA may also provide a checkpoint to control three-dimensional organization of NER complexes (Bartels and Lambert, 2007; Missura *et al.*, 2001). These data support the critical role for the XPA protein as well as its function in NER. Biochemical studies established the location of a PAR-binding motif in XPA and confirmed that the motif

conferred PAR binding (Fahrer *et al.*, 2007; Pleschke *et al.*, 2000), but the functional significance of this motif has not been defined.

In this study, we demonstrate that inhibition of PARP activity, or PARP-1 knockdown, causes retention of UVR-induced photoproducts in human keratinocytes. UVR exposure stimulated PARP activity and promoted association between XPA and PAR as well as XPA and PARP-1. Inhibition of PARP activity: 1) decreased the association between XPA and PARP-1 in whole cell extracts, 2) decreased the association between XPA and chromatin-bound PARP-1 and 3) blocked UVR-induced XPA association with chromatin, suggesting that these associations and XPA recruitment to chromatin is dependent on poly(ADP-ribosyl)ation. These results not only confirm a role for PARP-1 in NER, but suggest a mechanistic link for PARP activity in the repair of UVR-induced photoproducts.

2.2. Materials and Methods

Cell lines. The human keratinocyte cell line (HaCaT) was generously provided by Dr. Mitch Denning (Loyola University Medical Center, Maywood, IL). HaCaT cells were maintained as described previously (Ding *et al.*, 2009). PARP-1 HuSH cells were created by transfecting HaCaT cells with a PARP-1 shRNA (Origene, HuSH 29mer). Stable clones were selected using 0.5 μg/ml puromycin and maintained in growth media supplemented with 0.3 μg/ml puromycin. Decreased PARP-1 protein and mRNA was confirmed by western blot and northern blot analysis, respectively. Human embryonic kidney (HEK) 293 cells were cultured in Dulbecco's Modified Eagle's Medium (DMEM) supplemented with 10% fetal bovine serum (FBS), 2 mM L-glutamine and antibiotics

(penicillin, 100 U/ml and streptomycin, 100 µg/ml). Cells were cultured at 37 °C in 95% air/5% CO_2 humidified incubator.

Antibodies. Antibodies used include: Anti-PAR (Alexis Biochemical/Enzo Life Science), Anti-Thymine dimer clone KTM53 (CPD) and Anti-(6-4) photoproducts clone KTM50 (Kamiya Biomedical Company), Anti-XPA (Abcam, ab2352), Anti-XPA (Abcam, ab85914 for immunoprecipitation), Anti-PARP (Cell Signaling, #9542), Anti-PARP (Cell Signaling, #9532 for immunocytochemistry), Anti-GAPDH (Millipore), Anti-β tubulin (Santa Cruz), anti-rabbit and anti-mouse IgG, HRP conjugated (Promega), goat anti-rabbit IgG FITC conjugated and donkey anti-mouse IgG, Cy3 conjugated (Millipore).

UVR exposure and DPQ treatments. Cells at 50-60% confluent density were placed in phosphate buffered saline (PBS) and exposed to 3 kJ/m^2 solar-simulated ultraviolet radiation (ssUVR) using an Oriel 300W Watt Solar Ultraviolet Simulator (Newport Corporation, CA). The number of MED (minimal erythema dose) for 3 kJ/m^2 is 0.042 as measured by the Erythema UV and UVA Intensity Meter (Model 3D, Solar Light Company, PA). This dose resulted in 88% viability at 24hrs. After UVR exposure, PBS was replaced with growth media for times indicated in figures. Levels of UVR-induced photoproducts at zero time were performed, and there was no difference in initial photoproduct formation between HaCaT and PARP-1 HuSH cells. For the indicated studies, cells were exposed to 10µM 3,4-dihydro-5-[4-(1-piperidinyl)butoxyl]-1(2H)-isoquinolinone (DPQ, Santa Cruz Biotechnology) for 30 minute before UVR exposure. DPQ was present in the post-exposure incubation medium. Cells that were not treated are labeled as NT.

Western blotting. For total cell lysates, cells were collected in PARP lysis buffer (20mM Tris base (pH 7.5), 1mM EDTA, 1mM EGTA, 1% triton X-100, 25mM sodium pyrophosphate, 1mM β-glcycerol phosphate, 1mM sodium vanadate, 1μg/ml leupeptin and 2mM PMSF) and extracts clarified by centrifugation (8,000 rpm at 4^{o}C for five minutes). Cytoplasmic and nuclear cell fractions were obtained as described for the CellLytic NuCLEAR Extraction Kit (Sigma). Protein concentrations were measured using the BCA Protein Assay (Thermo Scientific). 30 μg protein in loading buffer (3x, 187.5mM Tris-HCl, pH 6.8, 6% w/v SDS, 30% glycerol, 150mM DTT and 0.03% (w/v) bromophenol blue) was heated at 100^{o}C for 5 minutes, resolved on a 10% sodium dodecyl sulfate (SDS)-polyacrylimide gel and transferred to nitrocellulose or polyvinylidene fluoride (PVDF) membranes. Proteins were detected as previously described (Qin *et al.*, 2008b). Band signal intensity was obtained using a Kodak 440CF Imager Digital Science Image Station. To control sample loading and protein transfer, membranes were stripped and re-probed to detect GAPDH. GAPDH was tested and found not to change following treatment conditions.

NAD Assay. Experiments were conducted according to the manufacturer's (Cell Technology Inc., CA) protocol for the Fluorescent NAD+/NADH Detection Kit.

Detection of UVR-induced photoproducts. 6-4 PPs or CPDs were detected as described in (Ding *et al.*, 2009) [protocol for 8-OHdG] with the following modifications: Fixed cells were not treated with RNase or proteinase K. Cells were incubated in 10% normal horse serum in PBS overnight. Anti 6-4 PP or CPD antibody was incubated with cells at a 1:1000 or 1:200 dilution, respectively, for 1 hour at 37^{o}C in a humid chamber. Cells were washed with PBS then incubated with secondary antibody

(1:300) for 1 hour at 37°C in a humid chamber. Following incubation with secondary antibody, cells were washed with PBS and mounted with Vectashield mounting media containing 2 μg/mL DAPI (Vector labs). Images were obtained using a Zeiss Axioscope 40 using a 40x objective with an Optronics MacroFire camera and PictureFrame 2.1 picture software. Images used for comparison were acquired with the same instrument settings and exposure times. Three to five images per cell type and time point were obtained and intensity measurements were quantified using Image J (NIH).

In addition, levels of genomic photoproducts were measured using a slot blot (Minifold II, Whatman International) immunoassay using antibodies to 6-4 PP (1:1000) and CPDs (1:2000). Sample preparation and slot blot procedure were conducted according to the Bio-Dot SF Instruction Manual (BioRad). Nitrocellulose membranes were placed in blocking solution for 1 hour (5% dried milk made in tris buffer saline with 0.05% Tween-20 [TBST]), primary antibodies were incubated for 1 hour followed by incubation with secondary antibodies for 1 hour. Membranes were washed for 20 minutes and signal intensity was obtained using a Kodak 440CF Imager Digital Science Image Station. After imaging, membranes were stained with methylene blue for 5 minutes in order to obtain total DNA in each well. Intensity measurements were normalized to total DNA in each well.

Immunoprecipitation. PAR, PARP-1 or XPA were immunoprecipitated from 750-1000 μg of protein in PARP lysis buffer as described in (Zhou *et al.*, 2011) with the following modifications. Primary antibodies (1:100 dilution) were incubated with protein for 1 hour at 4°C followed by addition of protein A agarose beads (Invitrogen) and further incubation for 1 hour at 4°C. Beads were isolated by centrifugation (4,500 rpm at

4°C for five minutes) and washed three times with PARP lysis buffer. To elute protein, loading buffer (see western blotting) was added to pelleted beads and heated at 100°C for 5 minutes and resolved by SDS- polyacrylimide gel as described above in the western blotting section.

Immunocytochemistry (ICC). In situ detection of XPA and PARP-1 was conducted as described in (Schwerdtle *et al.*, 2010) with the following modifications. XPA (1:50) and PARP-1 (1:150) antibodies were diluted in washing buffer (0.5% bovine albumin, 0.05% Tween-20). Secondary antibodies were used at 1:300 (FITC) and 1:500 (cy3) dilutions. Primary and secondary antibodies were added simultaneously during the appropriate steps. Five images per group were obtained using an LSM 510-META confocal with a 63x objective. For colocalization analysis, cy3 (XPA) and FITC (PARP-1) intensity measurements were obtained with individual masks for the respective channels and colocalization was determined in Slidebook 5.0 (Intelligent Imaging Innovations Inc., CO) using percent colocalization or Pearson's correlation coefficient.

Chip-on-western. Chromatin preparation was adapted from (Fousteri *et al.*, 2006) and collection protocol was followed as stated. Following collection, chromatin suspension was sonicated on ice (1 x 90sec) in RIPA buffer (0.01 M Tris-HCl ph 8.0, 0.14M NaCl, 1% Triton X-100, 0.1% deoxycholate, 1% SDS) using a Branson Sonifer (Output 5, Duty 40%, pulsed). Samples were isolated by centrifugation (13,200 rpm at 4°C for 15 minutes) with the supernatant containing cross-linked chromatin. A 50 µl aliquot of the supernatant was used to determine DNA concentration using the DNeasy Blood and Tissue Kit (Qiagen). For each sample, an equal amount of cross-linked chromatin (40-50 µg) was immunoprecipitated with 1:100 dilution of specific antibody

(XPA 12F5 or PARP-1 #9542). For immunoprecipitation of PARP-1, samples were incubated in primary for 1 hr at 4^{o}C. The immunocomplexes were absorbed onto pre-cleared sepharose Protein A beads (GE Healthcare) for 1 hr at 4^{o}C. Samples were washed three times in PARP lysis buffer and lastly in LiCl buffer (0.02 M Tris [pH 8.0], 0.25 M LiCl, 0.5% Triton X-100, 0.5% Na-deoxycholate), resuspended in loading buffer (see Western blotting), and boiled for 30 minutes at 100^{o}C before being loading onto a 10% polyacrylaminde gel. The western blotting protocol (above) was followed. The protocol for immunoprecipitation of XPA was adjusted as follows; samples were incubated in primary for 3 hrs at 4^{o}C. The immunocomplexes were absorbed onto pre-cleared Protein A and Protein G beads (1:1 ratio, Invitrogen) for 3 hrs at 4^{o}C. Beads were washed as stated in (Fousteri *et al.*, 2006), resuspended in loading buffer (see Western blotting), and boiled for 30 minutes at 100^{o}C before being loading onto a 10% polyacrylaminde gel. The western blotting protocol (above) was followed. For analysis, band signal intensity was obtained using a Kodak 440CF Imager Digital Science Image Station. All negative control samples were incubated with normal rabbit IgG-AC (Santa Cruz) and processed similar to samples incubated with primary antibody. We confirmed the presence of photolesions in the same soluble chromatin fraction used to perform immunoprecipitations by blotting the fraction onto a membrane using a slot blot apparatus (see above protocol, *Detection of UV-induced photoproducts*, slot blot).

Statistical Analysis. All graphs and statistical data were completed using GraphPad Prism 5 (GraphPad Software Inc., CA). Analysis used: unpaired t-test, Two-way ANOVA analysis with Bonferroni's correction, One-way ANOVA followed by Tukey's post-hoc multiple comparison test.

2.3. Results

UVR-induced photoproducts are retained following reduction of PARP activity through protein silencing or chemical inhibition - To investigate the impact of PARP-1 depletion on retention of UVR-induced photoproducts in cancer-relevant target cells, immortalized human keratinocytes (HaCaT) were transfected with a short hairpin RNA directed toward the PARP-1 protein (PARP-1 HuSH). A 60% reduction in PARP-1 protein levels was detected by western blotting (Fig 2.1A and 2.1B) which corresponded to a 60% reduction in basal PAR levels (Fig. 2.1C, NT) and a 70% reduction in PARP activation following a single dose of $3kJ/m^2$ solar simulated UVR (Fig. 2.1C, 1h). The accumulation of 6-4 PPs, as measured by fluorescent intensity, in PARP-1 HuSH cells remained elevated compared to HaCaT cells over a 6 hour time frame (Fig. 2.1D and 2.1E), suggesting decreased efficiency in repair mechanisms. Similar results were obtained using the slot blot technique for UVR-induced 6-4 PPs (Fig. 2.1F) and CPDs (Fig. 2.1G), further illustrating a role for PARP-1 in the repair of UV-induced lesions.

To expand on the above findings and examine the role of PARP activity, the PARP inhibitor 3,4-dihydro-5-[4-(1-piperidinyl)butoxyl]-1(2H)-isoquinolinone (DPQ) (Moroni *et al.*, 2001; Suto *et al.*, 1991) was used. This inhibitor significantly decreased UVR-stimulated PARP activity as measured by PAR production (Fig. 2.2A) and resulted in retention of 6-4 PPs (Fig. 2.2B) and CPDs (Fig. 2.2C). Taken together, these findings demonstrate that reduction of PARP activity, either by PARP-1 silencing or chemical inhibition, promotes retention of UVR-induced photolesions.

UVR promotes association between PARP-1 and XPA - PARP-1 activity was stimulated by UVR, as measured by decreased cellular NAD^+ (Fig. 2.3A)

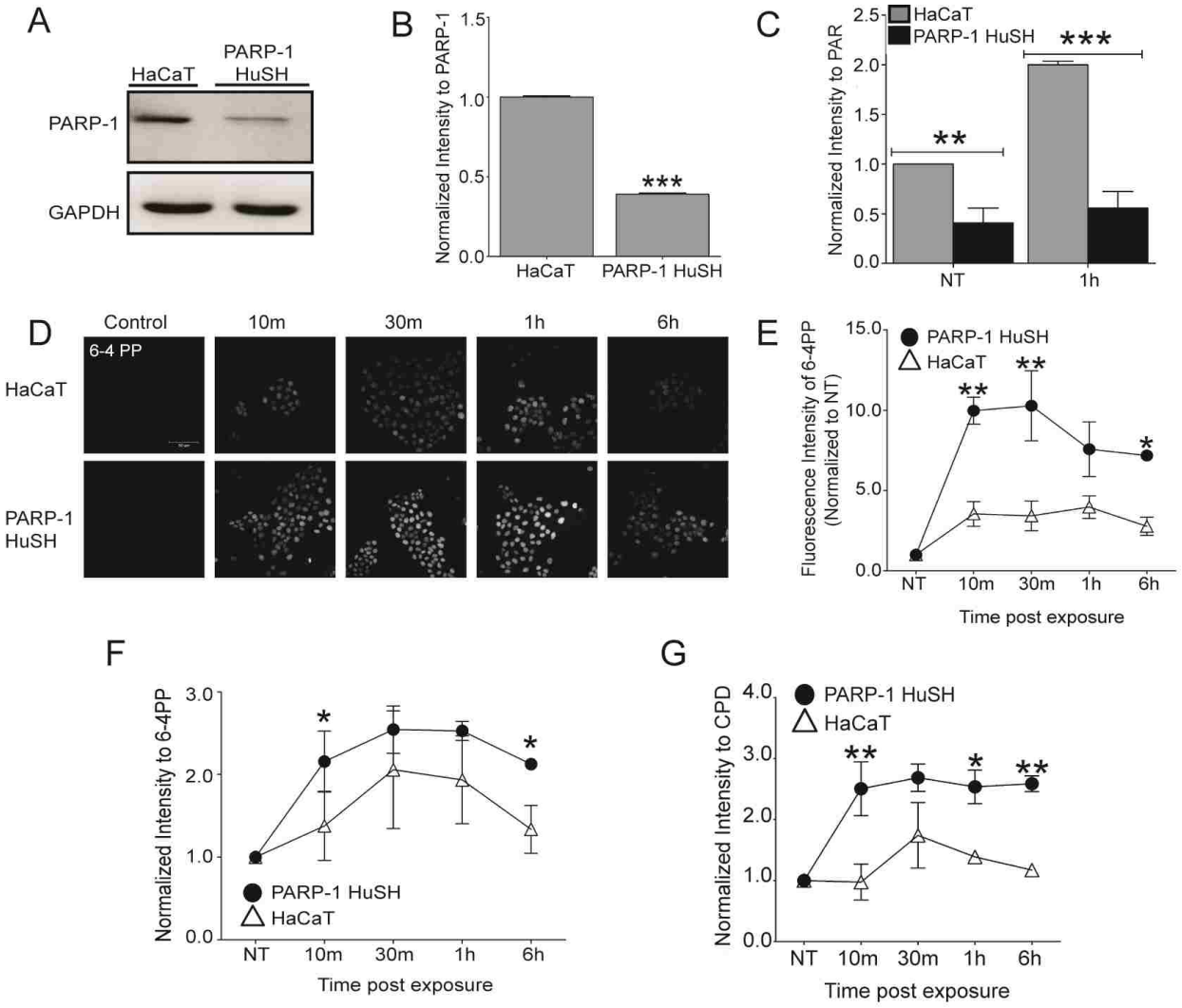

FIGURE 2.1. **Effects of PARP activity on retention of UVR-induced photoproducts.** *A,* Representative western blot comparing PARP-1 protein in HaCaT and PARP-1 HuSH cells. GAPDH is used as a loading control. *B,* Quantification of (A) by densitometry. PARP-1 intensity was normalized to GAPDH. Data presented as means ± SEM, n=3. *C,* Quantification of PAR western blots by densitometry in HaCaT and PARP-1 HuSH cells following UVR exposure. Data presented as means ± SEM, n=3. *D,* HaCaT cells and PARP-1 HuSH cells were exposed to a single dose of ssUVR (3 kJ/m^2) and collected at various times post exposure. Immunofluorescence was used to obtain images of 6-4 PPs. Initial UVR-induced photoproducts did not differ between HaCaT and PARP-1 HuSH cells. *E,* Fluorescence intensity obtained from images in (D). HaCaT (open triangles) and PARP-1 HuSH (closed circles). Intensities were normalized to NT sample. Data presented as means ± SEM, n=4. *F,G* Slot blot was performed on DNA extracted from HaCaT and PARP-1 HuSH cells. Quantification of lesion intensity by densitometry. Intensities normalized to NT. *F,* Intensity of 6-4 PPs formation. Data presented as means ± SEM, n=3. *G,* Intensity of CPD formation. Data presented as means ± SEM, n=3. *p<0.05, **p<0.01, ***p<0.001. Scale bar = 50μm.

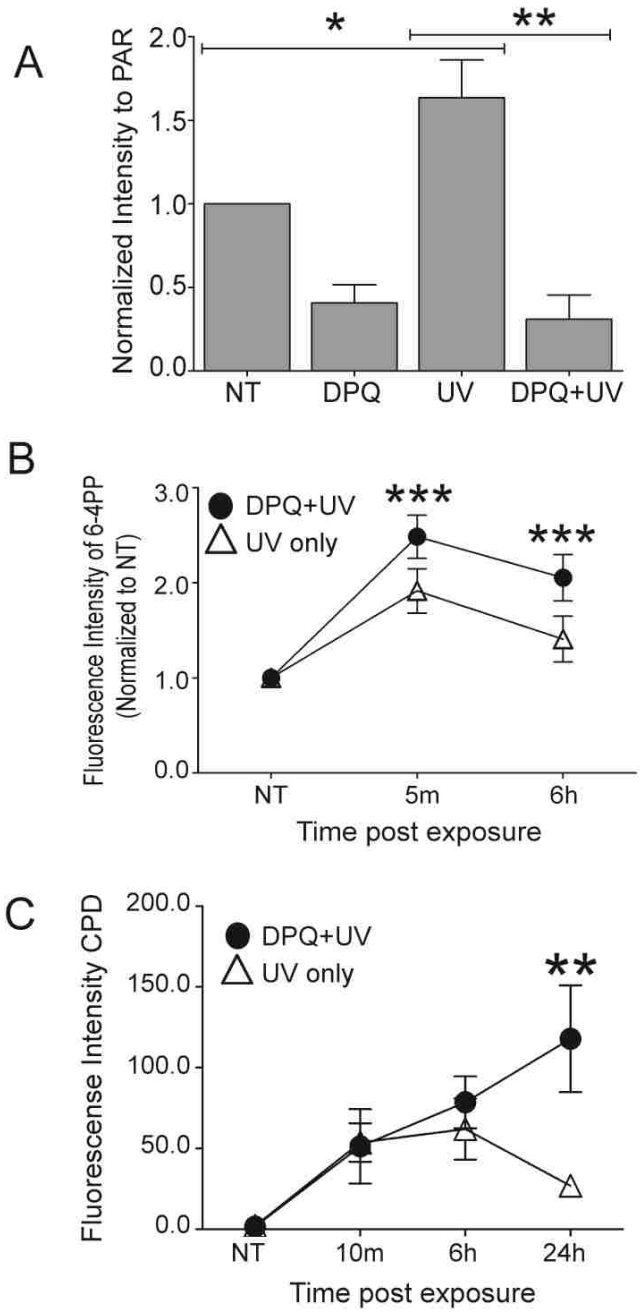

FIGURE 2.2. **Inhibition of PARP activity results in retention of UVR-induced lesions.** HaCaT cells were pre-exposed to a PARP inhibitor, DPQ, 30 minutes prior to a single dose of ssUVR (3 kJ/m^2) or exposed to UVR alone and collected at various times post exposure. *A*, Quantification of PAR western blots by densitometry. Data presented as means ± SEM, n=3. *B*, Quantification of 6-4 PPs obtained from immunofluorescent images. UV only samples (open triangles) and DPQ+UV samples (closed circles). Fluorescence intensity was normalized to NT sample. Data presented as means ± SEM, n=4. *C*, Quantification of CPDs obtained from immunofluorescent images. Fluorescence intensity of raw data. Data presented as means ± SEM, n=3. *p<0.05, **p<0.01, ***p<0.01.

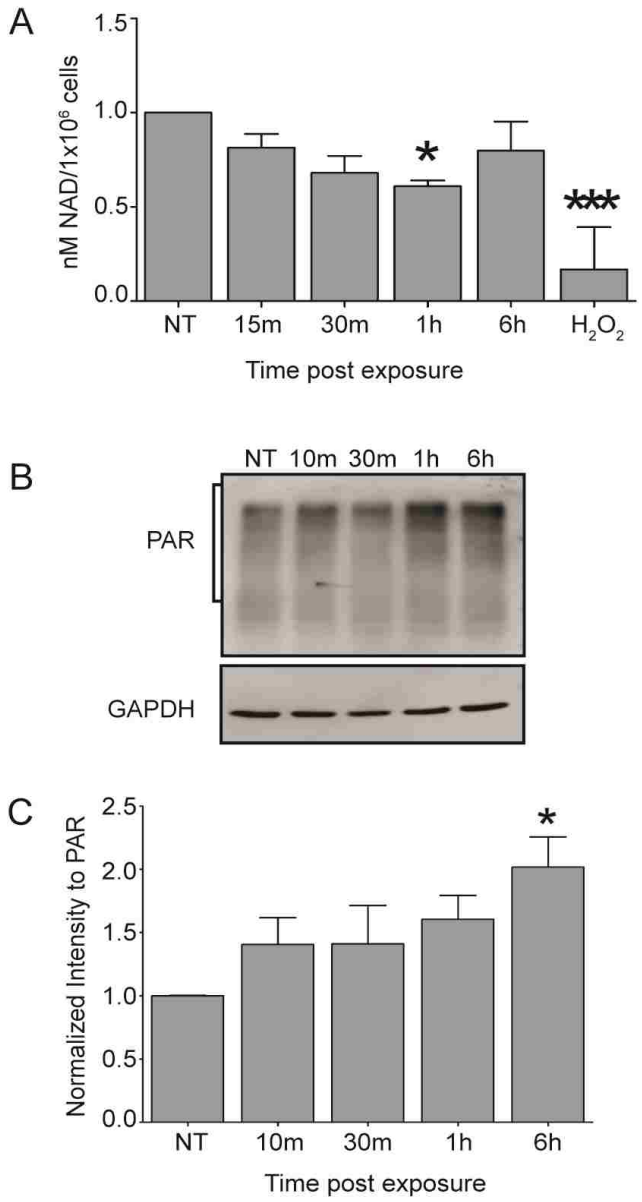

FIGURE 2.3. **PARP activity is increased following UVR exposure.** *A,* HaCaT cells were given a single dose of ssUVR (3 kJ/m^2) and allowed to incubate for various times post exposure. Following incubation, levels of NAD+ were assessed using a fluorescent detection method. Data presented as means ± SEM, n=4. *B,* HaCaT cells were given a single dose of ssUVR (3 kJ/m^2) and collected at various times post exposure. Representative western blot of PAR accumulation. GAPDH was used as loading control. *C,* Quantification of (B) by densitometry. PAR intensity was normalized to GAPDH. Data presented as means ± SEM, n=4. *p<0.05, ***p<0.001.

and a significant increase in PAR production (Fig. 2.3B and 2.3C). Given that biochemical assays established that XPA contains a PAR binding motif (Pleschke *et al.*, 2000), we examined whether association between XPA and PAR could be detected within an intact cellular system using co-immunoprecipitation of endogenous proteins. Association between XPA and PAR was detectable in unstimulated cells (Fig. 2.4A, NT) and this association was rapidly increased following UVR-exposure (Fig. 2.4A and Fig. 2.5A). Because PARP-1 is self-modified by PAR, we investigated the possible association between XPA and PARP-1. Co-immunoprecipitation revealed UVR-induced association between XPA and PARP-1 following immunoprecipitation of XPA (Fig.2.4B) and PARP-1 (Fig. 2.5B). Immunofluorescence detection was performed to evaluate co-localization of XPA and PARP-1 *in situ.* In agreement with the co-immunoprecipitation findings, a significant increase in XPA and PARP-1 co-localization was detected one hour post UVR exposure (Fig. 2.4C and 2.4D). The co-localization was transient with significant reduction apparent six hours following UVR (Fig. 2.4D). These results demonstrate that the identified PAR binding motif in XPA is functional within cells and suggest that it promotes UVR-induced associations of XPA with PAR and PARP-1.

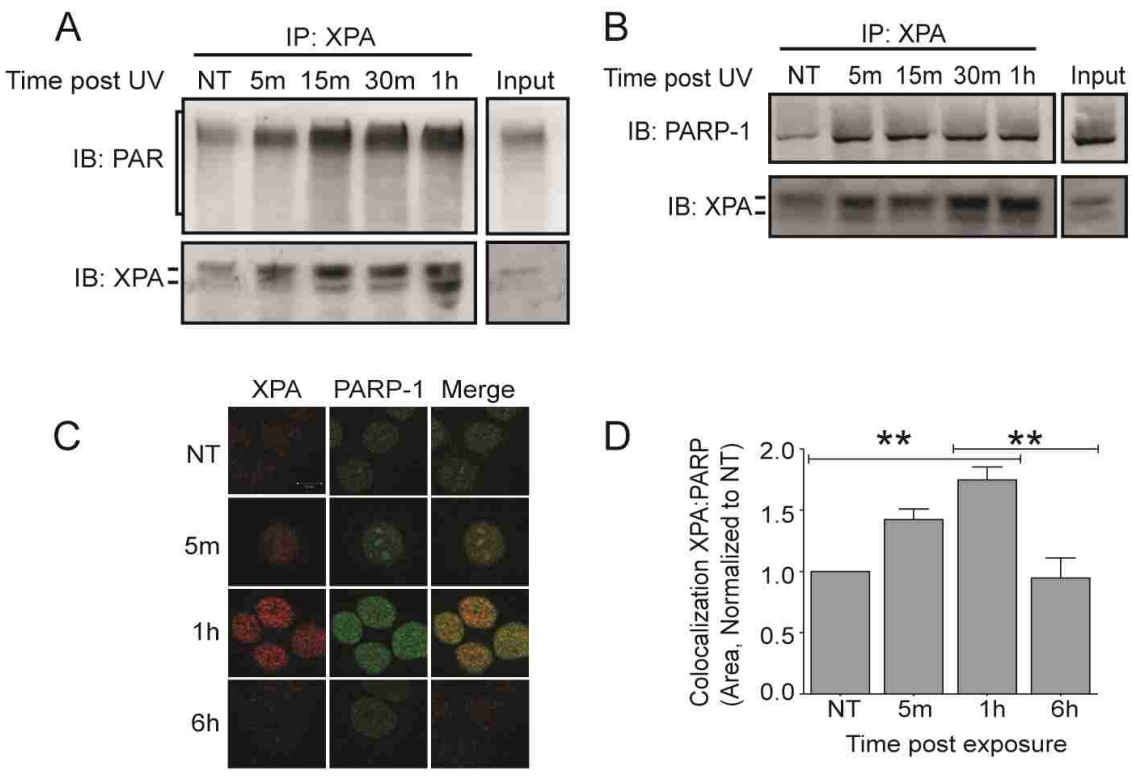

FIGURE 2.4. **UVR-induced associations between XPA and PARP-1.** HaCaT cells were given a single dose of ssUVR (3 kJ/m^2) and collected at various times post exposure. *A,* Representative image of co-immunoprecipitation. XPA was immunoprecipitated (IP) from cells and membranes were subsequently immunoblotted (IB) for PAR. Membranes were stripped and immunoblotted for XPA, as confirmation for immunoprecipitation, n=3 *B,* Representative image of co-immunoprecipitation. XPA was immunoprecipitated (IP) from cells and membranes were subsequently immunoblotted (IB) for PARP-1. Membranes were stripped and immunoblotted for XPA, as confirmation for immunoprecipitation, n=3 *C,* Dual staining with antibodies against XPA (red) and PARP-1 (green) was performed in order to assess the amount of colocalization (merge, yellow). *D,* Quantification of intensities from (C). Percent colocalization was determined as stated in Methods. Intensities were normalized to NT sample. Data presented as means ± SEM, n=3. ** $p<0.01$. Scale bar = 10μm.

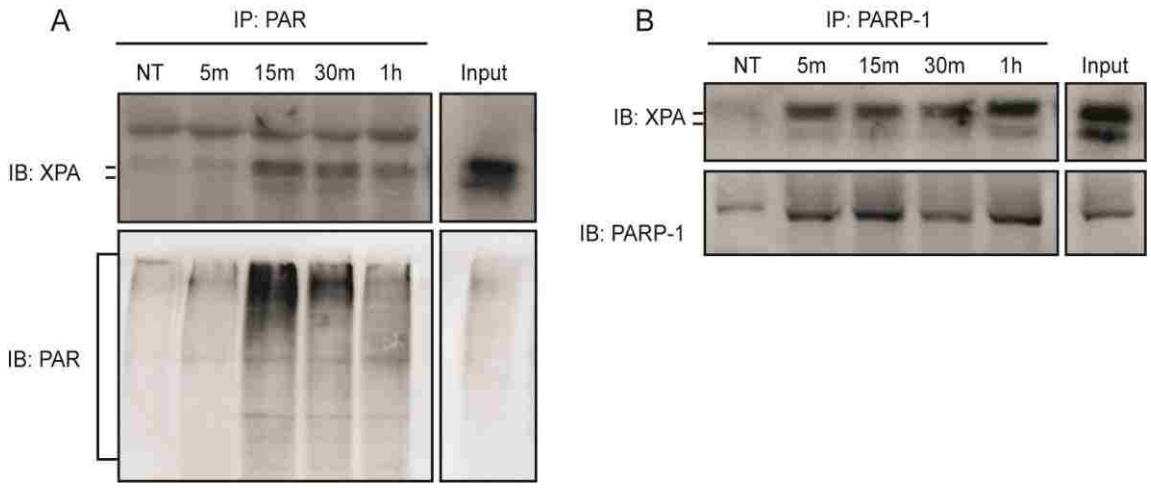

FIGURE 2.5. **Interactions between XPA and PARP-1.** HaCaT cells were given a single dose of ssUVR (3 kJ/m^2) and collected a various times post exposure. *A,* Representative image of co-immunoprecipitation. PAR was immunoprecipitated (IP) from cells and membranes were subsequently immunoblotted (IB) for XPA. Membranes were then stripped and immunoblotted for PAR, as confirmation for immunoprecipitation. *B,* Representative image of co-immunoprecipitation. PARP-1 was immunoprecipitated (IP) from cells and membranes were subsequently immunoblotted (IB) for XPA. Membranes were then stripped and immunoblotted for PARP-1, as confirmation for immunoprecipitation.

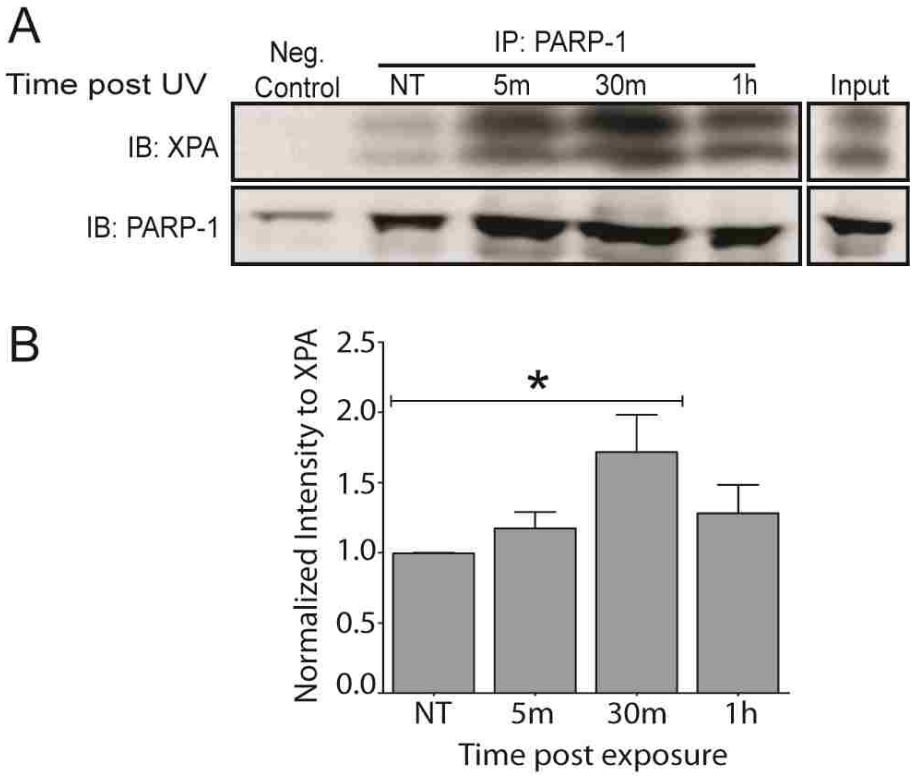

FIGURE 2.6. **UVR-induced associations between XPA and chromatin bound PARP-1.** HEK 293 cells were given a single dose of ssUVR (3 kJ/m^2) and collected at various times post exposure. A modified chromatin immunoprecipitation method (ChIP-on-western) was then performed. *A*, Representative image of co-immunoprecipitation. PARP-1 was immunoprecipitated (IP) from cells and membranes were subsequently immunoblotted (IB) for XPA. Membranes were stripped and immunoblotted for PARP-1, as confirmation for immunoprecipitation. *B*, Quantification of western blot by densitometry. Data presented as means ± SEM, n=5. * $p<0.05$

In order to observe this association in a more direct context for PARP-1 function, we isolated chromatin complexes using *in vivo* cross-linking followed by chromatin immunoprecipitation, as described in (Fousteri *et al.*, 2006). Chromatin fragments were immunoprecipitated with a PARP-1 specific antibody. Following UVR exposure, increased binding of PARP-1 with chromatin complexes was detected (Fig. 2.6A, IB: PARP-1), which was expected based on PARP-1's known function (Hassa and Hottiger, 2008). Furthermore, under conditions where PARP-1 had increased binding with chromatin, it also associated with XPA. This association was significant 30 minutes following UVR exposure (Fig. 2.6B). The extensive protocol used to isolate chromatin complexes highlights that the observed association between PARP-1 and XPA is not spurious. This relationship occurs under relevant conditions for NER proteins thus demonstrating its potential to be meaningful in lesion repair.

Decreased PARP activity through silencing or chemical inhibition, results in decreased association between PARP-1 and XPA – Next, we wanted to observe the association between PARP-1 and XPA within PARP-1 HuSH cells. Results from Fig.2.1 show that decreasing PARP-1 protein and subsequently PARP activity results in retention of UV-induced lesions. To better understand how PARP-1 associations with XPA may contribute to these findings, we conducted immunoprecipitations with a PARP-1 specific antibody in the PARP-1 HuSH cells. Immunoblotting for PARP-1 following its immunoprecipitation from PARP-1 HuSH cells showed a significant decrease in PARP-1 protein (Fig. 2.7A, Table 1A) and PAR bound to PARP-1 itself (Fig. 2.7A, Table 1A). This data corroborates results from Fig. 1A-C. More importantly, following immunoprecipitation of PARP-1 from PARP-1 HuSH cells there was a significant

decrease in its association with XPA when compared to HaCaT cells (Fig. 2.7A, Table 1A). Reciprocal immunoprecipitations also showed a decreased association between XPA and PARP-1 in PARP-1 HuSH cells (Fig. 2.7B, Table 2.1B). Taken together, these data suggest a contribution of the PARP-1 protein and/or its activity in its association with XPA.

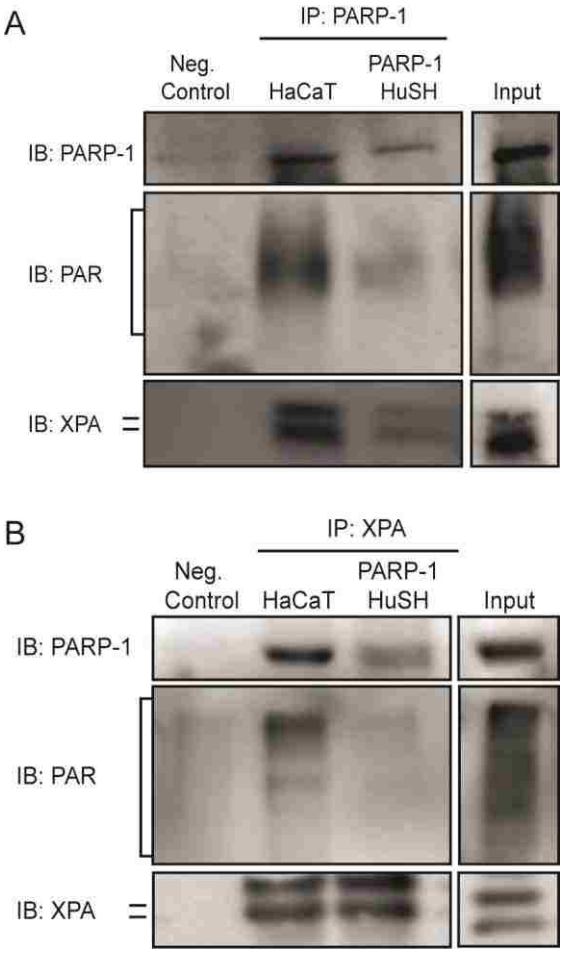

FIGURE 2.7. **Silencing PARP-1 protein leads to decreased association between PARP-1 and XPA.** Co-immunoprecipitations were performed in HaCaT and PARP-1 HuSH cells. *A,* Representative image of co-immunoprecipitations. PARP-1 was immunoprecipitated (IP) from cells and membranes were subsequently immunoblotted (IB) for PARP-1, PAR and XPA. *B,* Representative image of reciprocal co-immunoprecipitations. XPA was immunoprecipitated (IP) from cells and membranes were subsequently immunoblotted (IB) for PARP-1, PAR and XPA.

A

IP: PARP-1		
IB:	**% Decrease**	**p value**
PARP-1	75	<0.05
PAR	54	<0.05
XPA	82	<0.01

B

IP: XPA		
IB:	**% Decrease**	**p value**
PARP-1	50	<0.05
PAR	40	<0.01
XPA	10	n.s

TABLE 2.1. **Quantification summary of immunoprecipitation data from HaCaT and PARP-1 HuSH cells**. Statistical analysis of data obtained from western blots shown in Figure 5. *A,* Quantification of immunoprecipitations with PAPR-1 specific antibody. *B,* Quantification of immunoprecipitations with XPA specific antibody, n=3.

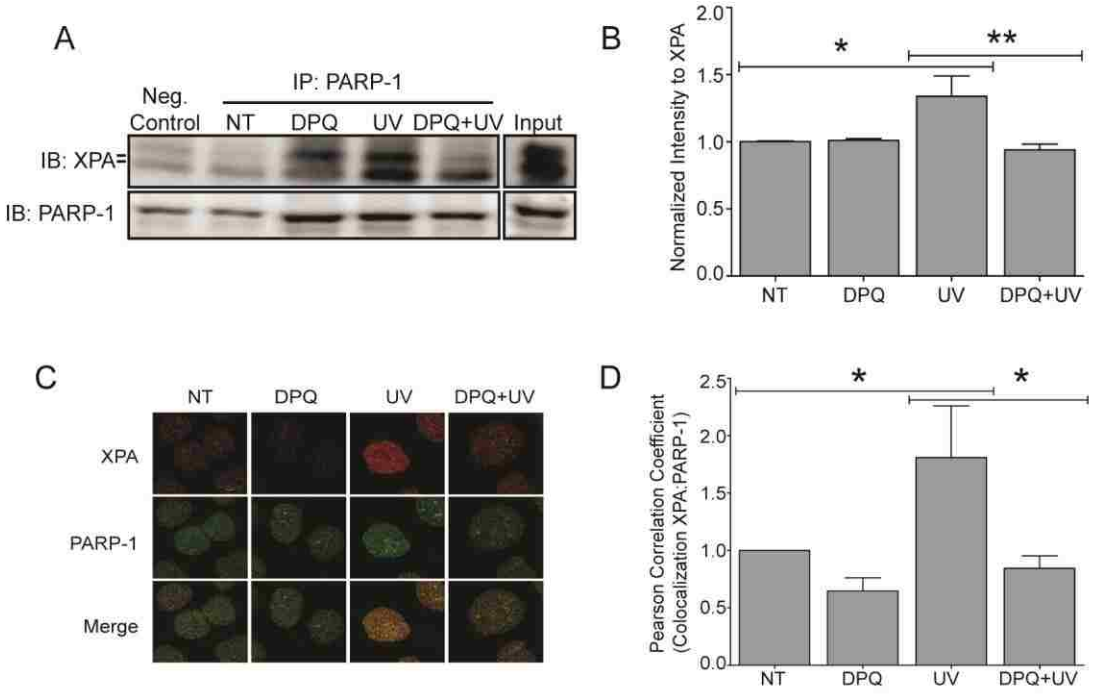

FIGURE 2.8. **Inhibition of PARP-1 activity also leads to decreased association between PARP-1 and XPA.** HaCaT cells were pre-exposed to a PARP inhibitor, DPQ, 30 minutes prior to UVR exposure. *A,* Cells were collected 30 minutes post UVR. Representative western blot obtained from modified chromatin immunoprecipitation method (ChIP-on-western). PARP-1 was immunoprecipitated from chromatin complexes. Membranes were immunoblotted (IB) for XPA and subsequently immunoblotted for PARP-1 as confirmation for immunoprecipitation. *B,* Quantification of western blot by densitometry. Data presented as means ± SEM, n=3. *C,* HaCaT cells were pre-exposed to a PARP inhibitor, DPQ, 30 minutes prior to UVR exposure and cells were fixed one hour post UVR. Dual staining with antibodies against XPA (red) and PARP-1 (green) was performed in order to assess the amount of colocalization (merge, yellow). *D,* Graph representing colocalization between XPA and PARP-1. Percent colocalization was determined using Pearson's Correlation Coefficient. Data presented as means ± SEM, n=3. * $p<0.05$, ** $p<0.01$. Scale bar = 10µm.

To investigate this further, we performed experiments using the pharmacological PARP inhibitor, DPQ. Chromatin binding experiments confirmed a significant increase in the association between chromatin-bound PARP-1 and XPA (Fig. 2.8A and 2.8B, UV) which was abolished following DPQ exposure (Fig. 2.8A and 2.8B, DPQ+UV), suggesting a role for PARP activation in the association between XPA and PARP. This decrease in association was also observed when XPA was immunoprecipitated from whole cell extracts and subsequently immunoblotted for PARP-1 (Fig. 2.9). Lastly, immunofluorescent experiments provided similar results. Following UVR, there was increased co-localization between PARP-1 and XPA (Fig. 2.8C, UV), again, following DPQ exposure this association was significantly decreased (Fig. 2.8D, DPQ+UV). Overall, these findings further demonstrate the importance of PARP activity in the association between PARP-1 and XPA.

PARP inhibition leads to changes in XPA function – The main functions of XPA are to bind DNA and interact with other NER proteins, thereby promoting DNA repair (Camenisch and Nageli, 2008). To ascertain whether there were any changes to XPA's DNA binding ability as a function of PARP activity, cells were exposed to UVR with or without DPQ treatment and collected five minutes post UVR. UVR exposure significantly increased XPA binding to chromatin compared to unexposed cells (Fig. 2.10A and 2.10B, UV) and DPQ significantly decreased UVR-induced XPA association with chromatin (Fig. 2.10B, DPQ+UV). These data demonstrate that PARP activity regulates UVR-induced XPA association with chromatin, which begins to provide a mechanistic link between PARP activity and NER.

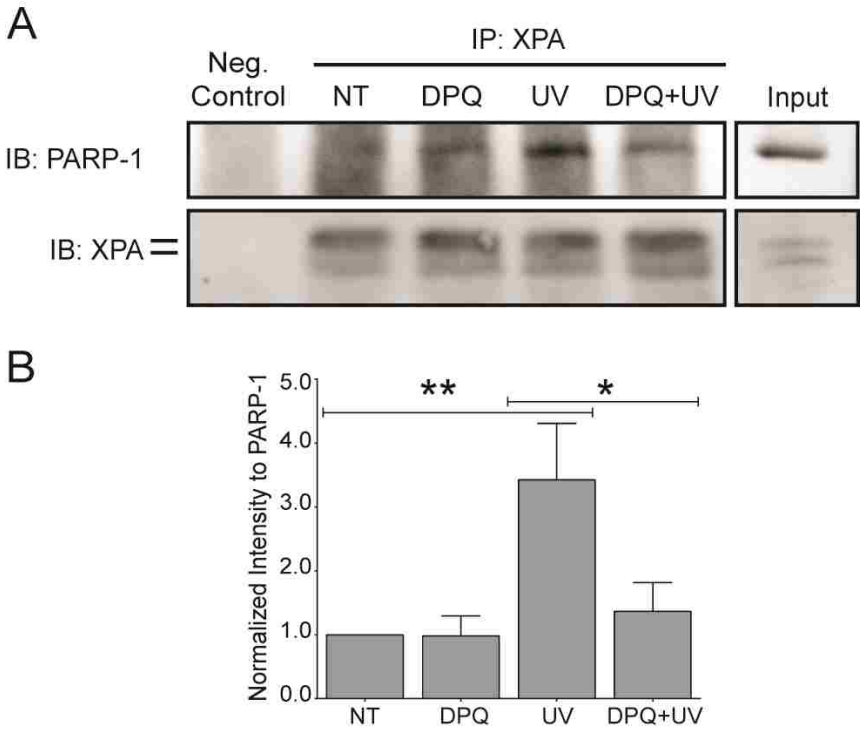

FIGURE 2.9. **Inhibition of PAPR activity decreases the association between PARP-1 and XPA.** HaCaT cells were pre-exposed to a PARP inhibitor, DPQ, 30 minutes prior to a single dose of UVR and collected five minutes post exposure. *A,* Representative image of co-immunoprecipitation. XPA was immunoprecipitated from cells (IP) and membranes were subsequently immunoblotted (IB) for PARP-1. Membranes were stripped and immunoblotted for XPA, as confirmation for immunoprecipitation. *B,* Quantification of western blot by densitometry. PARP-1 intensity was normalized to NT. Data presented as means ± SEM, n=5.

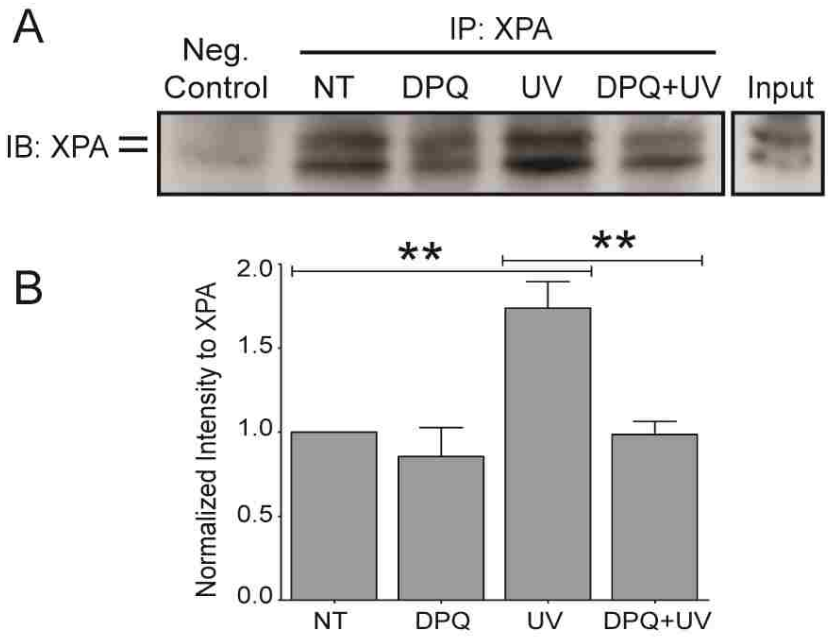

FIGURE 2.10. **Inhibition of PARP activity effects XPA function.** HEK 293 cells were pre-exposed to a PARP inhibitor, DPQ, 30 minutes prior to UVR exposure and collected five minutes post exposure. *A,* Representative western blot obtained from modified chromatin immunoprecipitation (ChIP-on-western). XPA was immunoprecipitated (IP) from samples and its ability to bind chromatin was assessed by subsequent immunoblotting (IB). *B,* Quantification by densitometry from ChIP-on-westerns. XPA intensity was normalized to NT. Data presented as means ± SEM, n=4. *p<0.05, **p<0.01.

2.4. Discussion

Production of PAR by PARP enzymes modulates the association of DNA repair proteins with sites of DNA damage and is important for the orchestration of DNA repair. Although the involvement of PARP-1 in BER is well characterized, there is limited knowledge regarding the contributions of PARP-1 to NER. Evidence to support a role for PARP-1 in NER include retention of UVR-induced photoproducts previously described (Flohr *et al.*, 2003; Ghodgaonkar *et al.*, 2008) and our data in keratinocytes (Fig. 2.1) following disruption of PARP activity by expression of the PARP-1 DNA binding domain, chemical inhibitors or RNAi. Current literature places a role for PARP-1 in the transcriptional coupled repair arm of NER with studies supporting a cooperative interplay between PARP-1 and Cockane syndrome B protein (CSB) (Flohr *et al.*, 2003; Ghodgaonkar *et al.*, 2008). Our studies provide a novel alternative mechanism which demonstrates an association between XPA and PARP-1 (Fig. 2.11). Because XPA is a core NER protein and both transcription coupled repair and global excision repair converge at an XPA-dependent step, these findings support the hypothesis that activated PARP contributes to the retention of UVR-induced DNA photoproducts through modulation of XPA.

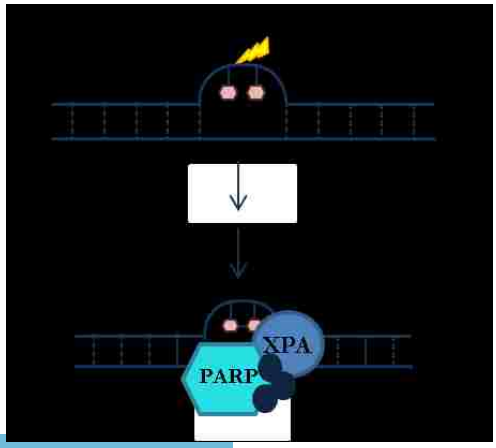

FIGURE 2.11. **Schematic of PARP-1 association with XPA.** Following UVR exposure PARP activity is increased leading to the formation of PAR which helps mediate the association between PARP-1 and XPA.

PARP-1 enzymatic activity is stimulated following DNA damage and the consequent assembly of PAR subunits recruits DNA repair proteins to the lesion. There are three main PAR- binding motifs responsible for mediating associations between PAR and acceptor proteins. One PAR binding motif is a highly conserved domain known as the 'macro domain' of approximately 130-190 amino acid residues. This motif is present in several PARP family members such as PARP-9, PARP-14 and PARP-15 (Han *et al.*, 2010; Karras *et al.*, 2005). Another PAR-binding motif is known as the PBZ domain. This domain is a putative C2H2 zinc-finger and has been identified in the checkpoint protein CHFR (checkpoint protein with forkhead-associated and RING domains) and the DNA damage response protein APLF (aprataxin PNK-like factor) (Ahel *et al.*, 2008; Li *et al.*, 2011). The best characterized PAR-binding motif contains approximately 20-25 amino acids with an N-terminal basic amino acid cluster followed by hydrophobic residues interspersed with basic amino acids. This motif has been identified in several of the core histones, p53, cyclin-dependent kinase inhibitor 1 (p21), XRCC1 and other proteins including XPA (Malanga *et al.*, 1998; Pleschke *et al.*, 2000; Schmitz *et al.*, 1998). The presence of a PAR-binding motif in XPA was predicted by sequence alignments that identified the 20-25 amino acid motif in the C-terminus of XPA. Polymer blot experiments confirmed PAR binding properties of amino acids between 215-237 (Pleschke *et al.*, 2000). Further *in vitro* analysis determined that polymers of ~16 PAR units were necessary for XPA binding and high affinity XPA binding was evident using immobilized long PAR chains (63-mer) (Fahrer *et al.*, 2007). While these studies suggested that PAR might influence XPA activity, the biochemical approaches did not demonstrate *in vivo* significance.

The current studies reveal that UVR promotes association of XPA with PAR subunits (Fig.2.4 and 2.5). Additionally, PAR production by activated PARP enhances UVR-dependent XPA association with bound PARP-1 (Fig. 2.8) and UVR stimulated XPA association with chromatin (Fig. 2.10). These findings illustrate that XPA:PAR associations occur in cells at endogenous protein levels and the association is relevant based on the observed modulation of UVR-dependent XPA:DNA binding as a function of PARP enzymatic activity *in vivo*. While the above data highlights a role for PAR-facilitated interactions, there may be additional contributions due to PARP-1 itself. PARP-1 silencing leading to decreased PARP-1 protein and enzyme activity (Fig. 2.1A-C and Fig. 2.7) decreased the association between PARP-1 and XPA to a greater magnitude than under conditions of pharmacologic PARP inhibition by DPQ. This suggests there may be a dual mechanism during lesion repair that relies upon PARP activation and PAR production which is augmented by direct protein interactions.

Additionally, we noted there was greater lesion retention in PARP-1 HuSH cells when compared to inhibition of PARP activity alone (Fig. 2.1E compared to Fig. 2.1F, 10m post UV). A possible explanation could be due to PARP-1 itself being involved in the recognition of UVR-induced photolesions in addition to it acting as a scaffold during lesion repair. PARP-1 is able to directly bind platinum lesions which are also large, bulky and helix-distorting (Zhu *et al.*, 2010). While this report showed decreased binding of PARP-1 to platinum lesions following its automodification, specific experiments with CPDs and 6-4 PPs would need to be conducted in order to determine the individual roles for the PARP-1 protein and its activity in lesion recognition.

NER is regulated by multiple post-translational modifications including PARylation, polyubiquitination and phosphorylation (Nouspikel, 2009). The breadth of protein modification and regulation by PAR is currently unknown; however a mass spectrometry based proteome-wide search for PAR-binding proteins and PAR-associated complexes using the 20-25 amino acid PAR-binding sequence identified hundreds of putative PAR-binding proteins (Gagne *et al.*, 2008). Fewer proteins have been identified with the alternate PAR binding motifs but database searches predicted 27 proteins containing the PAR binding macro domain and four proteins with the PBZ domain (Gagne *et al.*, 2008). Although only a fraction of putative PAR acceptor proteins have been analyzed, it is clear that in addition to PAR-dependent recruitment of BER proteins such as XRCC1 and DNA Ligase III to sites of DNA damage, PARP activation modulates multiple steps in the repair of DNA damage. PARylation of chromatin-associated proteins including histones and certain chromatin remodeling factors is believed to modify local chromatin structure at sites of DNA strand breaks or damage (Ahel *et al.*, 2009; Gottschalk *et al.*, 2009; Polo *et al.*, 2010) and recently, Iduna was identified as a PAR-dependent ubiquitin E3 ligase (Kang *et al.*, 2011a). These findings suggest that PARP activity and PAR production may influence numerous aspects of DNA repair.

Overall, our findings further extend the impact of PARP activation in DNA repair beyond the established role in BER by providing evidence for PAR-facilited modulation of XPA as had been predicted by the identification of its PAR-binding motif. Due to the centrality of XPA within NER, modulation of XPA by PAR provides a novel mechanism to account for the observed relationship between loss of PARP function and retention of

UVR-induced photolesions; thus, solidifying a role for PARP in NER. Further studies to assess the functional significance of identified or predicted PAR binding sites in other proteins will be necessary to delineate the scope of PARP activation in DNA repair and other regulatory pathways.

CHAPTER 3

The data within this paper is being submitted to the journal *DNA Repair*

Authors include: Brenee S. King, Ke Jian Liu, and Laurie G. Hudson

3. Evidence for Poly(ADP-ribose)polymerase-1 Interactions With Xeroderma Pigmentosum Complementation Group C (XPC)

3.1. Introduction

Poly(ADP-ribose)polymerase-1 (PARP-1) is the most abundant PARP enzyme in living cells. It has various functions in DNA damage repair, most notably base excision repair (BER). This pathway is responsible for repairing small, non-helix distorting lesions. For some time, it has been known that PARP-1 binds to DNA following damage. DNA binding stimulates enzymatic activity leading to production of poly (ADP-ribose) (PAR), and through its interactions with other BER proteins, such as XRCC1 and DNA polymerase β, PARP-1 acts as a scaffold for recruitment of other proteins (Almeida and Sobol, 2007; Caldecott *et al.*, 1996; Dantzer *et al.*, 2000). For example, experiments in cells indicate that PARP activation and subsequent formation of PAR subunits following oxidative damage facilitates XRCC1 assembly into nuclear foci (El-Khamisy *et al.*, 2003) and *in vitro* results demonstrate that XRCC1 preferentially binds to ribosylated PARP-1 (Masson *et al.*, 1998).

There is a more limited body of evidence to support a role for PARP-1 in nucleotide excision repair (NER). The NER pathway is responsible for repairing bulky, helix distorting lesions caused by exposure to ultraviolet radiation (UVR) and chemical or cross-linking agents. Inhibition of PARP activity by over expression of its DNA binding domain, gene silencing, or pharmacologic inhibitors leads to retention of

ultraviolet-induced DNA lesions such as cyclobutane pyrimidine dimers (CPDs) and 6-4 pryrimidine pyrimidone dimers (6-4 PPs) (Flohr *et al.*, 2003; Ghodgaonkar *et al.*, 2008). These studies suggest a role for PARP-1 in NER, but a mechanism to account for this observation has yet to be fully elucidated.

An important early event in NER is DNA lesion recognition. In the global genomic repair (GG-NER) arm of NER, xeroderma pigmentosum complementation group C (XPC) protein is responsible for lesion recognition (Sugasawa, 2008, 2011). This protein is part of a stable heterotrimeric complex which includes hHR23A or hHR23B (S. *cerevisiae* RAD23p homologs) and centrin 2 (Kamionka and Feigon, 2004) and is essential for initiation of GG-NER in *in vitro* and in intact cells (Sugasawa *et al.*, 1998; Volker *et al.*, 2001). Specifically, XPC detects strongly helix-distorting lesions with high affinity toward bubble structures and 6-4 PPs (Hey *et al.*, 2002). One potential mechanism to link PARP-1 to NER is through interaction with key NER proteins such as XPC. A proteome-wide search conducted by Gagne et al. using the well-established PAR-binding sequence based on the consensus motif *hxbxhhbbhhb*, initially identified XPC as a potential PAR-binding protein (Gagne *et al.*, 2008). Based on this information we hypothesized that XPC associates with PARP-1 and that this interaction is mediated, at least in part, through PAR.

In this study, we investigated potential interactions between XPC and PARP-1. We find an association between XPC and PARP-1 within the cellular context and when XPC is bound to chromatin. Importantly, PARP-1 did not interact with XPF, thereby suggesting a level of selectivity for the association. The association between PARP-1 and XPC is partially mediated by PAR and inhibition of PARP activity decreases UVR-

induced XPC binding to chromatin. Taken together, these findings provide evidence that the predicted PAR binding sequence on XPC (Gagne *et al.*, 2008) is functional within cells and that PARP activity leading to PAR production facilitates XPC binding to damaged DNA.

3.2. Materials and Methods

Cell lines. Human embryonic kidney (HEK) 293 cells were cultured in Dulbecco's Modified Eagle's Medium (DMEM) supplemented with 10% fetal bovine serum (FBS), 2 mM L-glutamine and antibiotics (penicillin, 100 U/ml and streptomycin, 100 μg/ml). Cells were cultured at 37°C in 95% air/5% CO_2 humidified incubator. The human keratinocyte cell line (HaCaT) was generously provided by Dr. Mitch Denning (Loyola University Medical Center, Maywood, IL). HaCaT cells were maintained as described previously (Ding *et al.*, 2009). PARP-1 HuSH cells were created by transfecting HaCaT cells with a PARP-1 shRNA (Origene, HuSH 29mer). Stable clones were selected using 0.5 μg/ml puromycin and maintained in growth media supplemented with 0.3 μg/ml puromycin. Decreased PARP-1 protein and mRNA were confirmed by western blot and northern blot analysis, respectively.

Antibodies. Antibodies used include: Anti-XPC (Santa Cruz, A-5, for immunoprecipitations), Anti-XPC (Abcam, ab20178, for western blotting), Anti-PAR (Alexis Biochemical/Enzo Life Science), Anti-PARP-1 (Cell Signaling, #9542), Anti-XPF (Abcam, ab7694) and anti-rabbit and anti-mouse IgG, HRP conjugated (Promega).

UVR exposure and AG-014699 treatments. Cells at 65-70% confluent density were exposed to 3 kJ/m^2 solar-simulated ultraviolet radiation (ssUVR) using an Oriel 300W Watt Solar Ultraviolet Simulator (Newport Corporation, CA). The number of

MED (minimal erythema dose) for 3 kJ/m^2 is 0.042 as measured by the Erythema UV and UVA Intensity Meter (Model 3D, Solar Light Company, PA). This dose resulted in 88% viability at 24hrs (data not shown). After UVR exposure, cells were placed back in the incubator for times indicated in figures. Cells were exposed to 50nM AG-014699 (Rucaparib, Selleck Chemicals) 1 hour before UVR exposure. AG-014699 was present in the post-exposure incubation medium. Cells that were not treated are labeled as NT.

Immunoprecipitation. PARP-1 was immunoprecipitated from 750 µg of protein as previously described in (Zhou *et al.*, 2011), with the following modifications: PARP-1 primary antibody (1:100 dilution) was incubated with protein for 1 hour at 4^{o}C followed by addition of pre-cleared sepharose Protein A beads (GE Healthcare) for 1 hour at 4^{o}C. Beads were isolated by centrifugation (1,815 x g at 4^{o}C for five minutes) and washed three times with lysis buffer (20mM Tris base (pH 7.5), 1mM EDTA, 1mM EGTA, 1% triton X-100, 25mM sodium pyrophosphate, 1mM β-glcycerol phosphate, 1mM sodium vanadate, 1µg/ml leupeptin and 2mM PMSF). To elute protein, loading buffer (3x, 187.5mM Tris-HCl, pH 6.8, 6% w/v SDS, 30% glycerol, 150mM DTT and 0.03% (w/v) bromophenol blue) was added to pelleted beads and heated at 100^{o}C for 5 minutes. Proteins were resolved on a 10% sodium dodecyl sulfate (SDS)-polyacrylimide gel. Proteins then transferred onto nitrocellulose (Biorad) or polyvinylidene fluoride (PVDF) membranes (Whatman). Proteins were detected as previously described (Qin *et al.*, 2008b). Band signal intensity was obtained using a Carestream 4000MM Pro Science Image Station and Carestream MI software.

Chip-on-western. Chromatin preparation was adapted from (Fousteri *et al.*, 2006) and collection protocol was followed as stated: following collection, chromatin

suspension was sonicated on ice (1 x 90sec) in RIPA buffer (0.01 M Tris-HCl ph 8.0, 0.14M NaCl, 1% Triton X-100, 0.1% deoxycholate, 1% SDS) using a Branson Sonifer (Output 5, Duty 40%, pulsed). Samples were isolated by centrifugation (15,600 x g at 4^{o}C for 15 minutes) with the supernatant containing cross-linked chromatin. A 50 µl aliquot of the supernatant was used to determine DNA concentration using the DNeasy Blood and Tissue Kit (Qiagen). For each sample, an equal amount of cross-linked chromatin (50 µg) was diluted in lysis buffer (20mM Tris base (pH 7.5), 1mM EDTA, 1mM EGTA, 1% triton X-100, 25mM sodium pyrophosphate, 1mM β-glcycerol phosphate, 1mM sodium vanadate, 1µg/ml leupeptin and 2mM PMSF) and immunoprecipitated with specific antibody. For immunoprecipitation of PARP-1, samples were incubated in primary antibody at 1:100 dilution for 1 hr at 4^{o}C. The immunocomplexes were absorbed onto pre-cleared sepharose Protein A beads (GE Healthcare) for 1 hr at 4^{o}C. Samples were washed three times in lysis buffer and lastly in LiCl buffer (0.02 M Tris [pH 8.0], 0.25 M LiCl, 0.5% Triton X-100, 0.5% Na-deoxycholate), resuspended in loading buffer (see immunoprecipitation protocol), and boiled for 30 minutes at 100^{o}C before being loading onto a 10% polyacrylaminde gel. The protocol for immunoprecipitation of XPC was adjusted as follows: samples were incubated in primary antibody at 1:100 dilution for 3 hrs at 4^{o}C. The immunocomplexes were absorbed onto pre-cleared sepharose Protein A beads (GE Healthcare) for 3 hrs at 4^{o}C and washed three times with lysis buffer and lastly in LiCl buffer. For protein elution, pelleted beads were resuspended in loading buffer, and boiled for 30 minutes at 100^{o}C before being loading onto a 10% polyacrylaminde gel. For analysis, band signal intensity was obtained using a Carestream 4000MM Pro Science Image Station and Carestream MI software. All negative control samples were

incubated with normal rabbit or mouse IgG-AC (Santa Cruz) and processed similar to samples incubated with primary antibody. We confirmed the presence of photolesions (6-4 PPs and CPDs) in the same soluble chromatin fraction used to perform immunoprecipitations by blotting the fraction onto a membrane using the slot blot technique (described in manufacturer's protocol, Bio-Dot SF Instruction Manual, BioRad). After imaging, membranes were stained with methylene blue for 5 minutes in order to obtain values for total DNA in each sample.

Statistical Analysis. All graphs and statistical data were completed using GraphPad Prism 5 (GraphPad Software Inc., CA). One-way ANOVA followed by Dunnett's Multiple Comparison Test (time course experiments) or Tukey's post-hoc multiple comparison test (AG-014699 experiments) were used for statistical analysis.

3.3. Results

UVR promotes the association between PARP-1 and XPC. XPC is important for the lesion recognition step of NER. A modified chromatin immunoprecipitation approach was used to detect XPC binding to chromatin and potential association with PAR and PARP-1. To detect DNA-binding proteins in a functional context, HEK 293 cells were exposed to a single dose of UVR and collected at various times post exposure. Endogenous proteins were cross-linked to DNA followed by immunoprecipitation with an XPC-specific antibody. Under these conditions, we observed a significant increase in XPC binding to chromatin at 5 minutes post-UVR (Fig 3.1A, IB: XPC and Fig. 3.1B). These binding kinetics are in accordance with other findings using fluorescence recovery after photobleaching (FRAP) (Hoogstraten *et al.*, 2008), thus supporting the modified chromatin immunoprecipitation approach.

A putative PAR binding motif was identified in XPC (Gagne *et al.*, 2008), but PAR binding of XPC has not been tested. To determine whether XPC binds PAR, the XPC chromatin complex was immunoprecipitated and immunoblotted using PAR-specific antibodies. PAR was observed at each time point post UVR exposure (Fig. 3.1A, IB: PAR). This time frame is sufficient to observe increases in total PAR following UVR in mouse embryonic fibroblasts (Vodenicharov *et al.*, 2005) and keratinocytes (data not shown). This finding suggests XPC and PAR can associate in an intact cellular system using endogenous proteins. The presence of PAR in the XPC chromatin immunoprecipitation suggested that PARP-1 might be present given that PARP-1 enzymatic activity is responsible for the majority of PAR produced in response to DNA damage (Burkle, 2001). Probing for PARP-1 revealed an increased association between XPC and PARP-1 at five minutes post UVR exposure (Fig. 3.1A, IP: PARP-1). Potential association between PARP-1 and XPC on chromatin has not been previously reported. The finding was confirmed by conducting the reciprocal experiment using the modified chromatin immunoprecipitation method. HEK 293 cells were exposed to a single dose of UVR, collected at various times post exposure and a PARP-1 specific antibody was used to isolate chromatin complexes. The association between PARP-1 and XPC was significantly increased 5 minutes post UVR exposure (Fig. 3.1C and 3.1D). Taken together, these results indicate that UVR stimulates XPC and PARP-1 binding to chromatin and immunoprecipitated XPC is associated with PAR and PARP-1. Because of evidence that PAR facilitates protein:protein interactions, it is possible that PAR production by activated PARP-1 contributes to the XPC:PARP-1 interaction.

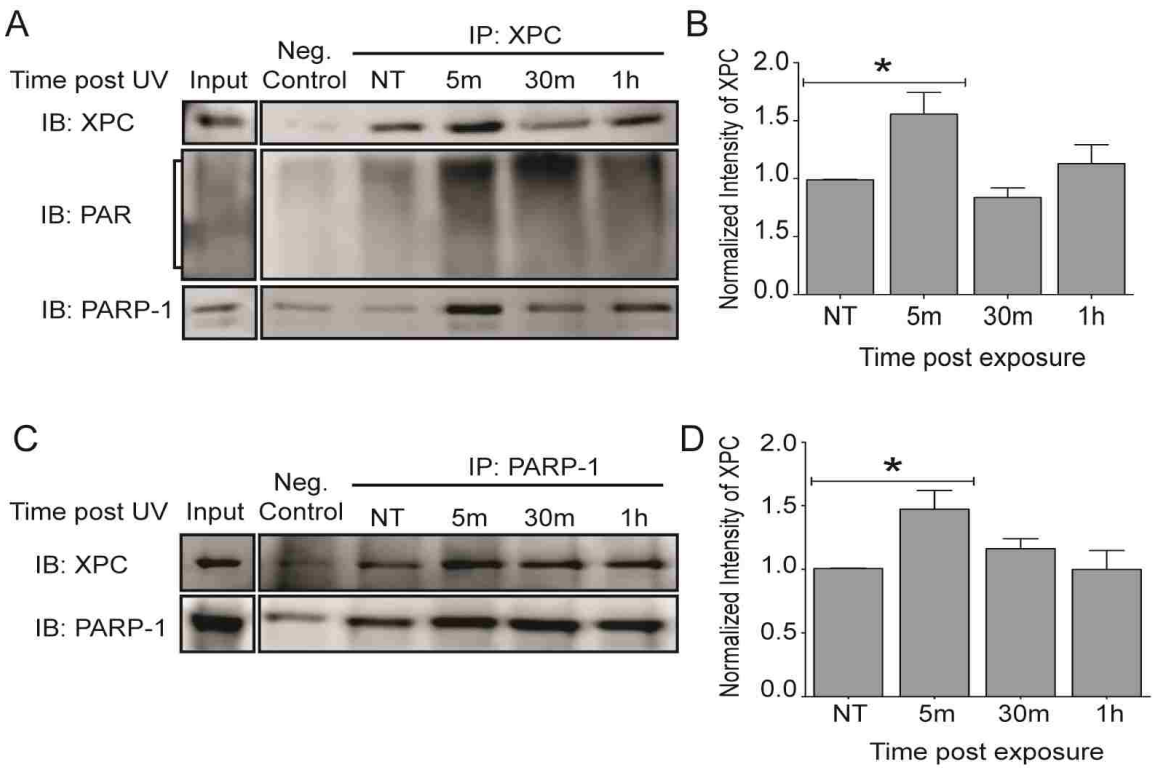

FIGURE 3.1. **UVR-induced associations between PARP-1 and XPC.** HEK 293 cells were given a single dose of ssUVR (3 kJ/m^2) and collected at various times post exposure. *A and C,* A modified chromatin immunoprecipitation method (ChIP-on-western) was performed. A, Representative image of co-immunoprecipitation. XPC was immunoprecipitated (IP) from cells and membranes were subsequently immunoblotted (IB) for XPC, PAR and PARP-1. *B,* Quantification of XPC western blot from (A) by densitometry. Data presented as means ± SEM, n=3 *C,* Representative image of co-immunoprecipitation. PARP-1 was immunoprecipitated (IP) from cells and membranes were subsequently immunoblotted (IB) for XPC. Membranes were stripped and immunoblotted for PARP-1, as confirmation of immunoprecipitation. *D,* Quantification of XPC western blot from (C) by densitometry. Data presented as means ± SEM, n=5. All samples were normalized to NT. * $p<0.05$.

Reductions in PARP-1 activity decrease association between PARP-1 and XPC. Previous findings showed PARP-1 silencing and enzyme inhibition led to retention of UVR-induced DNA lesions in hamster cells and skin fibroblasts (Flohr *et al.*, 2003; Ghodgaonkar *et al.*, 2008) so we used both approaches to investigate potential association between PARP-1 and XPC in cell lysates. To test the impact of PARP-1 protein knock-down, we compared PARP-1 association with XPC in an immortalized human keratinocyte cell line (HaCaT) to HaCat cells transfected with a PARP-1 shRNA (PARP-1 HuSH cells). Following immunoprecipitation of PARP-1 from both cell types, the PARP-1 protein and PAR production were decreased 75% and 80% respectively in HuSH cells compared to parental control cells (Fig. 3.2A). A modest (22%), but significant decrease in the association between PARP-1 and XPC was detected in the PARP-1 HuSH cells when compared to the HaCaT cells (Fig. 3.2B).

To gain more insight into the role of PARP activity in the association between XPC and PARP-1, we immunoprecipitated endogenous PARP-1 from cells treated with the PARP inhibitor AG-014699 (Hunter *et al.*, 2011; Kimbung *et al.*, 2012; Plummer *et al.*, 2008). Following UVR exposure autoribosylation of PARP-1 was increased (Fig. 3.2C, IB: PAR, UV), and pre-incubation with the PARP inhibitor reduced PAR bound to PARP-1 by 90% (Fig. 3.2C, IB: PAR, AG+UV). As observed using chromatin immunoprecipitation (Fig. 3.1), UVR exposure led to an increased association between PARP-1 and XPC as detected by co-immunoprecipitation from cell lysates (Fig. 3.2C, IB: XPC, UV). However, this UVR–stimulated association was ablated when cells were pretreated with the PARP inhibitor (Fig. 3.2C IB: XPC and 3.2D, AG+UV). These findings suggest that PAR subunits contribute to the interaction

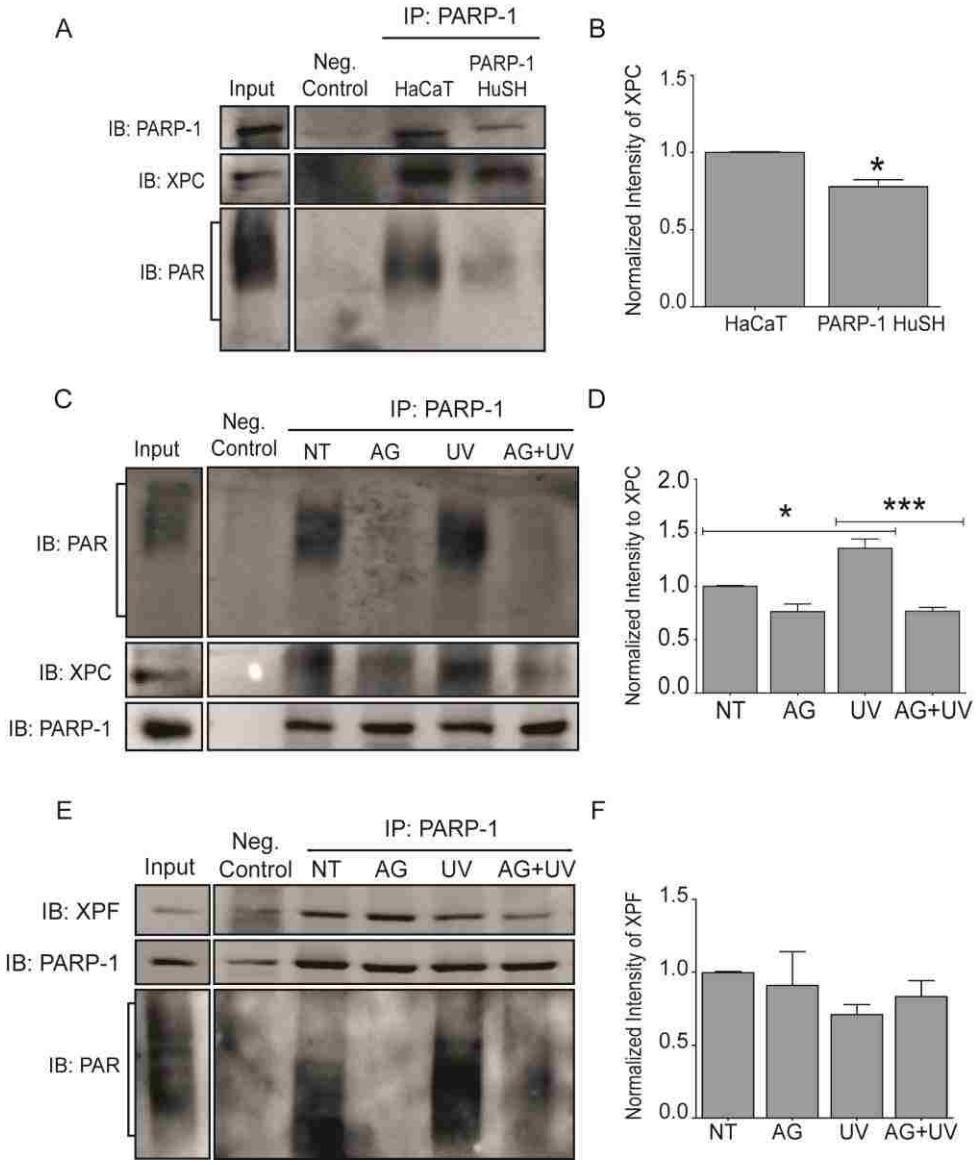

FIGURE 3.2. **Silencing of the PARP-1 protein or inhibition of its activity leads to a decreased association between PARP-1 and XPC.** *A,* Co-immunoprecipitations were performed in HaCaT and PARP-1 HuSH cells. Representative image of co-immunoprecipitation. PARP-1 was immunoprecipitated (IP) from cells and membranes were subsequently immunoblotted (IB) for PARP-1, XPC and PAR. *B,* Quantification of XPC western blot from (A) by densitometry. Data presented as means ± SEM, n=4. *C and E,* HaCaT cells were pre-exposed to the PARP inhibitor, AG-014699, 1 hour prior to UVR exposure and collected five minutes post exposure. *C,* Representative image of co-immunoprecipitation. PARP-1 was immunoprecipitated (IP) from cells and membranes were subsequently immunoblotted (IB) for PAR, XPC and PARP-1. *D,* Quantification of XPC western blot from (C) by densitometry. Data presented as means ± SEM, n=3. *E,* HaCaT cells were pre-exposed to the PARP inhibitor, AG-014699, 1 hour prior to UVR exposure and collected thirty minutes post exposure. Representative image of co-immunoprecipitation. PARP-1 was immunoprecipitated (IP) from cells and membranes were subsequently immunoblotted (IB) for XPF, PARP-1 and PAR. *F,* Quantification of XPF western blot from (E) by densitometry. Data presented as means ± SEM, n=4. All samples were normalized to NT. *p<0.05, ***p<0.001.

between PARP-1 and XPC in response to UVR.

In order to assess selectivity of PARP-1 association, co-immunoprecipitation studies were conducted for XPF, the last factor to enter the preincision complex during NER (Fagbemi *et al.*, 2011). In contrast to XPC, XPF does not have a putative PAR binding sequence, thus is not predicted to interact with PARP-1 following UVR activation. PARP-1 was immunoprecipitated from PARP-inhibitor treated and/or UVR-exposed cells. Immunoblot for XPF showed no significant changes in the association between PARP-1 and XPF under conditions where PARP-1 was activated (Fig. 3.2E, IB: PAR, UV) or when PARP activity was inhibited (Fig. 3.2E, IB; PAR, AG+UV) Together, the data surrounding XPC and XPF illustrate the importance of the PAR binding motif in PAR associations with NER proteins.

Inhibition of PARP-1 activity results in decreased binding of XPC to chromatin. The findings in Figure 3.2 demonstrate that PARP activity is essential for the UVR-induced co-immunoprecipitation of PARP-1 and XPC. Since XPC is essential in the recognition of UVR-induced photoproducts (Rastogi *et al.*, 2010; Rechkunova *et al.*, 2011; Sugasawa, 2008), the modified chromatin immunoprecipitation assay was used to assess changes to XPC binding under conditions of PARP inhibition. UVR exposure significantly increased XPC binding to chromatin (Fig. 3.3A and 3.3B, UV), similar to what is shown in Fig. 3.1A (IB: XPC, 5m). Pretreatment of cells with the PARP inhibitor AG-014699 significantly decreased UVR-induced XPC binding to chromatin (Fig. 3.3B, AG+UV). Lastly, we investigated how the PARP-1:XPC chromatin complex changed upon inhibition of PARP activity. Chromatin immunoprecipitation using PARP-1 as the

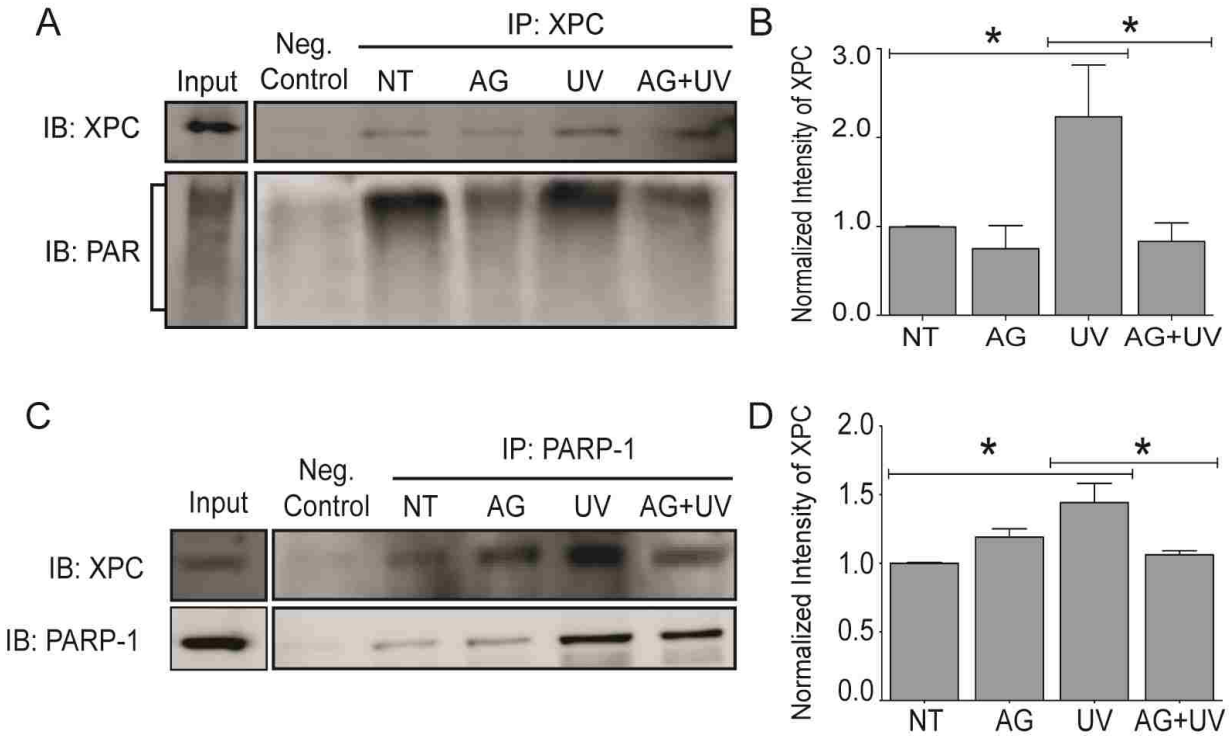

FIGURE 3.3. **Inhibition of PARP activity results in decreased binding of XPC to chromatin.** *A and C,* HEK 293 cells were pre-exposed to the PARP inhibitor, AG-014699, 1 hour prior to UVR exposure and collected five minutes post exposure. A modified chromatin immunoprecipitation method (ChIP-on-western) was performed. A, Representative image of co-immunoprecipitation. XPC was immunoprecipitated (IP) from cells and membranes were subsequently immunoblotted (IB) for XPC and PAR. *B,* Quantification of XPC western blot from (A) by densitometry. Data presented as means ± SEM, n=6. *C,* Representative image of co-immunoprecipitation. PARP-1 was immunoprecipitated (IP) from cells and membranes were subsequently immunoblotted (IB) for XPC. Membranes were stripped and immunoblotted for PARP-1, as confirmation of immunoprecipitation. *D,* Quantification of XPC western blot from (C) by densitometry. Data presented as means ± SEM, n=3. All samples were normalized to NT. *p<0.05.

probe demonstrated a significant increase in XPC following UVR exposure (Fig. 3.3C and 3.3D, UV), and this increase in XPC was blocked when PARP activity was inhibited (Fig. 3.3C and 3.3D, compare UV and AG+UV). Together, the data suggests PARP activity not only potentially regulates XPC binding in response to DNA damage, but it also participates in the formation of the PARP-1:XPC complex within chromatin.

3.4. Discussion

The proteome-wide search for PAR-binding proteins performed by Gagne et al. revealed a putative PAR binding motif in XPC (Gagne *et al.*, 2008). The current studies demonstrate that PAR was associated with endogenous XPC immunoprecipitated from cells in a time dependent manner following UVR exposure (Fig. 3.1A). Furthermore, chromatin-associated PARP-1 and XPC were co-immunoprecipited from UVR exposed cells suggesting that both proteins are part of a complex (Fig. 3.4). Use of the PARP inhibitor AG-014699, showed this complex was partially stabilized by PAR formation (Fig. 3.2C and 3.3C).

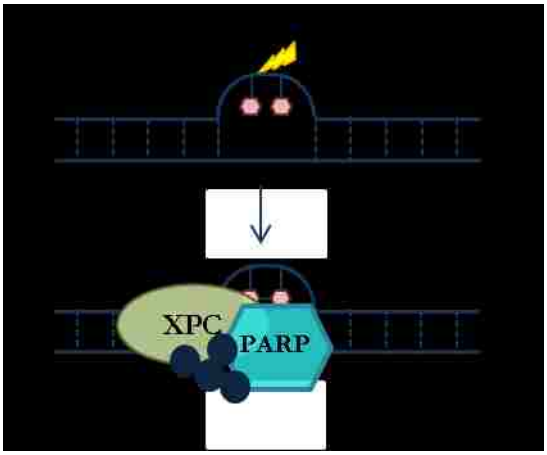

FIGURE 3.4. **Schematic of PARP-1 association with XPC.** Following UVR exposure PARP activity is increased leading to the formation of PAR which helps mediate the association between PARP-1 and XPC.

The importance of PAR in the BER repair pathway has been shown previously. DNA Ligase III was shown to directly bind PAR and preferentially bind automodified PARP-1 (Leppard *et al.*, 2003). Our data is novel because it reveals a possible mechanism for how PARP and its activity may contribute to NER.

Recently, Luijsterburg et al. demonstrated that PARP inhibition suppressed UVR-induced immobilization of XPC-GFP and reduced its recruitment to damaged sites (Luijsterburg *et al.*, 2012). Our findings extend these observations by showing a significant decrease in endogenous XPC binding to DNA complexes under conditions of PARP inhibition (Fig. 3.3A). Together, these results suggest that activation of PARP-1 in response to DNA damage and subsequent production of PAR may contribute to NER. Further support for this idea is provided by our findings that PARP-1 and XPA interact following UVR exposure (King *et al.*, 2012). Importantly, XPA contains a PAR binding sequence similar to the one predicated in XPC (Pleschke *et al.*, 2000). In contrast, following activation or inhibition of PARP activity, there were no significant changes in the association between PARP-1 and XPF, another protein in the pre-incision complex with no known PAR binding motif (Fig. 3.2F). These findings suggest that PAR binding motifs are an important determinant linking PARP-1 activation and interaction with NER proteins.

Other post-translational modifications of XPC have been identified including sumolyation and ubiquitylation (Sugasawa, 2006; Wang *et al.*, 2005). UV-induced sumolyation is thought to protect XPC from degradation once it leaves the NER complex, thereby allowing XPC to initiate a new round of damage recognition (Wang *et al.*, 2005). Additionally, polyubiquitulation of XPC augments its DNA binding activity (Sugasawa

et al., 2005). These findings, in conjunction with the work of Luijsterburg et al. and the data presented here, indicates the growing importance of understanding protein modification as mechanisms underlying XPC and other NER protein function. Evidence to support the presence of functional PAR-binding motifs in critical NER proteins support a role for PARP activation in NER and more specifically, how PAR may be able to regulate the function of central NER proteins such as XPC and thereby link PARP activity to retention or repair of UV-induced photolesions.

CHAPTER 4

4. *In vivo* inhibition of PARP activity by sodium arsenite results in retention of UVR-induced cyclobutane pyrimidine dimers

4.1. Introduction

4.1.1. Arsenic in the environment

Arsenic [As] is ubiquitous in the environment and is found in small quantities in rocks, soil, water, air and food (EPA, 1984). It is a toxic element that is classified as a human carcinogen. In the United States, India, Taiwan, Vietnam and Japan, the World Health Organization's set maximum contaminant levels for arsenic in drinking water is 10 µg/liter (Mohan and Pittman, 2007; WHO, 2004). Despite the current guidelines, it is not uncommon to find levels of arsenic above this standard in drinking water. The US Environmental Protection Agency (EPA) estimates that approximately 13 million people in the US are exposed to arsenic at levels above 10 µg/liter (EPA, 2001). At least four million people drink unhealthy arsenic levels in Mexico and several Latin American countries (Argentina, Chile, El Salvador, Peru and Nicaragua). It is estimated that more than 50 million people in Bangladesh drink water with levels of arsenic that exceed their national standard of 50 µg/liter (Bundschuh *et al.*; Camacho *et al.*, 2011; Mondal *et al.*, 2006). Overall, large populations are affected by arsenic exposure via ground water consumption.

4.1.2. Arsenic carcinogenesis

Chronic health effects of arsenic exposure include peripheral heart disease, ischemic heart disease, cerebral infraction, diabetes mellitus, hypertension and lastly skin and internal cancers (Jomova *et al.*, 2011; Yu *et al.*, 2006). In a 1984 health assessment

the EPA classified arsenic as a class I carcinogen based on epidemiologic data and the quantitative risk with regard to its routes of exposure (ingestion and inhalation) (EPA, 1984). Specifically, bladder, lung, kidney, liver and uterus are often considered arsenic-associated malignancies (Chen *et al.*, 2005; Ding *et al.*, 2000; Jomova *et al.*, 2011; Mead, 2005; Morales *et al.*, 2000; Steinmaus *et al.*, 2000). Currently there is *sufficient evidence* in humans for arsenic and inorganic arsenic compounds as lung, skin and urinary bladder carcinogens, and *some evidence* for these compounds as kidney, liver and prostate (IARC, 2009). Whole life exposure models (*in utero* through weaning and adulthood) demonstrate that arsenic is a complete carcinogen (Tokar *et al.*, 2010; Tokar *et al.*, 2011).

4.1.3. Genotoxicity

Arsenic does not cause point mutations in bacterial and standard mammalian cell mutation assays (Barrett *et al.*, 1989; Wang *et al.*, 1996) but does cause large deletion mutations in a human-hamster cell line (Hei *et al.*, 1998). Micronuclei were found in bone marrow of mice and in exfoliated bladder cells from exposed humans (Tinwell *et al.*, 1991; Warner *et al.*, 1994). Additionally, at high concentrations arsenic induced chromosome abberations (Lee *et al.*, 1988; Mahata *et al.*, 2003), and at lower concentrations it induced sister chromatid exchanges (Huang *et al.*, 1995; Kochhar *et al.*, 1996). The mechanisms of arsenic genotoxicity are not well understood, but arsenic can cause DNA damage through the formation of chemically reactive molecules.

Arsenic generates reactive oxygen species (ROS) and reactive nitrogen species (RNS) (Barchowsky *et al.*, 1999; Cooper *et al.*, 2007; Shi *et al.*, 2004). Production of reactive oxygen species following arsenic exposure can induce oxidative damage in cellular DNA. One type of damage is the formation of DNA strand breaks. The

development of single strand breaks can occur at low arsenite concentrations while generation of double strand breaks is seen at concentrations of 5 μM in mammalian cells (Martinez *et al.*, 2011a; Schwerdtle *et al.*, 2003b; Shi *et al.*, 2004). Oxidative damage also involves the formation of 8-OHdG adducts (Ding *et al.*, 2005; Qin *et al.*, 2008a; Wanibuchi *et al.*, 1997; Yamamoto *et al.*, 1997). Clinical studies showed a positive correlation between 8-OHdG staining and skin conditions such as arsenic-related skin neoplasms and arsenic keratosis (Matsui *et al.*, 1999). The combination of *in vitro* and *in vivo* studies demonstrates the mutagenic potential associated with DNA damage caused by arsenic-induced ROS.

4.1.4. Arsenic as a co-carcinogen

In addition to evidence that arsenic is a complete carcinogen, several studies demonstrate that arsenic can work in combination with other DNA damaging agents. The combination of ultraviolet radiation (UVR) and sodium arsenite resulted in a synergistic increase in cytotoxicity, chromosome aberrations and mutations to 6-thioguanine and in the *hprt* locus (Lee *et al.*, 1985; Li and Rossman, 1991) in cells and a synergism between arsenic and UVR in the development of skin tumors (Rossman *et al.*, 2001). Evidence suggests this is due to inhibition of DNA repair processes. Hartwig et al. exposed human fibroblasts to low, non-toxic levels, of arsenite (2.5 μM) and demonstrated interference with NER. The incision frequency was affected most severely and the ligation step was inhibited but only at cytotoxic concentrations of sodium arsenite (20 and 50 μM) (Hartwig *et al.*, 1997; Rossman *et al.*, 2004).

While the concept of arsenic as a co-carcinogen was discussed for some time, details regarding specific molecular targets were lacking. Using the rationale that

trivalent arsenic can inhibit the activity of thiol-containing enzymes, especially those containing two sulfhydryl groups in close proximity (Fluharty and Sanadi, 1961; Jennette, 1981), Li et al. investigated the role of arsenite inhibition on the activity of DNA ligase III and found it to be diminished following arsenite exposure (Li and Rossman, 1989).

Using the same rationale, Yager et al. investigated the inhibition of PARP-1 activity by arsenite treatment. They found a 50% decrease in PARP-1 enzymatic activity following exposure to 10 μM arsenite (Yager and Wiencke, 1997). In contrast, studies by Lynn et al. demonstrate a stimulatory effect of arsenite on PARP activity, it is pertinent to mention they were using concentrations of 40 μM arsenite or above in their studies (Lynn *et al.*, 1998). A few years later, Hartwig et al. confirmed the inhibition of PARP activity by arsenite exposure (Hartwig *et al.*, 2003). These initial reports of arsenite inhibition of DNA repair proteins provided the first data linking arsenite to a molecular targets and impairment of DNA repair processes.

4.1.5. Arsenic inhibition of DNA Repair

Arsenic is a trivalent oxyanion that contains an unshared pair of 4 s electrons. This characteristic allows it to bind proteins which could lead to conformational alterations of protein structure or inhibit enzymatic activities of proteins. Arsenic has been known to bind more than 200 proteins (Abernathy *et al.*, 1999) many of which have disulfide bonds (cysteine). Trivalent arsenicals bind with high affinity to proximal sulfhydryl groups which are commonly found in DNA-binding proteins, transcription factors and DNA-repair proteins (Kitchin, 2001; Kitchin and Wallace, 2005).

A common structural feature of DNA-binding proteins is the zinc finger. These small protein motifs contain finger-like protrusions that coordinate zinc which stabilizes the secondary structure of a protein. Certain zinc finger-containing proteins such as DNA ligase III, PARP-1 and XPA have been shown to be affected by arsenic exposure (Li and Rossman, 1989; Schwerdtle *et al.*, 2003a; Yager and Wiencke, 1997). Inhibition of enzyme activity by arsenic exposure could lead to spontaneous or induced mutations in key genetic sites leading to the possible development of cancer.

Data from our lab and our collaborators demonstrated arsenic interaction with the zinc finger domains of PARP-1. Using mass spectrometry, Ding et al. showed covalent binding of arsenite to an apopeptide of the PARP-1 zinc finger that could be reversed by addition of zinc (Ding *et al.*, 2009). In addition, zinc partially restored PARP activity and diminished the exacerbating effects of arsenite on DNA damage (Qin *et al.*, 2008a). The interaction between arsenite and the PARP-1 zinc finger was further examined in studies describing selectivity of arsenite for C3H1 and C4 zinc finger motifs (Zhou *et al.*, 2011). Several conclusions can be drawn from this series of studies: (1) arsenite is able to inhibit PARP activity in cells, (2) inhibition of PARP activity in combination with other damaging agents (H_2O_2 or UVR) can exacerbate DNA damage (8-OHdG or DNA strand breaks), and (3) arsenite is able to inhibit PARP-1 through binding to its zinc-finger domain. Overall, these data describe a molecular mechanism for arsenite inhibition of DNA repair pathways. An animal study to test the potential interaction between arsenite exposure and ultraviolet radiation was conducted to help confirm *in vitro* data surrounding a role for PARP-1 in NER.

4.2. Materials and Methods

Animal handling and treatments. SKH-1 mice (21-25 days old) were purchased from Charles River Laboratories (Wilmington, MA). Studies were performed under an approved Institutional Animal Care and Use Committee (IACUC) protocol (#09-100408-HSC). Animals were housed for seven days before start of treatments. All UVR exposures were whole body with no restraints. For dose response studies: Animals were exposed to varying doses of solar simulated ultraviolet radiation (ssUVR) [7 kJ/m^2 to 35 kJ/m^2] and all samples were collected one hour post exposure. For time course studies: Animals were given a single dose (28 kJ/m^2) of ssUVR. Following exposure, animals were returned to their cages and samples collected at the appropriate time points post exposure. For acute UVR exposure studies after arsenic treatment: Animals were housed by treatment group and administered sodium arsenite (5 mg/l), zinc chloride (10 mg/l), both or neither in the drinking water for 28 days. Water was changed every other day, consumption monitored and volumes compared to untreated control animals to ensure equivalent water consumption (data not shown). Controls and treated animals were provided standard mouse chow *ad lib*. Animals randomly selected from each treatment group were then exposed to a single dose (28 kJ/m^2), 1.2 minimum erythema dose (MED) of ssUVR, then euthanized 30 minutes post exposure. This time point was established in preliminary studies and reflects a time point leading to significant, but not maximal, levels of DNA damage (data not shown). For all studies: the irradiated and UVR naïve dorsal skin was collected, preserved in 10% neutral buffered formalin and paraffin blocks were prepared using standard procedures.

Immunohistochemistry (IHC). Paraffin embedded tissue was sectioned using a rotary microtome (Microm HM315) at a thickness of 10 μm. For staining, slides were deparaffinized with three exchanges of xylene (ten minutes each) followed by a one minute exchange in absolute ethanol. Sections were rehydrated by sequential one minute immersions in 95%, 75%, and 50% ethanol followed by five minutes in water. Slides were then placed in a 1:10 dilution of H_2O_2 and methanol for twenty minutes. A DNA unwinding step was performed using 0.125% trypsin for ten minutes at room temperature, followed by three rinses with 1X phosphate-buffered saline (PBS). Slides were then placed in 1N HCl for thirtry minutes at room temperature and subsequently rinsed with 1X PBS. Slides were blocked in 5% BSA containing 10% goat serum for ten minutes, then incubated with anti-CPD antibody (Thymine clone KTM53; Kamiya Biomedical) at 1:250 dilution or poly(ADP) ribose [PAR] (Alexis Biochemicals) at 1:100 dilution overnight followed by anti-mouse secondary antibody conjugated to Cy3 (Chemicom) at 1:200 for one hour. Slides were mounted with VectaShield plus DAPI (Vector Laboratories) and images were collected on a Zeiss LSM-510 META confocal microscope using a 40x objective. A minimum of four images per section were taken and the number of stained nuclei were counted and divided by the total number of nuclei in each image to give the percentage of stained cells.

Western blotting. After sacrifice, dorsal skin was collected from irradiated and UVR naïve mice. The collected skin sample was immediately placed flat, dermis side down, on a metal block surrounded by dry ice in order to freeze the skin. The sample was then scraped with the edge of a dissecting blade and the removed epidermis was place into an eppendorf tube containing PARP lysis buffer (20mM Tris base (pH 7.5), 1mM

EDTA, 1mM EGTA, 1% triton X-100, 25mM sodium pyrophosphate, 1mM β-glcycerol phosphate, 1mM sodium vanadate, 1µg/ml leupeptin and 2mM PMSF) or RIPA buffer (0.01 M Tris-HCl (pH 8.0), 0.14M NaCl, 1% Triton X-100, 0.1% deoxycholate, 1% sodium dodecyl sulfate [SDS], 1mM sodium vanadate, 1µg/ml leupeptin and 2mM PMSF). Tubes containing tissue samples were placed on dry ice and transferred to a -80^{o}C freezer. Before use, samples were allowed to defrost and were then sonicated on ice using a Branson Sonifer (Output 5, Duty 40%) for two minutes and clarified by centrifugation at 20,000 x g. Samples were transferred to a new eppendorf tube, being careful not to transfer non-dermal portions. Protein concentrations were obtained using the BCA Protein Assay (Thermo Scientific). 10 µg of protein in loading buffer (3x, 187.5mM Tris-HCl, pH 6.8, 6% w/v SDS, 30% glycerol, 150mM DTT and 0.03% (w/v) bromophenol blue) was heated at 100^{o}C for 5 minutes, resolved on a 10% SDS-polyacrylimide gel and transferred to a nitrocellulose membrane. Anti-PAR antibody (Alexis Biochemcials) was used at a 1:100 dilution. Band signal intensity was obtained using a Kodak 440CF Imager Digital Science Image Station. To control sample loading and protein transfer, membranes were stripped and re-probed to detect GAPDH (Millipore, 1:300 dilution).

Statistics. All graphs and statistical data were completed using GraphPad Prism 5 (GraphPad Software Inc., CA). Analysis used: Two-way ANOVA analysis followed by Bonferroni's correction.

4.3. Results

DNA damage and PARP activation in mouse skin following exposure to ssUVR. With the end goal of obtaining *in vivo* results on the actions of combined arsenite and UVR exposure, the appropriate ssUVR dose and time frames for PARP activation and

DNA damage needed to be obtained. Dose response experiments were performed with SKH-1 hairless mice. Mice were exposed to varying doses of ssUVR and dorsal skin was collected one hour post exposure. Subsequently, immunohistochemistry was performed on skin removed from irradiated or UVR naive mice. PARP activation was detected using specific antibodies against PAR. Colocalization was observed between PAR and DAPI stained nuclei at doses of 7 kJ/m^2 or greater (Fig. 4.1A, merge; white arrows). Additionally, levels of direct DNA damage were investigated using specific antibodies against CPDs. Increased lesion formation was clearly seen at doses of 28 kJ/m^2 or higher (Fig. 4.1B, merge, white arrows). From these results a dose of 28 kJ/m^2 was selected for time course experiments.

PARP activation and CPD formation are maximal at early times post UVR exposure. Once a UVR dose was established, a time point for PARP activation and DNA damage formation was determined. Mice were exposed to a single dose of ssUVR and dorsal skin was collected at multiple time points (0-48 h) post UVR exposure. PARP activation was determined by PAR staining. Colocalization between PAR and DAPI stained nuclei was seen at early time points post exposure (30m and 1h) and appeared to remain elevated four hours post exposure (Fig. 4.2, merge). These results regarding PARP activation are similar to previously published results in cellular systems following UVB exposure (Vodenicharov *et al.*, 2005). CPD stained nuclei were observed one hour post exposure and remained present at 24 hours post exposure. The majority of CPDs were removed by 48 hours post UVR exposure (Fig. 4.3). These results are consistent with data in the literature regarding CPD formation and repair in SKH-1 mouse skin

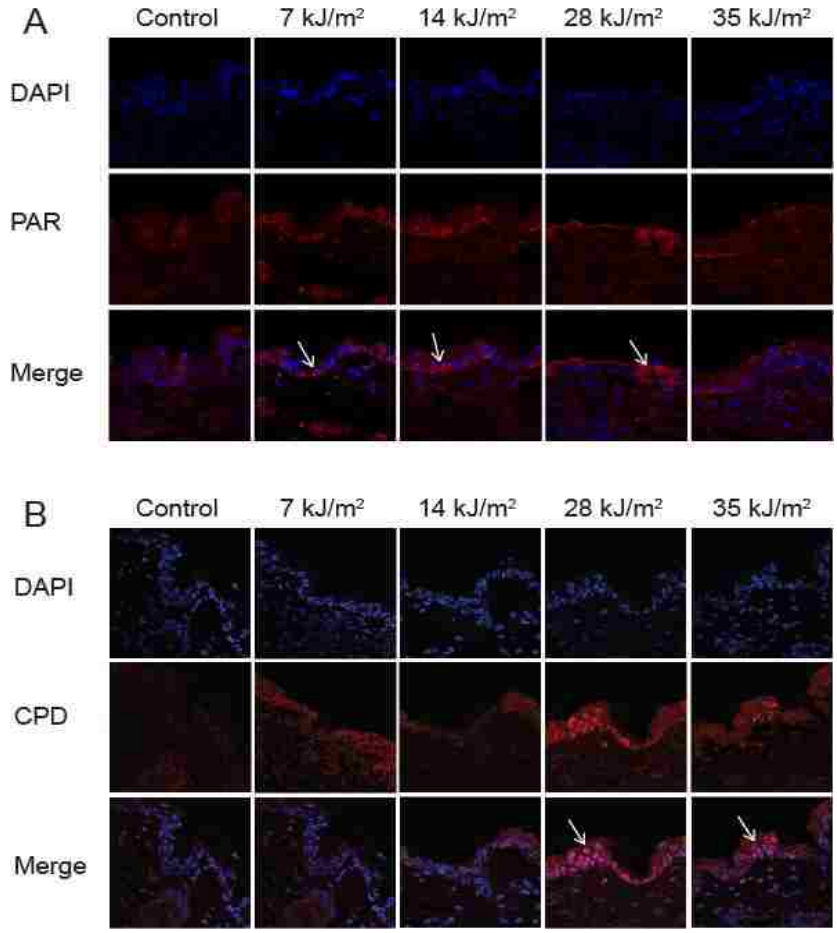

FIGURE 4.1 **PARP activation and UVR-induced DNA damage following varying concentrations of ssUVR.** SKH-1 mice were exposed to varying concentrations of solar-simulated ultraviolet radiation (ssUVR) and subsequently collected one hour post UVR exposure. Dorsal skin was collected, paraffin embedded and IHC was performed. *A,* Staining for PAR to evaluate changes in PARP activation following UVR exposure. Cell nuclei are in blue (DAPI), PAR (red) and areas where the two overlap can be seen in purple (Merge). *B,* Staining for CPDs to assess the amount of UV-induced DNA damage following UVR exposure. Cell nuclei are in blue (DAPI), CPD (red) and areas where the two overlap can be seen in purple (Merge). White areas indicate areas of colocalization.

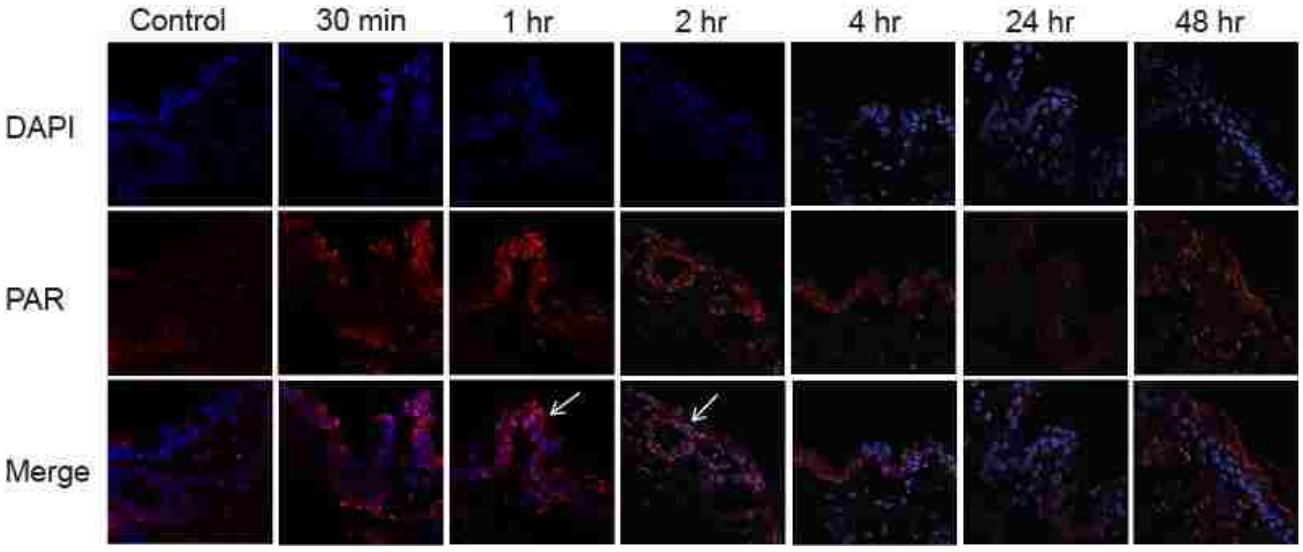

FIGURE 4.2 **Time course of PARP activation following ssUVR exposure.** SKH-1 mice were exposed to a single dose of ssUVR (28 kJ/m^2) and euthanized at the indicated times post UVR exposure. Dorsal skin was collected, paraffin embedded and IHC was performed. Samples were stained for PAR to observe PARP activation following UVR exposure. Cell nuclei are in blue (DAPI), PAR (red) and areas where the two overlap can be seen in purple (Merge). White arrows indicate areas of colocalization.

following UVR exposure (Lu *et al.*, 1999). From these studies a dose of 28 kJ/m^2 and a time point at 30 minutes post UVR exposure were used for the acute arsenite studies.

Dual exposure to arsenite and ssUVR results in increased retention of UVR-induced DNA damage. Using the UVR dose and time point parameters obtained from preliminary experiments, SKH-1 mice were exposed to 5 mg/l of sodium arsenite in their drinking water for 28 days. On the last day of arsenite exposure, mice were exposed to a single dose of ssUVR (28 kJ/m^2) and dorsal skin was collected 30 minutes post UVR exposure. Changes in UVR-induced DNA damaged were observed by using specific antibodies for CPDs. As expected, animals exposed to UVR alone had an increased number of CPD stained cells when compared to unexposed mice (Fig. 4.4A and 4.4B, UV only). Animals given sodium arsenite in their drinking water followed by ssUVR had an increased number of CPD stained cells compared to UVR exposure alone, suggesting retention of CPDs upon arsenite exposure (Fig, 4.4A and 4.4B, As+UV). These results complement cellular studies regarding delayed repair of CPDs following co-exposure of arsenite and UVR (Ding *et al.*, 2008).

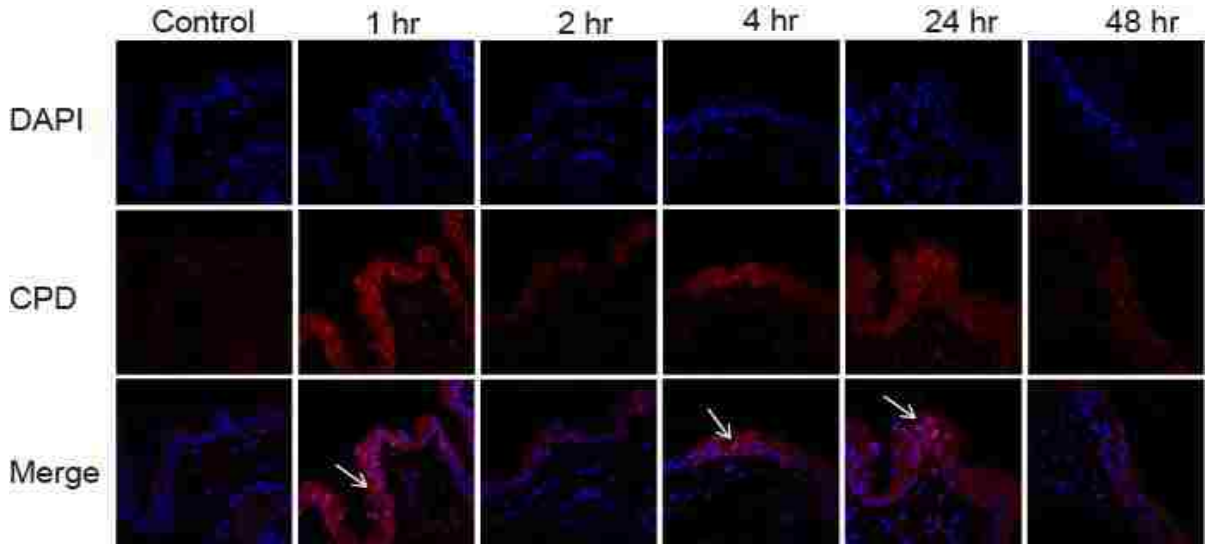

FIGURE 4.3 **Time course of UVR-induced DNA damage following ssUVR exposure.** SKH-1 mice were exposed to a single dose of ssUVR (28 kJ/m^2) and euthanized at various times post UV exposure. Dorsal skin was collected, paraffin embedded and IHC was performed. Samples were stained for CPDs to observe UVR-induced DNA damage following UVR exposure. Cell nuclei are in blue (DAPI), CPD (red) and areas where the two overlap can be seen in purple (Merge). White arrows indicate areas of colocalization.

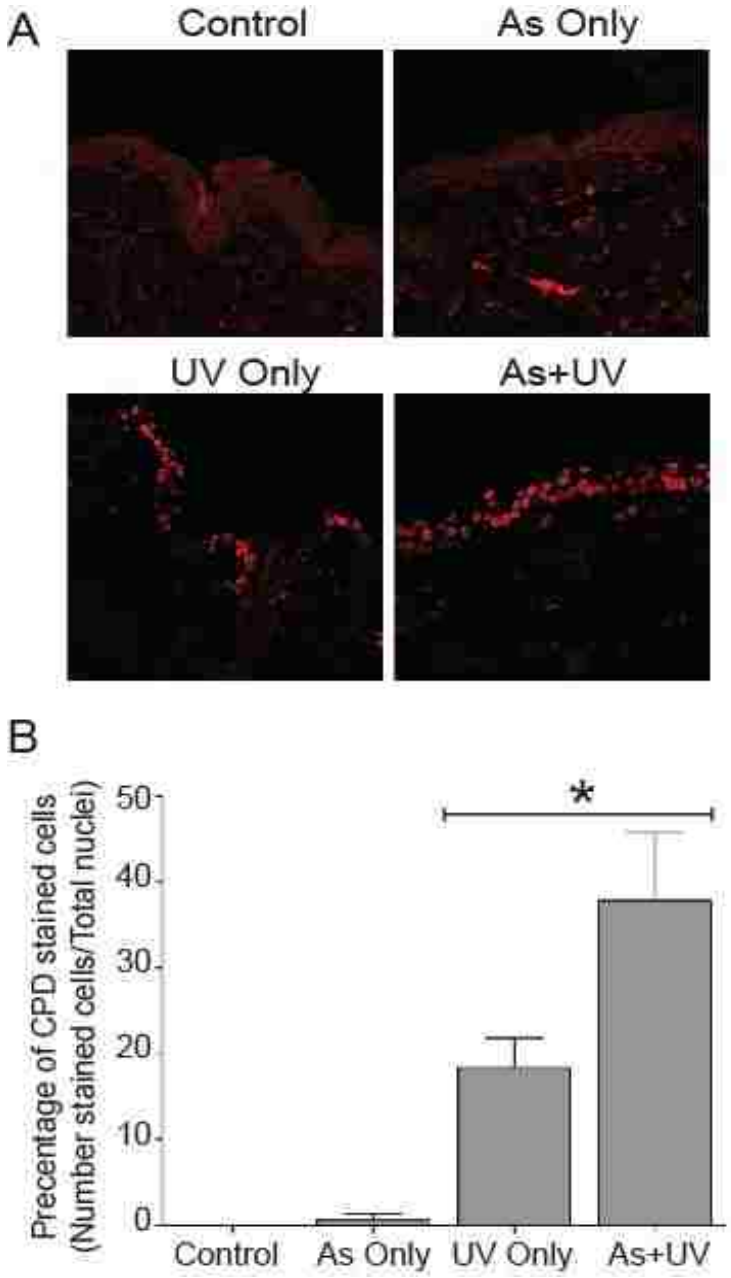

FIGURE 4.4 **Co-exposure of arsenite and UVR results in retention of UVR-induced DNA damage.** SKH-1 mice were exposed to 5 mg/l of sodium arsenite in their drinking water for 28 days. Mice where there exposure to a single dose of ssUVR (28 kJ/m^2). Dorsal skin was collected 30 minutes post UVR exposure, paraffin embedded and the amount of UVR-induced DNA damage was observed by performing IHC with antibodies against CPDs. *A,* Representative image of CPD stained cells [red nuclei]) for each treatment group. *B,* Quantification of CPD staining for each treatment group. The number of CPD stained cells was divided by the total number of cells in the image (DAPI stain, not shown) to obtain percentage of stained cells. n=5 animals. *$p < 0.05$

Arsenite inhibits in vivo PARP activation. Arsenic interferes with the activity of important DNA repair enzymes (Li and Rossman, 1989; Lynn *et al.*, 1997). More specifically, arsenite inhibits the activity of PARP-1 (Ding *et al.*, 2009; Hartwig *et al.*, 2003; Qin *et al.*, 2008a; Qin *et al.*, 2008b; Yager and Wiencke, 1997). This inhibition could provide a mechanistic link to explain the observed lesion retention under conditions where mice were co-exposed to arsenite and ssUVR. Protein samples were collected from dorsal skin of irradiated and UVR naïve mice. Proteins were separated on a polyacrylaminde gel and subsequently probed for PAR as a marker for PARP activation. Decreased PAR formation was observed in animals co-exposed to arsenite and UVR when compared to animals exposed to UVR alone (Fig. 4.5). This suggests *in vivo* inhibition of PARP activity following exposure to arsenite.

Zinc supplementation can counteract the effects of arsenite exposure. Co-exposure of arsenite and zinc results in counteraction of the inhibitory effects of arsenite on PARP activity and DNA repair in cells (Qin *et al.*, 2008a; Qin *et al.*, 2008b). To investigate this observation *in vivo*, SKH-1 hairless mice were exposed to 10 mg/l zinc chloride in their drinking water either alone or in combination with sodium arsenite. Mice were subsequently given a single dose of ssUVR and direct DNA damage was measured by quantification of CPD stained nuclei. Mice that were co-exposed to arsenite and zinc in their drinking water had a comparable number of CPD stained nuclei then mice exposed to UV alone (Fig. 4.6 As+Zn+UV compared to Fig.4.4 UV only). This was a significant reduction compared to mice exposed to a combination of arsenite and UV, which display an increased number of CPD stained cells when compared to UV alone (Fig. 4.6 As+UV compared to As+Zn+UV).

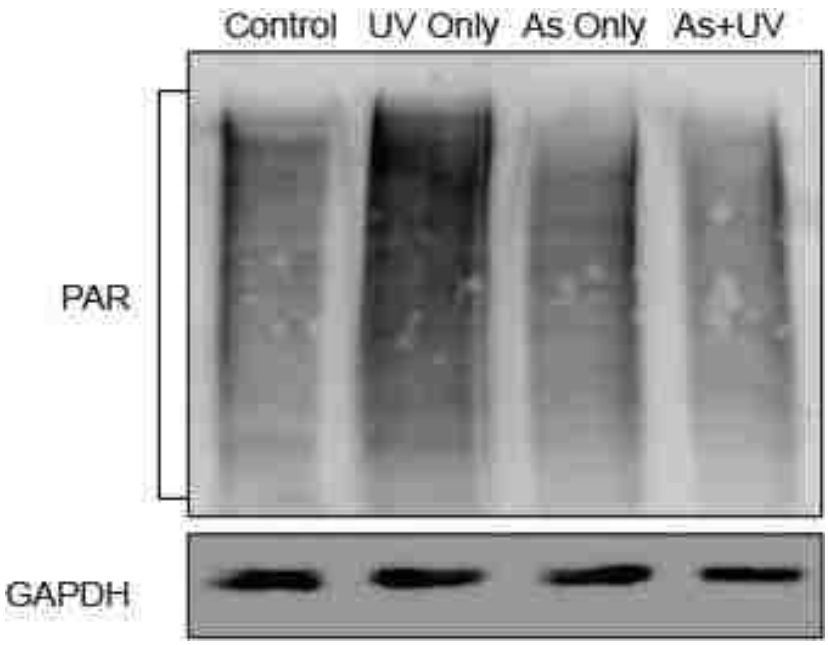

FIGURE 4.5 **Exposure to arsenite is able to inhibit *in vivo* PARP activity.** SKH-1 mice were exposed to 5 mg/l of sodium arsenite in their drinking water for 28 days. Mice where there exposure to a single dose of ssUVR (28 kJ/m^2). Dorsal skin was collected 30 minutes post UVR exposure and epidermal protein was collected as described in Materials and Methods. Proteins were separated on a polyacrylaminde gel and probed for PAR in order to observe changes in PARP activity. GAPDH was used as a loading control.

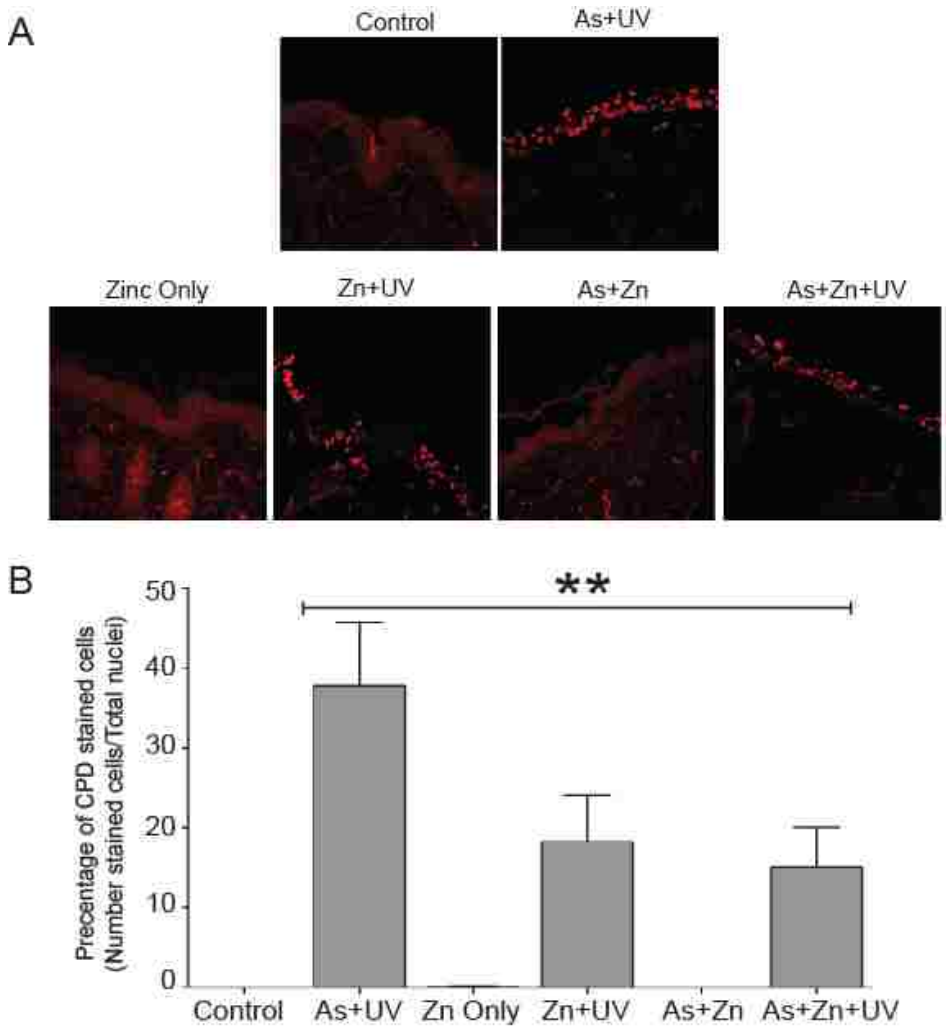

FIGURE 4.6 **Zinc supplementation is able to restore the deleterious effects of arsenic exposure.** SKH-1 mice were exposed to 5 mg/l of sodium arsenite, 10 mg/l of zinc chloride or a combination of both in their drinking water for 28 days. Mice where then exposed to a single dose of ssUVR (28 kJ/m^2). Dorsal skin was collected 30 minutes post UVR exposure, paraffin embedded and the amount of UV-induced DNA damage was observed by performing IHC with antibodies against CPDs. *A,* Representative image of CPD stained cells [red nuclei]) for the indicated treatment groups. *B,* Quantification of CPD staining for all treatment groups. The number of CPD stained cells was divided by the total number of cells in the image (DAPI stain, not shown) to obtain percentage of stained cells. n=5 animals. **$p < 0.01$

This data confirms cellular results regarding the ability of zinc to counter effects of arsenite exposure *in vivo*.

4.4. Discussion

Arsenic is defined as a class I human carcinogen (Martinez *et al.*, 2011b) but its mechanism of action remains under investigation. Many modes of action for arsenic carcinogenesis have been identified, in particular its ability to act as a co-carcinogen (Rossman *et al.*, 2004; Yu *et al.*, 2006). Arsenic inhibits proteins involved in BER and single strand break repair (SSBR) but its effects in NER are under studied. Early reports concluded that arsenite exposure creates partially repair-deficient conditions by impairing the incision step in NER (Hartwig *et al.*, 1997). Additionally, co-exposure of arsenite and UVR resulted in increased mutagenicity in a human lymphoblast cell line (Danaee *et al.*, 2004). SKH-1 mice exposed to arsenic for 28 days and exposed to a single dose of ssUVR retained more CPDs one hour post exposure then mice exposed to UVR alone (Fig.4.4) suggesting arsenite exposure can effect CPD formation and/or repair in an *in vivo* system. These results are similar to those obtained *in vitro* (Ding *et al.*, 2008). Very few studies have investigated arsenic's ability to affect specific proteins in NER.

PARP-1 is a DNA repair protein known to be involved in BER and SSBR (Woodhouse and Dianov, 2008). While the role of PARP-1 in NER is still under investigation, several studies show decreases in PARP activity result in retention of UVR-induced photoproducts such as 6-4 PPs and CPDs (Flohr *et al.*, 2003; Ghodgaonkar *et al.*, 2008) and (Chapter 2, Figure 2.1). Arsenic inhibits PARP activity following exposure to H_2O_2 and UVR exposure *in vitro* (Qin *et al.*, 2008a; Qin *et al.*, 2008b; Walter *et al.*, 2007). To our knowledge, there is no data showing inhibition of PARP activity by

arsenite *in vivo*. Using protein obtained from dorsal skin of mice exposed to arsenite alone, UVR alone, or a combination of both, we observed decreased PARP activity in mice co-exposed to arsenite and UVR (Fig. 4.5). This data suggests that lesion retention following co-exposure to arsenite and UVR may, in part, be due to inhibition of important DNA repair proteins such as PARP-1. Additionally, I am currently investigating the association of PARP-1 with NER proteins such as XPA and XPC. Inhibition of PARP activity decreases the association between PARP-1 and XPA (Chapter 2) and PARP-1 and XPC (Chapter 3). It is possible that *in vitro* experiments translate *in vivo* and UVR-induced photoproduct retention is a result of arsenite inhibition of PARP activity and decreased association with important NER proteins.

While data suggests inhibition of DNA repair through decreased PARP function, there is also the possibility of direct inhibition of established NER proteins by arsenite exposure. Nollan et al. showed decreases in XPC protein level as well as decreased accumulation of XPC at damaged sites following 24 hour incubation with sodium arsenite in human skin fibroblasts. They suggest the decreases in XPC protein is most likely due to inhibition of XPC gene expression by arsenite (Nollen *et al.*, 2009). Additionally, several studies have investigated arsenic's effects on XPA. Trivalent arsenicals release zinc from a synthetic peptide based on the zinc finger region of XPA (Beyersmann and Hartwig, 2008; Kitchin and Wallace, 2008). This data has recently been complemented with studies showing arsenite selectivity for C4 zinc fingers, such as the one found in XPA, leading to zinc loss and disruption in protein activity (Zhou *et al.*, 2011). These studies show that arsenic's ability to affect UVR-induced photoproducts involves several mechanisms. Lastly, the effects observed by arsenite exposure appear to

be partially reversible. Co-exposure of arsenite and zinc results in decreased retention of UVR-induced CPDs. *In vitro* and cellular studies show zinc is able to reduce the effects of arsenite-induced oxidative or direct damage (Qin *et al.*, 2008a; Qin *et al.*, 2008b) and (Cooper et al. unpublished).These results are most likely due to partially restored function of the zinc finger domains found in PARP-1which are essential for DNA damage recognition. Overall, this data suggests the results obtained *in vitro* and in cellular systems occur *in vivo*.

CHAPTER 5

5. Discussion and Future directions

PARP-1 is an enzyme with many functions throughout the cell. To date, its best understood functions in DNA repair pathways have been centered on base excision repair (BER). The data presented in this dissertation expands the knowledge on the role of PARP in an additional arm in DNA repair, nucleotide excision repair (NER). Currently, there is limited information regarding PARP's mechanism of action in NER.

Ghodgaonkar et al. and Flohr et al. suggest a cooperative interaction between PARP and CSB in repair mechanisms following UVR exposure (Flohr *et al.*, 2003; Ghodgaonkar *et al.*, 2008). CSB is involved in the transcription coupled-repair (TC-NER) arm of NER. Following stalling of RNA polymerase II, CSB is proposed to assist in the assembly of repair factors (Fousteri and Mullenders, 2008; Rastogi *et al.*, 2010). In contrast, the XP family members are associated with global genomic repair (GG-NER) and the steps common to both TC-NER and GG-NER. My findings provide strong evidence that PARP is also involved in GG-NER through interactions with XPC and XPA (Fig. 5.1).

Following UVR exposure, there is rapid activation of PARP-1 leading to the formation of poly(ADP-ribose) [PAR]. Within this timeframe of PARP activation we show PAR-enhanced association with NER proteins. Using co-immunoprecipitations of endogenous proteins from cell lysates we observed UVR-enhanced associations between PARP-1 and XPA as well as PARP-1 and XPC. A modified chromatin immunoprecipitation method allowed us to monitor interactions of chromatin-associated NER proteins. Within this environment, we again found UVR-enhanced associations

between PARP-1 and XPA and PARP-1 and XPC. Due to the presence of a PAR-binding motif within their sequences, both XPA and XPC have been identified as potential PAR-associated proteins (Gagne *et al.*, 2008; Pleschke *et al.*, 2000).

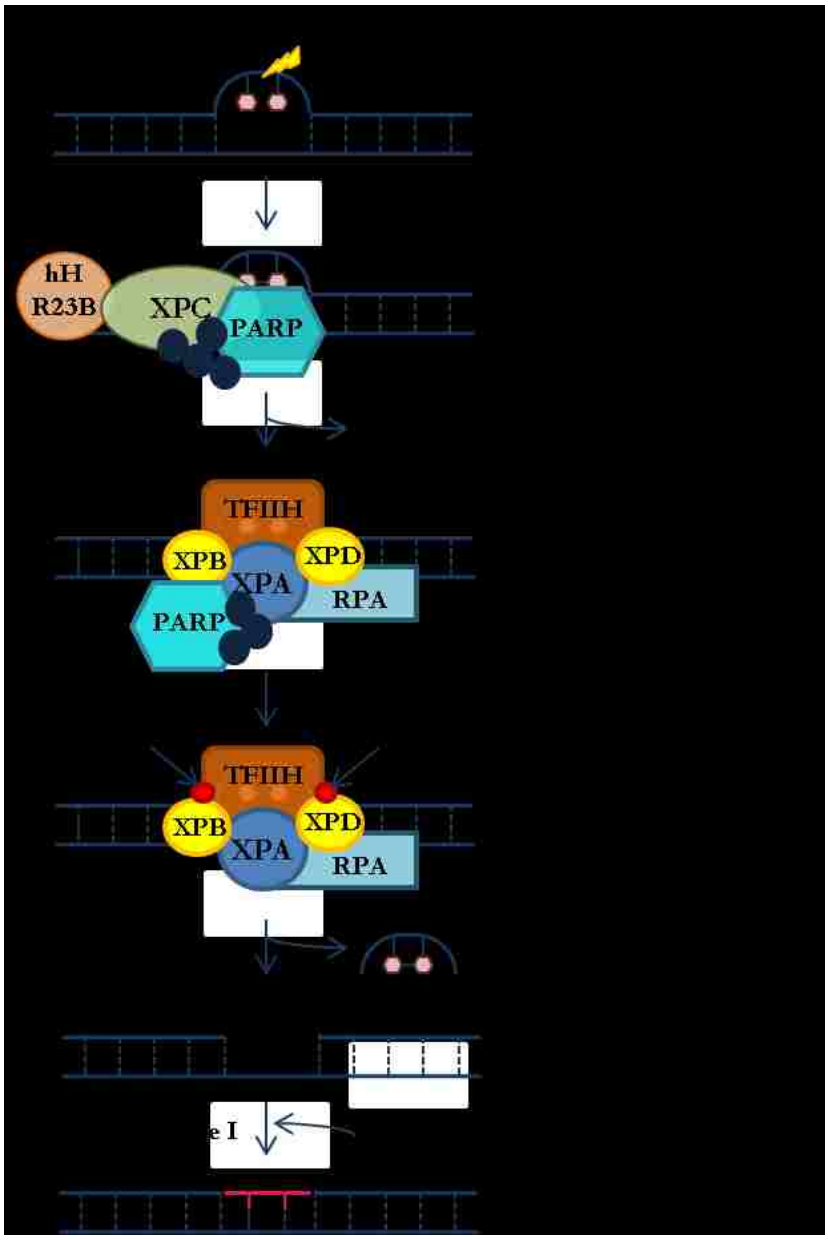

FIGURE 5.1. **Schematic illustrating potential role of PARP-1 in NER.** Following UVR exposure PARP activity is increased leading to the formation of PAR which allows PARP-1 to associate with important NER proteins such as XPC and XPA.

The importance of PAR in mediating interactions was demonstrated using PARP inhibitors where decrease PAR production led to decreased associations between XPA and XPC with PARP-1. Co-immunoprecipitations with PARP-1 and XPF, another XP protein in NER with no known PAR-binding motif, did not show UVR-enhanced association and PARP inhibition had no significant effect on the interaction between these proteins. These results not only demonstrate the importance of PAR within NER but also the PAR-binding sequence which can aid in selectivity for PARP-1 associations with NER proteins.

XPC and XPA are crucial for two distinct roles in NER (Fig. 1.2). XPC enters the damaged site early and is involved in lesion recognition. Once the DNA is unwound and open, XPA enters the damaged area and assists in binding to various proteins within NER. The ability of PAR to interact with two important NER proteins such as XPC and XPA leads to further questions on the potential contributions of PARP to NER.

5.1. XPC: Potential for PARP activity in lesion recognition

XPC is a central protein in lesion recognition within NER. While there is ample information surrounding the types of lesions bound by XPC and the timing for XPC lesion recognition (Hoogstraten *et al.*, 2008; Rechkunova *et al.*, 2011), the mechanism by which XPC locates a lesion within the vastness of undamaged DNA is not clear (Rastogi *et al.*, 2010). PARP activation could assist at this stage in the repair process. Following UVR exposure, PARP becomes active generating PAR as early as 15 seconds post exposure and peaking around 5 minutes (Vodenicharov *et al.*, 2005). This time frame corresponds to XPC entry to the damaged area (Hoogstraten *et al.*, 2008). It is possible that PAR production following PARP activation could act in two ways. In one scenario,

PARP-1 binding to damaged DNA and formation of PAR leads to recruitment of XPC to the damaged site. Another possibility is that PARP and XPC enter the damaged area simultaneously and PAR helps stabilize XPC binding to DNA during lesion recognition. An experimental approach to further investigate this step would be to perform live cell imaging using fluorescence recovery after photobleaching (FRAP). Recently, Hoogstraten et al. used this method to gain insight into XPC mobility following cell exposure to DNA damaging agents (Hoogstraten *et al.*, 2008). Similar experiments that monitor XPC mobility could be conducted using GFP-XPC under normal conditions and under conditions where PARP activity was inhibited. The use of FRAP is advantageous because it allows one to investigate actions of proteins seconds after insult. Monitoring these very early events will be crucial to further understanding PAR/PARP-1 contributions to the entrance of proteins into a damaged area.

5.2. XPA: Potential for PARP activity in complex stability

While XPA shows affinity for damaged DNA it is not recruited to DNA lesions without prior recognition of the damage by XPC (Volker *et al.*, 2001). Thus, a DNA verification function has been proposed for XPA's DNA binding ability (Camenisch *et al.*, 2006; Sugasawa *et al.*, 1998). It is thought that following initial recognition by XPC, binding of XPA helps to confirm the lesion is an NER substrate, thereby leading to a higher degree of damage discrimination (Sugasawa *et al.*, 1998). Our studies show that inhibition of PARP activity leads to decreased binding of XPA to chromatin (Chapter 2). Loss of XPA binding could decrease repair of UV-induced photoproducts and lead to increased cell sensitivity to DNA damage. It is possible that PAR helps to stabilize XPA binding. To further investigate the affects of PARP activity on XPA binding,

electrophoretic mobility shift assays (EMSA) could be conducted with XPA specific substrates under conditions of increased or decreased PARP activity. Additionally, an EMSA to help determine if binding of PARP-1 protein has an effect on XPA binding independent of its activity. It is also possible that PAR enhances the interaction between XPA and other NER proteins, in this case acting as a scaffold with NER.

5.3. PARP activity as a scaffold in NER

One important implication of this work is that PARP activation and PAR production may play a more extensive role in assembly of DNA repair complexes than previously understood. The data presented in this dissertation supports the hypothesis that PARP-1 activation modulates NER, at least in part, through interactions between PARP-1 and important NER proteins through a PAR-binding motif. Currently there are three known PAR binding motifs (Gagne *et al.*, 2008); the most studied being the 25 amino acid PAR-binding consensus sequence found within proteins such as XPA (Pleschke *et al.*, 2000). Gagne et al. conducted a proteome-wide search for PAR-associated proteins using this 25 amino acid consensus sequence and found more than 300 potential PAR-associated proteins (Gagne *et al.*, 2008). XPC was on the list of potential candidates along with DNA binding protein 1 (DDB1). While our data supports the functionality of the predicted PAR-binding motif in XPC, overall, the data only provides a snapshot of NER proteins that might interact with PARP-1. Additionally, our data suggests it is likely that PARP activation will be important for assembly of multi-protein DNA repair complexes.

As a first attempt to address this question, matrix-assisted laser desorption/ionization mass spectrometry (MALDI-MS) followed by tandem mass

spectrometry was employed to identify additional PARP-1 interacting NER proteins. The experiment was to also serve as verification for PARP-1 interaction with both XPA and XPC. The experimental design was to conduct ChIP-on-western experiments on control or UVR-exposed HEK 293 cells using PARP-1 specific antibodies. Analysis of the resulting immunoprecipitates identified a PARP-1 peak as expected; while proteins such as mono-ADP-ribosyltransferase 3 (ART3) were detected, no NER proteins were identified. It is possible that the strong intensity of the PARP-1 peak made it difficult to identify low abundance proteins in the samples or that the MALDI-MS method is not sufficiently sensitive for our purposes. Future studies would need to involve liquid chromatography mass spectrometry in addition to MADLI-MS followed by tandem mass spectrometry (LC-MALDI MS and MS/MS). Initial separation of proteins using LC increases sensitivity and selectivity when compared to MALDI alone. Because the goal is to identify endogenous proteins bound to chromatin following DNA damage, it is likely that the increased sensitivity of LC-MALDI MS would be needed to help capture many of the low abundant NER proteins in the complex. It is hoped that these future experiments would help to construct a more detailed view of PARP-1's role in NER.

5.4. Significance

Gaining a more complete understanding of PARP-1 in DNA repair pathways has broad implications. Currently, PARP's function in BER is being utilized to treat cancer. More specifically, PARP inhibitors are being used to act as sensitizers to DNA damaging chemotherapy or radiation (Telli and Ford, 2010; Tentori *et al.*, 2002). PARP inhibitors show enhanced chemopotentiation when used in combination with methylating agents (i.e. temozolomide, TZM) and topoisomerase inhibitors (Drew and Plummer, 2009;

Megnin-Chanet *et al.*, 2010). Additionally, they show enhanced cytotoxcity when in combination with radiotherapies (Dungey *et al.*, 2008; Megnin-Chanet *et al.*, 2010).

Another strategy for the use of PARP inhibitors is in genetically susceptible cells. In this case, cell populations that already harbor altered DNA repair pathways in combination with PARP inhibitors result in synthetic lethality, where loss of function of two genes leads to cell death. This is a common strategy in cells with BRAC1 and BRAC2 mutations. These cells have defective homologous recombination (HR) pathways. When a PARP inhibitor is administered the repair of endogenous single-strand breaks (SSBs) is decreased leading to persistent SSBs which are converted to double strand breaks (DSBs) at replication forks. Cells with functioning HR can repair the breaks and survive, but BRCA1/BRAC2 deficient cells cannot repair the DSBs and are susceptible to the lethality of PARP inhibitors (Helleday, 2011; Kummar *et al.*, 2012; Ratner *et al.*, 2012; Telli and Ford, 2010). This use of PARP inhibitors takes advantage of PARP's role in BER.

Based on the novel results presented in this dissertation there is the potential for therapeutic application of PARP function in NER. Ideally, this new information could be useful with drugs and/or compounds known to cause damage repaired by NER. A class of potential candidates includes the numerous platinum (Pt)-based chemotherapeutics such as cisplatin, carboplatin and oxaliplatin. These drugs intercalate into the cell forming various DNA lesions which eventually inhibit DNA replication leading to cell death. There are three main lesions formed as a result of platinum exposure: monoadducts, intrastrand crosslinks and interstrand crosslinks. These lesions bend the DNA double helix toward the major groove creating bulky DNA lesions (Di Francesco *et al.*, 2002).

Platinum lesions can be recognized and repaired by NER, mismatch repair or homologous recombination (HR). Given the structure and ability of platinum lesions to distort the DNA helix and obstruct transcription and replication, NER is the most important repair pathway in the efficacy of platinum chemotherapy (Danford *et al.*, 2005; Rabik and Dolan, 2007). Administration of PARP inhibitors in combination with platinum drugs would be predicted to decrease lesion repair and increase DNA damage potentially leading to cell death.

In conclusion, the data presented throughout this dissertation advances the current knowledge regarding the contributions of PARP in NER. It not only provides a novel mechanism regarding interactions between PARP and important NER proteins but also showcases the importance of PAR in this pathway. As such, this data opens the door to possibly expand the knowledge and use of therapies involving PARP inhibition. More specifically, this work could have broad implication in cancer chemotherapy.

APPENDIX A: PARP inhibition and its effects on XPA nuclear localization

Introduction

UVR exposure has been reported to increase nuclear localization of XPA through a mobilized fraction of the protein (Shell *et al.*, 2009; Wu *et al.*, 2007). In an effort to observe this aspect of XPA function we investigated if there were any changes to its localization under conditions of PARP activation and PARP inhibition.

Results

Within our system, there was no change to total XPA (Fig. A.1A and A.1B) over a 6 hour time period following UVR, but there was a significant increase in nuclear XPA one hour post exposure (Fig. A.1D). This data was confirmed using colocalization techniques. Quantification of nuclear XPA showed a significant increase following exposure to UVR alone (Fig. A.2A, UV). A pharmacologic inhibitor of PARP, DPQ, was used to probe the impact of PARP activity on XPA localization. The observed UVR-induced increase in nuclear XPA was diminished in cells treated with DPQ (Fig. A.2A, DPQ+UV). Biochemical analysis of subcellular fractions obtained from cells exposed to UVR in the absence or presence of DPQ confirmed the results obtained by colocalization techniques (Fig. A.2B, UV and DPQ+UV). These findings illustrate that PARP activity may regulate nuclear localization of XPA.

Discussion

The data presented in Appendix B strengthens the results presented in Chapter 2, Fig. 2.7 which shows functional changes to XPA chromatin binding following PARP

inhibition. Overall, the combination of these data illustrate that PARP activity may be important in the regulation of NER proteins which could contribute to the retention of UVR-induced photolesions following PAPR inhibition.

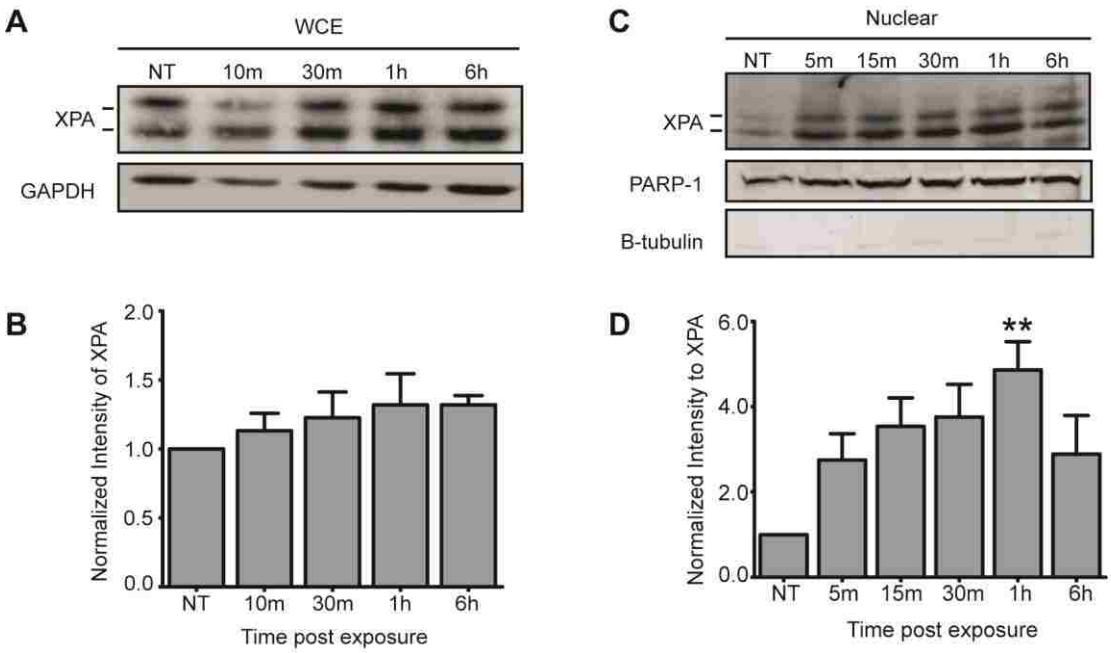

FIGURE A.1. **Changes in XPA localization following UVR exposure.** HaCaT cells were given a single dose of ssUVR (3 kJ/m^2) and whole cell extracts (WCE) were collected at various times post exposure. *A*, Representative western blot showing total XPA protein over time following UVR exposure. *B*, Quantification of (A) by densitometry. GAPDH was used as a loading control. XPA intensity was normalized to NT. Data presented as means ± SEM, n=6. HaCaT cells were given a single dose of ssUVR (3 kJ/m^2) and nuclear fractions were collected at various times post exposure. *C*, Representative western blot showing XPA in the nuclear fraction following UVR exposure. PARP-1 and β-tubulin were used as controls for nuclear and cytoplasmic fractions, respectively. *D*, Quantification of (C) by densitometry. XPA intensity was normalized to NT. Data presented as means ± SEM, n=4. **p<0.01.

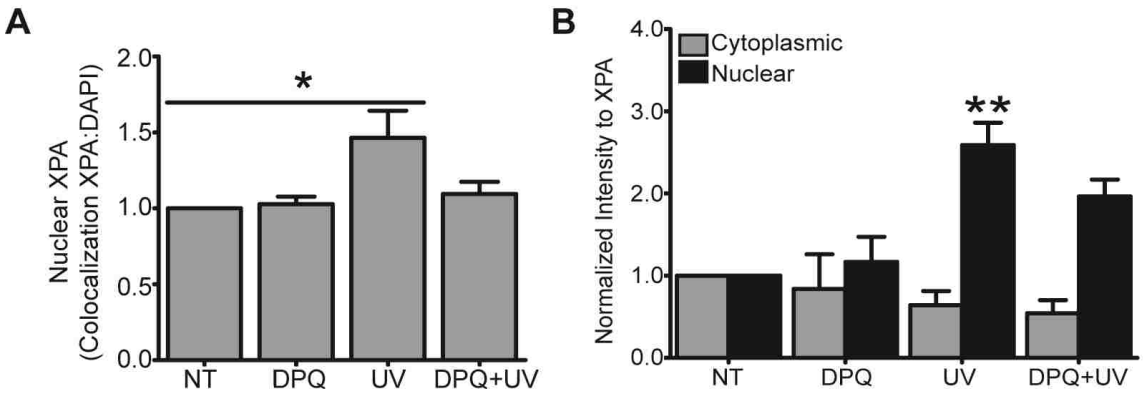

FIGURE A.2. **PARP inhibition and its effects on XPA nuclear localization.** HaCaT cells were pre-exposed to a PARP inhibitor, DPQ, 30 minutes prior to UVR exposure. They were subsequently fixed one hour post exposure. *A,* Graph representing quantification of fluorescent images where colocalization between XPA and DAPI (Nuclear XPA) were calculated. Data normalized to NT sample. Data presented as means ± SEM, n=4. Significance compared to NT. *B,* Graph representing XPA protein in nuclear and cytoplasmic fractions obtained from HaCaT cells. Data represents densitometry obtained from western blots. Data presented as means ± SEM, n=3. Significance compared to NT. * $p<0.05$, ** $p<0.01$.

APPENDIX B: PARP-1 and DDB1

Introduction

The paper published by Gagne et al. identified hundreds of proteins predicated to associate with PAR (Gagne *et al.*, 2008). From this report we investigated the protein XPC and found it to associate with PAR following UVR-exposure (Chapter 3, Fig. 3.1). Additionally, we were able to observe that XPC was part of a complex with automodified PARP-1 that is dependent on PAR formation (Chapter 3, Fig. 3.2). An additional NER protein identified within this paper was the DNA damage binding protein 1 (DDB1). DDB1 is associated with lesion recognition of both CPDs and 6-4 PPs (Sugasawa, 2009; Wakasugi *et al.*, 2002). In the case of CPDs, Sugasawa et al. and others have proposed a model where DDB binds first to CPDs and then recruits XPC to the damaged site (Fitch *et al.*, 2003; Sugasawa, 2006). This is important for CPD repair because they tend to distort the DNA helix less than 6-4 PPs (Rastogi *et al.*, 2010). A functional experiment within the Gagne et al. paper confirmed that DDB1 was able to be immunoprecipitated using antibodies specific to PAR (Gagne *et al.*, 2008). To expand on this data we investigated if DDB1 might form a complex with automodified PARP-1.

Results

HaCaT cells were exposed to UVR and whole cell extracts were collected at various times post exposure. Using these samples, antibodies specific to PARP-1 were used for immunoprecipitation. Co-immunoprecipitation methods were performed to see if there was an association between PARP-1 and DDB1 following UVR exposure. We observed a significant increase in the association between PARP-1 and DDB1 at all times post UVR-exposure (Fig. B.1A and B.1B). Similar to XPA (Chapter 2) and XPC

(Chapter 3) we wanted to investigate the importance of PAR formation in the association between PARP-1 and DDB1. We conducted experiments using the PARP inhibitor AG-014699 to reduce the levels of cellular PAR. We observed an increased association between DDB1 and PARP-1 five minutes post UVR-exposure (Fig. B.1D). Following PARP inhibition we did not see a significant change in association between PARP-1 and DDB1 as noted with other NER proteins (XPA and XPC). Overall, these data show that there is a UVR-induced increase in the association between PARP-1 and DDB1 but it may not rely on PAR formation.

Discussion

The data obtained for DDB1 differs from what we observed for XPA and XPC. The association between other NER proteins (XPA and XPC) and PARP-1 was found to be dependent on PAR formation. On the contrary, there was no change in DDB1 binding to PARP-1 following PARP inhibition. This may be due to the time point used. These experiments were performed five minutes post UVR-exposure. While Fig. B.1B showed a significant association at this time point, this data was not reproducible as seen in Fig. B.1D. Experiments performed 30 minutes post UVR-exposure may provide a better picture of the association between PARP-1 and DDB1. Additionally, this data could be indicating that there is a direct interaction between PARP-1 and DDB1 as opposed to a PAR-enhanced interaction. Additional biochemical experiments will need to be conducted to better understand the nature of the interaction between PARP-1 and DDB1.

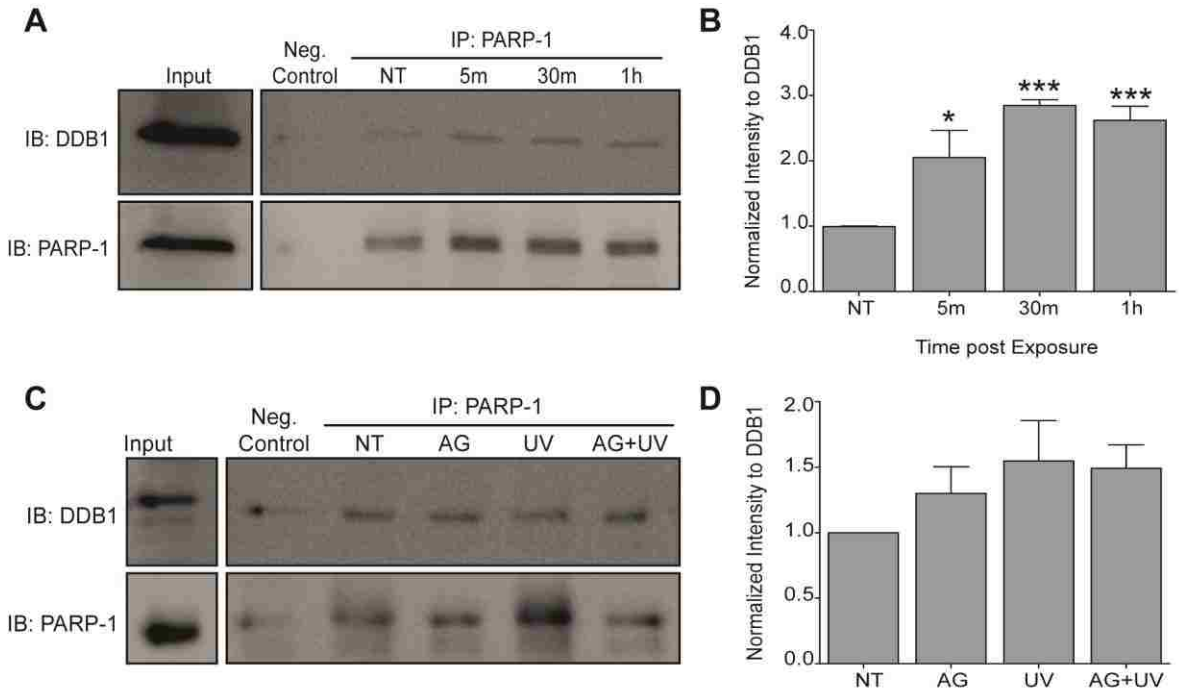

FIGURE B.1. **PARP inhibition does not affect the association between PARP-1 and DDB1.** HaCaT cells were given a single dose of ssUVR (3 kJ/m^2) and collected at various times post exposure. *A*, Representative image of co-immunoprecipitation. PARP-1 was immunoprecipitated (IP) from cells and membranes were subsequently immunoblotted (IB) for DDB1. Membranes were stripped and immunoblotted for PARP-1, as confirmation for immunoprecipitation. *B*, Quantification of DDB1 western blot from (A) by densitometry. Data presented as means ± SEM, n=4. *C*, HaCaT cells were pre-exposed to the PARP inhibitor, AG-014699, 1 hour prior to UVR exposure and collected five minutes post exposure. Representative image of co-immunoprecipitation. PARP-1 was immunoprecipitated (IP) from cells and membranes were subsequently immunoblotted (IB) for DDB1. *D*, Quantification of DDB1 western blot from (C) by densitometry. Data presented as means ± SEM, n=4. *$p < 0.05$. ***$p < 0.001$.

REFERENCES

Abernathy CO, Liu YP, Longfellow D, Aposhian HV, Beck B, Fowler B, *et al.* (1999) Arsenic: health effects, mechanisms of actions, and research issues. *Environ Health Perspect* 107:593-597.

Aboussekhra A, Biggerstaff M, Shivji MK, Vilpo JA, Moncollin V, Podust VN, *et al.* (1995) Mammalian DNA nucleotide excision repair reconstituted with purified protein components. *Cell* 80:859-868.

Ahel D, Horejsi Z, Wiechens N, Polo SE, Garcia-Wilson E, Ahel I, *et al.* (2009) Poly(ADP-ribose)-dependent regulation of DNA repair by the chromatin remodeling enzyme ALC1. *Science* 325:1240-1243.

Ahel I, Ahel D, Matsusaka T, Clark AJ, Pines J, Boulton SJ, *et al.* (2008) Poly(ADP-ribose)-binding zinc finger motifs in DNA repair/checkpoint proteins. *Nature* 451:81-85.

Alam M, Ratner D (2001) Cutaneous squamous-cell carcinoma. *N Engl J Med* 344:975-983.

Allinson SL, Dianova, II, Dianov GL (2003) Poly(ADP-ribose) polymerase in base excision repair: always engaged, but not essential for DNA damage processing. *Acta Biochim Pol* 50:169-179.

Almeida KH, Sobol RW (2007) A unified view of base excision repair: lesion-dependent protein complexes regulated by post-translational modification. *DNA Repair (Amst)* 6:695-711.

Alvarez-Gonzalez R, Jacobson MK (1987) Characterization of polymers of adenosine diphosphate ribose generated in vitro and in vivo. *Biochemistry* 26:3218-3224.

Ame JC, Rolli V, Schreiber V, Niedergang C, Apiou F, Decker P, *et al.* (1999) PARP-2, A novel mammalian DNA damage-dependent poly(ADP-ribose) polymerase. *J Biol Chem* 274:17860-17868.

Ame JC, Spenlehauer C, de Murcia G (2004) The PARP superfamily. *Bioessays* 26:882-893.

Andrabi SA, Dawson TM, Dawson VL (2008) Mitochondrial and nuclear cross talk in cell death: parthanatos. *Ann N Y Acad Sci* 1147:233-241.

Barchowsky A, Klei LR, Dudek EJ, Swartz HM, James PE (1999) Stimulation of reactive oxygen, but not reactive nitrogen species, in vascular endothelial cells exposed to low levels of arsenite. *Free Radic Biol Med* 27:1405-1412.

Barrett JC, Lamb PW, Wang TC, Lee TC (1989) Mechanisms of arsenic-induced cell transformation. *Biol Trace Elem Res* 21:421-429.

Bartels CL, Lambert MW (2007) Domains in the XPA protein important in its role as a processivity factor. *Biochem Biophys Res Commun* 356:219-225.

Batista LF, Kaina B, Meneghini R, Menck CF (2009) How DNA lesions are turned into powerful killing structures: insights from UV-induced apoptosis. *Mutat Res* 681:197-208.

Bergoglio V, Magnaldo T (2006) Nucleotide excision repair and related human diseases. *Genome Dyn* 1:35-52.

Besaratinia A, Kim SI, Pfeifer GP (2008) Rapid repair of UVA-induced oxidized purines and persistence of UVB-induced dipyrimidine lesions determine the mutagenicity of sunlight in mouse cells. *FASEB J* 22:2379-2392.

Beyersmann D, Hartwig A (2008) Carcinogenic metal compounds: recent insight into molecular and cellular mechanisms. *Arch Toxicol* 82:493-512.

Boehler C, Gauthier LR, Mortusewicz O, Biard DS, Saliou JM, Bresson A, *et al.* (2011) Poly(ADP-ribose) polymerase 3 (PARP3), a newcomer in cellular response to DNA damage and mitotic progression. *Proc Natl Acad Sci U S A* 108:2783-2788.

Bonicalzi ME, Haince JF, Droit A, Poirier GG (2005) Regulation of poly(ADP-ribose) metabolism by poly(ADP-ribose) glycohydrolase: where and when? *Cell Mol Life Sci* 62:739-750.

Bradford PT, Goldstein AM, Tamura D, Khan SG, Ueda T, Boyle J, *et al.* (2011) Cancer and neurologic degeneration in xeroderma pigmentosum: long term follow-up characterises the role of DNA repair. *J Med Genet* 48:168-176.

Bundschuh J, Litter MI, Parvez F, Roman-Ross G, Nicolli HB, Jean JS, *et al.* One century of arsenic exposure in Latin America: A review of history and occurrence from 14 countries. *Sci Total Environ* 429:2-35.

Burkle A (2001) Physiology and pathophysiology of poly(ADP-ribosyl)ation. *Bioessays* 23:795-806.

Burkle A (2005) Poly(ADP-ribose). The most elaborate metabolite of NAD+. *FEBS J* 272:4576-4589.

Cadet J, Sage E, Douki T (2005) Ultraviolet radiation-mediated damage to cellular DNA. *Mutat Res* 571:3-17.

Caldecott KW (2008) Single-strand break repair and genetic disease. *Nat Rev Genet* 9:619-631.

Caldecott KW, Aoufouchi S, Johnson P, Shall S (1996) XRCC1 polypeptide interacts with DNA polymerase beta and possibly poly (ADP-ribose) polymerase, and DNA ligase III is a novel molecular 'nick-sensor' in vitro. *Nucleic Acids Res* 24:4387-4394.

Caldecott KW, McKeown CK, Tucker JD, Ljungquist S, Thompson LH (1994) An interaction between the mammalian DNA repair protein XRCC1 and DNA ligase III. *Mol Cell Biol* 14:68-76.

Caldecott KW, Tucker JD, Stanker LH, Thompson LH (1995) Characterization of the XRCC1-DNA ligase III complex in vitro and its absence from mutant hamster cells. *Nucleic Acids Res* 23:4836-4843.

Callen JP, Bickers DR, Moy RL (1997) Actinic keratoses. *J Am Acad Dermatol* 36:650-653.

Camacho LM, Gutierrez M, Alarcon-Herrera MT, Villalba Mde L, Deng S (2011) Occurrence and treatment of arsenic in groundwater and soil in northern Mexico and southwestern USA. *Chemosphere* 83:211-225.

Camenisch U, Dip R, Schumacher SB, Schuler B, Naegeli H (2006) Recognition of helical kinks by xeroderma pigmentosum group A protein triggers DNA excision repair. *Nat Struct Mol Biol* 13:278-284.

Camenisch U, Nageli H (2008) XPA gene, its product and biological roles. *Adv Exp Med Biol* 637:28-38.

Charlier M, Helene C (1972) Photochemical reactions of aromatic ketones with nucleic acids and their components. I. Purine and pyrimidine bases and nucleosides. *Photochem Photobiol* 15:71-87.

Chen CJ, Hsu LI, Wang CH, Shih WL, Hsu YH, Tseng MP, *et al.* (2005) Biomarkers of exposure, effect, and susceptibility of arsenic-induced health hazards in Taiwan. *Toxicol Appl Pharmacol* 206:198-206.

Chinem VP, Miot HA (2011) Epidemiology of basal cell carcinoma. *An Bras Dermatol* 86:292-305.

Clark NJ, Kramer MA, Muthurajan UM, Luger K (2012) Alternative binding modes of Poly (ADP-ribose) Polymerase 1 to free DNA and nucleosomes. *J Biol Chem*.

Clayton E, Doupe DP, Klein AM, Winton DJ, Simons BD, Jones PH (2007) A single type of progenitor cell maintains normal epidermis. *Nature* 446:185-189.

Cooper KL, Liu KJ, Hudson LG (2007) Contributions of reactive oxygen species and mitogen-activated protein kinase signaling in arsenite-stimulated hemeoxygenase-1 production. *Toxicol Appl Pharmacol* 218:119-127.

Croteau DL, Peng Y, Van Houten B (2008) DNA repair gets physical: mapping an XPA-binding site on ERCC1. *DNA Repair (Amst)* 7:819-826.

D'Amours D, Desnoyers S, D'Silva I, Poirier GG (1999) Poly(ADP-ribosyl)ation reactions in the regulation of nuclear functions. *Biochem J* 342 (Pt 2):249-268.

Danaee H, Nelson HH, Liber H, Little JB, Kelsey KT (2004) Low dose exposure to sodium arsenite synergistically interacts with UV radiation to induce mutations and alter DNA repair in human cells. *Mutagenesis* 19:143-148.

Danford AJ, Wang D, Wang Q, Tullius TD, Lippard SJ (2005) Platinum anticancer drug damage enforces a particular rotational setting of DNA in nucleosomes. *Proc Natl Acad Sci U S A* 102:12311-12316.

Dantzer F, de La Rubia G, Menissier-De Murcia J, Hostomsky Z, de Murcia G, Schreiber V (2000) Base excision repair is impaired in mammalian cells lacking Poly(ADP-ribose) polymerase-1. *Biochemistry* 39:7559-7569.

Desmarais Y, Menard L, Lagueux J, Poirier GG (1991) Enzymological properties of poly(ADP-ribose)polymerase: characterization of automodification sites and NADase activity. *Biochim Biophys Acta* 1078:179-186.

Di Francesco AM, Ruggiero A, Riccardi R (2002) Cellular and molecular aspects of drugs of the future: oxaliplatin. *Cell Mol Life Sci* 59:1914-1927.

DiGiovanna JJ, Kraemer KH (2012) Shining a light on xeroderma pigmentosum. *J Invest Dermatol* 132:785-796.

Ding M, Shi X, Castranova V, Vallyathan V (2000) Predisposing factors in occupational lung cancer: inorganic minerals and chromium. *J Environ Pathol Toxicol Oncol* 19:129-138.

Ding W, Hudson LG, Liu KJ (2005) Inorganic arsenic compounds cause oxidative damage to DNA and protein by inducing ROS and RNS generation in human keratinocytes. *Mol Cell Biochem* 279:105-112.

Ding W, Hudson LG, Sun X, Feng C, Liu KJ (2008) As(III) inhibits ultraviolet radiation-induced cyclobutane pyrimidine dimer repair via generation of nitric oxide in human keratinocytes. *Free Radic Biol Med* 45:1065-1072.

Ding W, Liu W, Cooper KL, Qin XJ, de Souza Bergo PL, Hudson LG, *et al.* (2009) Inhibition of Poly(ADP-ribose) Polymerase-1 by Arsenite Interferes with Repair of Oxidative DNA Damage. *J Biol Chem* 284:6809-6817.

Douki T, Perdiz D, Grof P, Kuluncsics Z, Moustacchi E, Cadet J, *et al.* (1999) Oxidation of guanine in cellular DNA by solar UV radiation: biological role. *Photochem Photobiol* 70:184-190.

Douki T, Reynaud-Angelin A, Cadet J, Sage E (2003) Bipyrimidine photoproducts rather than oxidative lesions are the main type of DNA damage involved in the genotoxic effect of solar UVA radiation. *Biochemistry* 42:9221-9226.

Drew Y, Plummer R (2009) PARP inhibitors in cancer therapy: two modes of attack on the cancer cell widening the clinical applications. *Drug Resist Updat* 12:153-156.

Drobetsky EA, Turcotte J, Chateauneuf A (1995) A role for ultraviolet A in solar mutagenesis. *Proc Natl Acad Sci U S A* 92:2350-2354.

Dungey FA, Loser DA, Chalmers AJ (2008) Replication-dependent radiosensitization of human glioma cells by inhibition of poly(ADP-Ribose) polymerase: mechanisms and therapeutic potential. *Int J Radiat Oncol Biol Phys* 72:1188-1197.

El-Khamisy SF, Masutani M, Suzuki H, Caldecott KW (2003) A requirement for PARP-1 for the assembly or stability of XRCC1 nuclear foci at sites of oxidative DNA damage. *Nucleic Acids Res* 31:5526-5533.

EPA (1984) Health Assessment Document for Inorganic Arsenic. *Environmental Protection Agency* 600/8-83/021F.

EPA (2001) Technical Fact Sheet: Final Rule for Arsenic in Drinking Water. *Environmental Protection Agency* 815-F-00-016.

Eustermann S, Videler H, Yang JC, Cole PT, Gruszka D, Veprintsev D, *et al.* (2011) The DNA-binding domain of human PARP-1 interacts with DNA single-strand breaks as a monomer through its second zinc finger. *J Mol Biol* 407:149-170.

Fagbemi AF, Orelli B, Scharer OD (2011) Regulation of endonuclease activity in human nucleotide excision repair. *DNA Repair (Amst)* 10:722-729.

Fahrer J, Kranaster R, Altmeyer M, Marx A, Burkle A (2007) Quantitative analysis of the binding affinity of poly(ADP-ribose) to specific binding proteins as a function of chain length. *Nucleic Acids Res* 35:e143.

Fan L, Arvai AS, Cooper PK, Iwai S, Hanaoka F, Tainer JA (2006) Conserved XPB core structure and motifs for DNA unwinding: implications for pathway selection of transcription or excision repair. *Mol Cell* 22:27-37.

Fan L, Fuss JO, Cheng QJ, Arvai AS, Hammel M, Roberts VA, *et al.* (2008) XPD helicase structures and activities: insights into the cancer and aging phenotypes from XPD mutations. *Cell* 133:789-800.

Fitch ME, Nakajima S, Yasui A, Ford JM (2003) In vivo recruitment of XPC to UV-induced cyclobutane pyrimidine dimers by the DDB2 gene product. *J Biol Chem* 278:46906-46910.

Flohr C, Burkle A, Radicella JP, Epe B (2003) Poly(ADP-ribosyl)ation accelerates DNA repair in a pathway dependent on Cockayne syndrome B protein. *Nucleic Acids Research* 31:5332-5337.

Fluharty AL, Sanadi DR (1961) On the mechanism of oxidative phosphorylation. II. Effects of arsenite alone and in combination with 2,3-dimercaptopropanol. *J Biol Chem* 236:2772-2778.

Fousteri M, Mullenders LH (2008) Transcription-coupled nucleotide excision repair in mammalian cells: molecular mechanisms and biological effects. *Cell Res* 18:73-84.

Fousteri M, Vermeulen W, van Zeeland AA, Mullenders LH (2006) Cockayne syndrome A and B proteins differentially regulate recruitment of chromatin remodeling and repair factors to stalled RNA polymerase II in vivo. *Mol Cell* 23:471-482.

Freeman SE, Gange RW, Sutherland JC, Matzinger EA, Sutherland BM (1987) Production of pyrimidine dimers in DNA of human skin exposed in situ to UVA radiation. *J Invest Dermatol* 88:430-433.

Freeman SE, Hacham H, Gange RW, Maytum DJ, Sutherland JC, Sutherland BM (1989) Wavelength dependence of pyrimidine dimer formation in DNA of human skin irradiated in situ with ultraviolet light. *Proc Natl Acad Sci U S A* 86:5605-5609.

Frost C, Williams G, Green A (2000) High incidence and regression rates of solar keratoses in a queensland community. *J Invest Dermatol* 115:273-277.

Fuchs E, Raghavan S (2002) Getting under the skin of epidermal morphogenesis. *Nat Rev Genet* 3:199-209.

Fujihara H, Ogino H, Maeda D, Shirai H, Nozaki T, Kamada N, *et al.* (2009) Poly(ADP-ribose) Glycohydrolase deficiency sensitizes mouse ES cells to DNA damaging agents. *Curr Cancer Drug Targets* 9:953-962.

Gagne JP, Hendzel MJ, Droit A, Poirier GG (2006) The expanding role of poly(ADP-ribose) metabolism: current challenges and new perspectives. *Curr Opin Cell Biol* 18:145-151.

Gagne JP, Isabelle M, Lo KS, Bourassa S, Hendzel MJ, Dawson VL, *et al.* (2008) Proteome-wide identification of poly(ADP-ribose) binding proteins and poly(ADP-ribose)-associated protein complexes. *Nucleic Acids Res* 36:6959-6976.

Ghodgaonkar MM, Zacal N, Kassam S, Rainbow AJ, Shah GM (2008) Depletion of poly(ADP-ribose) polymerase-1 reduces host cell reactivation of a UV-damaged adenovirus-encoded reporter gene in human dermal fibroblasts. *DNA Repair* 7:617-632.

Gloster HM, Jr., Neal K (2006) Skin cancer in skin of color. *J Am Acad Dermatol* 55:741-760; quiz 761-744.

Gottschalk AJ, Timinszky G, Kong SE, Jin J, Cai Y, Swanson SK, *et al.* (2009) Poly(ADP-ribosyl)ation directs recruitment and activation of an ATP-dependent chromatin remodeler. *Proc Natl Acad Sci U S A* 106:13770-13774.

Guetens G, De Boeck G, Highley M, van Oosterom AT, de Bruijn EA (2002) Oxidative DNA damage: biological significance and methods of analysis. *Crit Rev Clin Lab Sci* 39:331-457.

Han W, Li X, Fu X (2010) The macro domain protein family: structure, functions, and their potential therapeutic implications. *Mutat Res* 727:86-103.

Hanai S, Kanai M, Ohashi S, Okamoto K, Yamada M, Takahashi H, *et al.* (2004) Loss of poly(ADP-ribose) glycohydrolase causes progressive neurodegeneration in Drosophila melanogaster. *Proc Natl Acad Sci U S A* 101:82-86.

Hartwig A, Groblinghoff UD, Beyersmann D, Natarajan AT, Filon R, Mullenders LH (1997) Interaction of arsenic(III) with nucleotide excision repair in UV-irradiated human fibroblasts. *Carcinogenesis* 18:399-405.

Hartwig A, Pelzer A, Asmuss M, Burkle A (2003) Very low concentrations of arsenite suppress poly(ADP-ribosyl)ation in mammalian cells. *Int J Cancer* 104:1-6.

Hassa PO, Hottiger MO (2008) The diverse biological roles of mammalian PARPS, a small but powerful family of poly-ADP-ribose polymerases. *Front Biosci* 13:3046-3082.

Heeres JT, Hergenrother PJ (2007) Poly(ADP-ribose) makes a date with death. *Curr Opin Chem Biol* 11:644-653.

Hei TK, Liu SX, Waldren C (1998) Mutagenicity of arsenic in mammalian cells: role of reactive oxygen species. *Proc Natl Acad Sci U S A* 95:8103-8107.

Helleday T (2011) The underlying mechanism for the PARP and BRCA synthetic lethality: clearing up the misunderstandings. *Mol Oncol* 5:387-393.

Hermanson-Miller IL, Turchi JJ (2002) Strand-specific binding of RPA and XPA to damaged duplex DNA. *Biochemistry* 41:2402-2408.

Hey T, Lipps G, Sugasawa K, Iwai S, Hanaoka F, Krauss G (2002) The XPC-HR23B complex displays high affinity and specificity for damaged DNA in a true-equilibrium fluorescence assay. *Biochemistry* 41:6583-6587.

Hoogstraten D, Bergink S, Ng JM, Verbiest VH, Luijsterburg MS, Geverts B, *et al.* (2008) Versatile DNA damage detection by the global genome nucleotide excision repair protein XPC. *J Cell Sci* 121:2850-2859.

Huang RN, Ho IC, Yih LH, Lee TC (1995) Sodium arsenite induces chromosome endoreduplication and inhibits protein phosphatase activity in human fibroblasts. *Environ Mol Mutagen* 25:188-196.

Huang XX, Bernerd F, Halliday GM (2009) Ultraviolet A within sunlight induces mutations in the epidermal basal layer of engineered human skin. *Am J Pathol* 174:1534-1543.

Hunter JE, Willmore E, Irving JA, Hostomsky Z, Veuger SJ, Durkacz BW (2011) NF-kappaB mediates radio-sensitization by the PARP-1 inhibitor, AG-014699. *Oncogene* 31:251-264.

IARC (2009) A review of human carcinogens - Part C: metals, arsenic, dusts, and fibers. *IARC Press; Lyon* 10:453-454.

Ikegami T, Kuraoka I, Saijo M, Kodo N, Kyogoku Y, Morikawa K, *et al.* (1998) Solution structure of the DNA- and RPA-binding domain of the human repair factor XPA. *Nat Struct Biol* 5:701-706.

Ikehata H, Ono T (2011) The mechanisms of UV mutagenesis. *J Radiat Res* 52:115-125.

Jacobs AL, Schar P (2012) DNA glycosylases: in DNA repair and beyond. *Chromosoma* 121:1-20.

Jennette KW (1981) The role of metals in carcinogenesis: biochemistry and metabolism. *Environ Health Perspect* 40:233-252.

Jerant AF, Johnson JT, Sheridan CD, Caffrey TJ (2000) Early detection and treatment of skin cancer. *Am Fam Physician* 62:357-368, 375-356, 381-352.

Jomova K, Jenisova Z, Feszterova M, Baros S, Liska J, Hudecova D, *et al.* (2011) Arsenic: toxicity, oxidative stress and human disease. *J Appl Toxicol* 31:95-107.

Jones P, Simons BD (2008) Epidermal homeostasis: do committed progenitors work while stem cells sleep? *Nat Rev Mol Cell Biol* 9:82-88.

Kamionka M, Feigon J (2004) Structure of the XPC binding domain of hHR23A reveals hydrophobic patches for protein interaction. *Protein Sci* 13:2370-2377.

Kang HC, Lee YI, Shin JH, Andrabi SA, Chi Z, Gagne JP, *et al.* (2011a) Iduna is a poly(ADP-ribose) (PAR)-dependent E3 ubiquitin ligase that regulates DNA damage. *Proc Natl Acad Sci U S A* 108:14103-14108.

Kang TH, Reardon JT, Sancar A (2011b) Regulation of nucleotide excision repair activity by transcriptional and post-transcriptional control of the XPA protein. *Nucleic Acids Res* 39:3176-3187.

Karras GI, Kustatscher G, Buhecha HR, Allen MD, Pugieux C, Sait F, *et al.* (2005) The macro domain is an ADP-ribose binding module. *EMBO J* 24:1911-1920.

Kimbung S, Biskup E, Johansson I, Aaltonen K, Ottosson-Wadlund A, Gruvberger-Saal S, *et al.* (2012) Co-targeting of the PI3K pathway improves the response of BRCA1 deficient breast cancer cells to PARP1 inhibition. *Cancer Lett* 319:232-241.

King BS, Cooper KL, Liu KJ, Hudson LG (2012) Poly(ADP-ribose) contributes to an association between Poly(ADP-ribose)polymerase-1 and Xeroderma pigmentosum complementation group A in nucleotide excision repair. *J Biol Chem* epub.

Kitchin KT (2001) Recent advances in arsenic carcinogenesis: modes of action, animal model systems, and methylated arsenic metabolites. *Toxicol Appl Pharmacol* 172:249-261.

Kitchin KT, Wallace K (2005) Arsenite binding to synthetic peptides based on the Zn finger region and the estrogen binding region of the human estrogen receptor-alpha. *Toxicol Appl Pharmacol* 206:66-72.

Kitchin KT, Wallace K (2008) The role of protein binding of trivalent arsenicals in arsenic carcinogenesis and toxicity. *J Inorg Biochem* 102:532-539.

Koberle B, Roginskaya V, Wood RD (2006) XPA protein as a limiting factor for nucleotide excision repair and UV sensitivity in human cells. *DNA Repair (Amst)* 5:641-648.

Kochhar TS, Howard W, Hoffman S, Brammer-Carleton L (1996) Effect of trivalent and pentavalent arsenic in causing chromosome alterations in cultured Chinese hamster ovary (CHO) cells. *Toxicol Lett* 84:37-42.

Koh DW, Lawler AM, Poitras MF, Sasaki M, Wattler S, Nehls MC, *et al.* (2004) Failure to degrade poly(ADP-ribose) causes increased sensitivity to cytotoxicity and early embryonic lethality. *Proc Natl Acad Sci U S A* 101:17699-17704.

Koster MI (2009) Making an epidermis. *Ann N Y Acad Sci* 1170:7-10.

Kubota Y, Nash RA, Klungland A, Schar P, Barnes DE, Lindahl T (1996) Reconstitution of DNA base excision-repair with purified human proteins: interaction between DNA polymerase beta and the XRCC1 protein. *EMBO J* 15:6662-6670.

Kummar S, Chen A, Parchment RE, Kinders RJ, Ji J, Tomaszewski JE, *et al.* (2012) Advances in using PARP inhibitors to treat cancer. *BMC Med* 10:25.

Lan L, Nakajima S, Oohata Y, Takao M, Okano S, Masutani M, *et al.* (2004) In situ analysis of repair processes for oxidative DNA damage in mammalian cells. *Proc Natl Acad Sci U S A* 101:13738-13743.

Langelier MF, Ruhl DD, Planck JL, Kraus WL, Pascal JM (2010) The Zn3 domain of human poly(ADP-ribose) polymerase-1 (PARP-1) functions in both DNA-dependent poly(ADP-ribose) synthesis activity and chromatin compaction. *J Biol Chem* 285:18877-18887.

Langelier MF, Servent KM, Rogers EE, Pascal JM (2008) A third zinc-binding domain of human poly(ADP-ribose) polymerase-1 coordinates DNA-dependent enzyme activation. *J Biol Chem* 283:4105-4114.

Lee TC, Huang RY, Jan KY (1985) Sodium arsenite enhances the cytotoxicity, clastogenicity, and 6-thioguanine-resistant mutagenicity of ultraviolet light in Chinese hamster ovary cells. *Mutat Res* 148:83-89.

Lee TC, Tanaka N, Lamb PW, Gilmer TM, Barrett JC (1988) Induction of gene amplification by arsenic. *Science* 241:79-81.

Leppard JB, Dong Z, Mackey ZB, Tomkinson AE (2003) Physical and functional interaction between DNA ligase IIIalpha and poly(ADP-Ribose) polymerase 1 in DNA single-strand break repair. *Mol Cell Biol* 23:5919-5927.

Li GY, McCulloch RD, Fenton AL, Cheung M, Meng L, Ikura M, *et al.* (2011) Structure and identification of ADP-ribose recognition motifs of APLF and role in the DNA damage response. *Proc Natl Acad Sci U S A* 107:9129-9134.

Li JH, Rossman TG (1989) Inhibition of DNA ligase activity by arsenite: a possible mechanism of its comutagenesis. *Mol Toxicol* 2:1-9.

Li JH, Rossman TG (1991) Comutagenesis of sodium arsenite with ultraviolet radiation in Chinese hamster V79 cells. *Biol Met* 4:197-200.

Li L, Lu X, Peterson CA, Legerski RJ (1995) An interaction between the DNA repair factor XPA and replication protein A appears essential for nucleotide excision repair. *Mol Cell Biol* 15:5396-5402.

Li RY, Calsou P, Jones CJ, Salles B (1998) Interactions of the transcription/DNA repair factor TFIIH and XP repair proteins with DNA lesions in a cell-free repair assay. *J Mol Biol* 281:211-218.

Lilyestrom W, van der Woerd MJ, Clark N, Luger K (2010) Structural and biophysical studies of human PARP-1 in complex with damaged DNA. *J Mol Biol* 395:983-994.

Ljungquist S, Kenne K, Olsson L, Sandstrom M (1994) Altered DNA ligase III activity in the CHO EM9 mutant. *Mutat Res* 314:177-186.

Lu YP, Lou YR, Yen P, Mitchell D, Huang MT, Conney AH (1999) Time course for early adaptive responses to ultraviolet B light in the epidermis of SKH-1 mice. *Cancer Res* 59:4591-4602.

Ludwig A, Behnke B, Holtlund J, Hilz H (1988) Immunoquantitation and size determination of intrinsic poly(ADP-ribose) polymerase from acid precipitates. An analysis of the in vivo status in mammalian species and in lower eukaryotes. *J Biol Chem* 263:6993-6999.

Luijsterburg MS, Lindh M, Acs K, Vrouwe MG, Pines A, van Attikum H, *et al.* (2012) DDB2 promotes chromatin decondensation at UV-induced DNA damage. *J Cell Biol* 197:267-281.

Lynn S, Lai HT, Gurr JR, Jan KY (1997) Arsenite retards DNA break rejoining by inhibiting DNA ligation. *Mutagenesis* 12:353-358.

Lynn S, Shiung JN, Gurr JR, Jan KY (1998) Arsenite stimulates poly(ADP-ribosylation) by generation of nitric oxide. *Free Radic Biol Med* 24:442-449.

Mackey ZB, Ramos W, Levin DS, Walter CA, McCarrey JR, Tomkinson AE (1997) An alternative splicing event which occurs in mouse pachytene spermatocytes generates a form of DNA ligase III with distinct biochemical properties that may function in meiotic recombination. *Mol Cell Biol* 17:989-998.

Maddodi N, Setaluri V (2008) Role of UV in cutaneous melanoma. *Photochem Photobiol* 84:528-536.

Mahata J, Basu A, Ghoshal S, Sarkar JN, Roy AK, Poddar G, *et al.* (2003) Chromosomal aberrations and sister chromatid exchanges in individuals exposed to arsenic through drinking water in West Bengal, India. *Mutat Res* 534:133-143.

Malanga M, Althaus FR (2005) The role of poly(ADP-ribose) in the DNA damage signaling network. *Biochem Cell Biol* 83:354-364.

Malanga M, Pleschke JM, Kleczkowska HE, Althaus FR (1998) Poly(ADP-ribose) binds to specific domains of p53 and alters its DNA binding functions. *J Biol Chem* 273:11839-11843.

Marintchev A, Mullen MA, Maciejewski MW, Pan B, Gryk MR, Mullen GP (1999) Solution structure of the single-strand break repair protein XRCC1 N-terminal domain. *Nat Struct Biol* 6:884-893.

Marks R, Rennie G, Selwood TS (1988) Malignant transformation of solar keratoses to squamous cell carcinoma. *Lancet* 1:795-797.

Martinez VD, Vucic EA, Adonis M, Gil L, Lam WL (2011a) Arsenic biotransformation as a cancer promoting factor by inducing DNA damage and disruption of repair mechanisms. *Mol Biol Int* 2011:718974.

Martinez VD, Vucic EA, Becker-Santos DD, Gil L, Lam WL (2011b) Arsenic exposure and the induction of human cancers. *J Toxicol* 2011:431287.

Maruta H, Matsumura N, Tanuma S (1997) Role of (ADP-ribose)n catabolism in DNA repair. *Biochem Biophys Res Commun* 236:265-269.

Masson M, Niedergang C, Schreiber V, Muller S, Menissier-de Murcia J, de Murcia G (1998) XRCC1 is specifically associated with poly(ADP-ribose) polymerase and negatively regulates its activity following DNA damage. *Mol Cell Biol* 18:3563-3571.

Matsui M, Nishigori C, Toyokuni S, Takada J, Akaboshi M, Ishikawa M, *et al.* (1999) The role of oxidative DNA damage in human arsenic carcinogenesis: detection of 8-hydroxy-2'-deoxyguanosine in arsenic-related Bowen's disease. *J Invest Dermatol* 113:26-31.

Mead MN (2005) Arsenic: in search of an antidote to a global poison. *Environ Health Perspect* 113:A378-386.

Megnin-Chanet F, Bollet MA, Hall J (2010) Targeting poly(ADP-ribose) polymerase activity for cancer therapy. *Cell Mol Life Sci* 67:3649-3662.

Meyer RG, Meyer-Ficca ML, Jacobson EL, Jacobson MK (2003) Human poly(ADP-ribose) glycohydrolase (PARG) gene and the common promoter sequence it shares with inner mitochondrial membrane translocase 23 (TIM23). *Gene* 314:181-190.

Missura M, Buterin T, Hindges R, Hubscher U, Kasparkova J, Brabec V, *et al.* (2001) Double-check probing of DNA bending and unwinding by XPA-RPA: an architectural function in DNA repair. *EMBO J* 20:3554-3564.

Mohan D, Pittman CU, Jr. (2007) Arsenic removal from water/wastewater using adsorbents--A critical review. *J Hazard Mater* 142:1-53.

Mondal P, Majumder CB, Mohanty B (2006) Laboratory based approaches for arsenic remediation from contaminated water: recent developments. *J Hazard Mater* 137:464-479.

Morales KH, Ryan L, Kuo TL, Wu MM, Chen CJ (2000) Risk of internal cancers from arsenic in drinking water. *Environ Health Perspect* 108:655-661.

Moroni F, Meli E, Peruginelli F, Chiarugi A, Cozzi A, Picca R, *et al.* (2001) Poly(ADP-ribose) polymerase inhibitors attenuate necrotic but not apoptotic neuronal death in experimental models of cerebral ischemia. *Cell Death Differ* 8:921-932.

Moser J, Kool H, Giakzidis I, Caldecott K, Mullenders LH, Fousteri MI (2007) Sealing of chromosomal DNA nicks during nucleotide excision repair requires XRCC1 and DNA ligase III alpha in a cell-cycle-specific manner. *Mol Cell* 27:311-323.

Moser J, Volker M, Kool H, Alekseev S, Vrieling H, Yasui A, *et al.* (2005) The UV-damaged DNA binding protein mediates efficient targeting of the nucleotide excision repair complex to UV-induced photo lesions. *DNA Repair (Amst)* 4:571-582.

Mouret S, Philippe C, Gracia-Chantegrel J, Banyasz A, Karpati S, Markovitsi D, *et al.* (2010) UVA-induced cyclobutane pyrimidine dimers in DNA: a direct photochemical mechanism? *Org Biomol Chem* 8:1706-1711.

Mu D, Park CH, Matsunaga T, Hsu DS, Reardon JT, Sancar A (1995) Reconstitution of human DNA repair excision nuclease in a highly defined system. *J Biol Chem* 270:2415-2418.

Narayanan DL, Saladi RN, Fox JL (2010) Ultraviolet radiation and skin cancer. *Int J Dermatol* 49:978-986.

Nash RA, Caldecott KW, Barnes DE, Lindahl T (1997) XRCC1 protein interacts with one of two distinct forms of DNA ligase III. *Biochemistry* 36:5207-5211.

Nazarkina Zh K, Khodyreva SN, Marsin S, Radicella JP, Lavrik OI (2007) Study of interaction of XRCC1 with DNA and proteins of base excision repair by photoaffinity labeling technique. *Biochemistry (Mosc)* 72:878-886.

Nishi R, Alekseev S, Dinant C, Hoogstraten D, Houtsmuller AB, Hoeijmakers JH, *et al.* (2009) UV-DDB-dependent regulation of nucleotide excision repair kinetics in living cells. *DNA Repair (Amst)* 8:767-776.

Nollen M, Ebert F, Moser J, Mullenders LH, Hartwig A, Schwerdtle T (2009) Impact of arsenic on nucleotide excision repair: XPC function, protein level, and gene expression. *Mol Nutr Food Res* 53:572-582.

Nouspikel T (2009) DNA repair in mammalian cells : Nucleotide excision repair: variations on versatility. *Cell Mol Life Sci* 66:994-1009.

Ogi T, Limsirichaikul S, Overmeer RM, Volker M, Takenaka K, Cloney R, *et al.* (2010) Three DNA polymerases, recruited by different mechanisms, carry out NER repair synthesis in human cells. *Mol Cell* 37:714-727.

Oka J, Ueda K, Hayaishi O, Komura H, Nakanishi K (1984) ADP-ribosyl protein lyase. Purification, properties, and identification of the product. *J Biol Chem* 259:986-995.

Orelli B, McClendon TB, Tsodikov OV, Ellenberger T, Niedernhofer LJ, Scharer OD (2010) The XPA-binding domain of ERCC1 is required for nucleotide excision repair but not other DNA repair pathways. *J Biol Chem* 285:3705-3712.

Overmeer RM, Moser J, Volker M, Kool H, Tomkinson AE, van Zeeland AA, *et al.* (2011) Replication protein A safeguards genome integrity by controlling NER incision events. *J Cell Biol* 192:401-415.

Park CH, Mu D, Reardon JT, Sancar A (1995) The general transcription-repair factor TFIIH is recruited to the excision repair complex by the XPA protein independent of the TFIIE transcription factor. *J Biol Chem* 270:4896-4902.

Park CJ, Choi BS (2006) The protein shuffle - Sequential interactions among components of the human nucleotide excision repair pathway. *Febs Journal* 273:1600-1608.

Parsons JL, Dianova, II, Allinson SL, Dianov GL (2005) Poly(ADP-ribose) polymerase-1 protects excessive DNA strand breaks from deterioration during repair in human cell extracts. *FEBS J* 272:2012-2021.

Perdiz D, Grof P, Mezzina M, Nikaido O, Moustacchi E, Sage E (2000) Distribution and repair of bipyrimidine photoproducts in solar UV-irradiated mammalian cells. Possible role of Dewar photoproducts in solar mutagenesis. *J Biol Chem* 275:26732-26742.

Pfeifer GP, Besaratinia A (2011) UV wavelength-dependent DNA damage and human non-melanoma and melanoma skin cancer. *Photochem Photobiol Sci* 11:90-97.

Pfeifer GP, You YH, Besaratinia A (2005) Mutations induced by ultraviolet light. *Mutat Res* 571:19-31.

Pleschke JM, Kleczkowska HE, Strohm M, Althaus FR (2000) Poly(ADP-ribose) binds to specific domains in DNA damage checkpoint proteins. *J Biol Chem* 275:40974-40980.

Plo I, Liao ZY, Barcelo JM, Kohlhagen G, Caldecott KW, Weinfeld M, *et al.* (2003) Association of XRCC1 and tyrosyl DNA phosphodiesterase (Tdp1) for the repair of topoisomerase I-mediated DNA lesions. *DNA Repair (Amst)* 2:1087-1100.

Plummer R, Jones C, Middleton M, Wilson R, Evans J, Olsen A, *et al.* (2008) Phase I study of the poly(ADP-ribose) polymerase inhibitor, AG014699, in combination with temozolomide in patients with advanced solid tumors. *Clin Cancer Res* 14:7917-7923.

Polo SE, Kaidi A, Baskcomb L, Galanty Y, Jackson SP (2010) Regulation of DNA-damage responses and cell-cycle progression by the chromatin remodelling factor CHD4. *EMBO J* 29:3130-3139.

Prasad R, Beard WA, Batra VK, Liu Y, Shock DD, Wilson SH (2011) A review of recent experiments on step-to-step "hand-off" of the DNA intermediates in mammalian base excision repair pathways. *Mol Biol (Mosk)* 45:586-600.

Proksch E, Brandner JM, Jensen JM (2008) The skin: an indispensable barrier. *Exp Dermatol* 17:1063-1072.

Protic M, Hirschfeld S, Tsang AP, Wagner M, Dixon K, Levine AS (1989) Induction of a novel damage-specific DNA binding protein correlates with enhanced DNA repair in primate cells. *Mol Toxicol* 2:255-270.

Qin XJ, Hudson LG, Liu W, Ding W, Cooper KL, Liu KJ (2008a) Dual actions involved in arsenite-induced oxidative DNA damage. *Chem Res Toxicol* 21:1806-1813.

Qin XJ, Hudson LG, Liu W, Timmins GS, Liu KJ (2008b) Low concentration of arsenite exacerbates UVR-induced DNA strand breaks by inhibiting PARP-1 activity. *Toxicol Appl Pharmacol* 232:41-50.

Rabik CA, Dolan ME (2007) Molecular mechanisms of resistance and toxicity associated with platinating agents. *Cancer Treat Rev* 33:9-23.

Rass K, Reichrath J (2008) UV damage and DNA repair in malignant melanoma and nonmelanoma skin cancer. *Adv Exp Med Biol* 624:162-178.

Rastogi RP, Richa, Kumar A, Tyagi MB, Sinha RP (2010) Molecular mechanisms of ultraviolet radiation-induced DNA damage and repair. *J Nucleic Acids* 2010:592980.

Ratner ES, Sartorelli AC, Lin ZP (2012) Poly (ADP-ribose) polymerase inhibitors: on the horizon of tailored and personalized therapies for epithelial ovarian cancer. *Curr Opin Oncol* 24:564-571.

Rechkunova NI, Krasikova YS, Lavrik OI (2011) Nucleotide excision repair: DNA damage recognition and preincision complex assembly. *Biochemistry (Mosc)* 76:24-35.

Rice PA (1999) Holding damaged DNA together. *Nat Struct Biol* 6:805-806.

Roewert-Huber J, Lange-Asschenfeldt B, Stockfleth E, Kerl H (2007) Epidemiology and aetiology of basal cell carcinoma. *Br J Dermatol* 157 Suppl 2:47-51.

Rossman TG, Uddin AN, Burns FJ (2004) Evidence that arsenite acts as a cocarcinogen in skin cancer. *Toxicol Appl Pharmacol* 198:394-404.

Rossman TG, Uddin AN, Burns FJ, Bosland MC (2001) Arsenite is a cocarcinogen with solar ultraviolet radiation for mouse skin: an animal model for arsenic carcinogenesis. *Toxicol Appl Pharmacol* 176:64-71.

Rouleau M, Aubin RA, Poirier GG (2004) Poly(ADP-ribosyl)ated chromatin domains: access granted. *J Cell Sci* 117:815-825.

Ruf A, Mennissier de Murcia J, de Murcia G, Schulz GE (1996) Structure of the catalytic fragment of poly(AD-ribose) polymerase from chicken. *Proc Natl Acad Sci U S A* 93:7481-7485.

Satoh MS, Lindahl T (1992) Role of poly(ADP-ribose) formation in DNA repair. *Nature* 356:356-358.

Scharer OD (2008) XPG: its products and biological roles. *Adv Exp Med Biol* 637:83-92.

Schmitz AA, Pleschke JM, Kleczkowska HE, Althaus FR, Vergeres G (1998) Poly(ADP-ribose) modulates the properties of MARCKS proteins. *Biochemistry* 37:9520-9527.

Schreiber V, Ame JC, Dolle P, Schultz I, Rinaldi B, Fraulob V, *et al.* (2002) Poly(ADP-ribose) polymerase-2 (PARP-2) is required for efficient base excision DNA repair in association with PARP-1 and XRCC1. *J Biol Chem* 277:23028-23036.

Schreiber V, Dantzer F, Ame JC, de Murcia G (2006) Poly(ADP-ribose): novel functions for an old molecule. *Nat Rev Mol Cell Biol* 7:517-528.

Schultz P, Fribourg S, Poterszman A, Mallouh V, Moras D, Egly JM (2000) Molecular structure of human TFIIH. *Cell* 102:599-607.

Schwerdtle T, Ebert F, Thuy C, Richter C, Mullenders LH, Hartwig A (2010) Genotoxicity of soluble and particulate cadmium compounds: impact on oxidative DNA damage and nucleotide excision repair. *Chem Res Toxicol* 23:432-442.

Schwerdtle T, Walter I, Hartwig A (2003a) Arsenite and its biomethylated metabolites interfere with the formation and repair of stable BPDE-induced DNA adducts in human cells and impair XPAzf and Fpg. *DNA Repair (Amst)* 2:1449-1463.

Schwerdtle T, Walter I, Mackiw I, Hartwig A (2003b) Induction of oxidative DNA damage by arsenite and its trivalent and pentavalent methylated metabolites in cultured human cells and isolated DNA. *Carcinogenesis* 24:967-974.

Shell SM, Li Z, Shkriabai N, Kvaratskhelia M, Brosey C, Serrano MA, *et al.* (2009) Checkpoint kinase ATR promotes nucleotide excision repair of UV-induced DNA damage via physical interaction with xeroderma pigmentosum group A. *J Biol Chem* 284:24213-24222.

Shen MR, Zdzienicka MZ, Mohrenweiser H, Thompson LH, Thelen MP (1998) Mutations in hamster single-strand break repair gene XRCC1 causing defective DNA repair. *Nucleic Acids Res* 26:1032-1037.

Shi H, Hudson LG, Ding W, Wang S, Cooper KL, Liu S, *et al.* (2004) Arsenite causes DNA damage in keratinocytes via generation of hydroxyl radicals. *Chem Res Toxicol* 17:871-878.

Simonin F, Hofferer L, Panzeter PL, Muller S, de Murcia G, Althaus FR (1993) The carboxyl-terminal domain of human poly(ADP-ribose) polymerase. Overproduction in Escherichia coli, large scale purification, and characterization. *J Biol Chem* 268:13454-13461.

Simpson CL, Patel DM, Green KJ (2011) Deconstructing the skin: cytoarchitectural determinants of epidermal morphogenesis. *Nat Rev Mol Cell Biol* 12:565-580.

Sinha RP, Hader DP (2002) UV-induced DNA damage and repair: a review. *Photochem Photobiol Sci* 1:225-236.

Smith S (2001) The world according to PARP. *Trends Biochem Sci* 26:174-179.

Steinmaus C, Moore L, Hopenhayn-Rich C, Biggs ML, Smith AH (2000) Arsenic in drinking water and bladder cancer. *Cancer Invest* 18:174-182.

Sugasawa K (2006) UV-induced ubiquitylation of XPC complex, the UV-DDB-ubiquitin ligase complex, and DNA repair. *J Mol Histol* 37:189-202.

Sugasawa K (2008) XPC: its product and biological roles. *Adv Exp Med Biol* 637:47-56.

Sugasawa K (2009) UV-DDB: a molecular machine linking DNA repair with ubiquitination. *DNA Repair (Amst)* 8:969-972.

Sugasawa K (2011) Multiple DNA damage recognition factors involved in mammalian nucleotide excision repair. *Biochemistry (Mosc)* 76:16-23.

Sugasawa K, Ng JM, Masutani C, Iwai S, van der Spek PJ, Eker AP, *et al.* (1998) Xeroderma pigmentosum group C protein complex is the initiator of global genome nucleotide excision repair. *Mol Cell* 2:223-232.

Sugasawa K, Okuda Y, Saijo M, Nishi R, Matsuda N, Chu G, *et al.* (2005) UV-induced ubiquitylation of XPC protein mediated by UV-DDB-ubiquitin ligase complex. *Cell* 121:387-400.

Suto MJ, Turner WR, Arundel-Suto CM, Werbel LM, Sebolt-Leopold JS (1991) Dihydroisoquinolinones: the design and synthesis of a new series of potent inhibitors of poly(ADP-ribose) polymerase. *Anticancer Drug Des* 6:107-117.

Tao Z, Gao P, Hoffman DW, Liu HW (2008) Domain C of human poly(ADP-ribose) polymerase-1 is important for enzyme activity and contains a novel zinc-ribbon motif. *Biochemistry* 47:5804-5813.

Taylor RM, Wickstead B, Cronin S, Caldecott KW (1998) Role of a BRCT domain in the interaction of DNA ligase III-alpha with the DNA repair protein XRCC1. *Curr Biol* 8:877-880.

Tebbs RS, Flannery ML, Meneses JJ, Hartmann A, Tucker JD, Thompson LH, *et al.* (1999) Requirement for the Xrcc1 DNA base excision repair gene during early mouse development. *Dev Biol* 208:513-529.

Telli ML, Ford JM (2010) PARP inhibitors in breast cancer. *Clin Adv Hematol Oncol* 8:629-635.

Tentori L, Portarena I, Graziani G (2002) Potential clinical applications of poly(ADP-ribose) polymerase (PARP) inhibitors. *Pharmacol Res* 45:73-85.

Thomas MC, Chiang CM (2006) The general transcription machinery and general cofactors. *Crit Rev Biochem Mol Biol* 41:105-178.

Thompson LH, Brookman KW, Dillehay LE, Carrano AV, Mazrimas JA, Mooney CL, *et al.* (1982) A CHO-cell strain having hypersensitivity to mutagens, a defect in DNA strand-break repair, and an extraordinary baseline frequency of sister-chromatid exchange. *Mutat Res* 95:427-440.

Thompson LH, Brookman KW, Jones NJ, Allen SA, Carrano AV (1990) Molecular cloning of the human XRCC1 gene, which corrects defective DNA strand break repair and sister chromatid exchange. *Mol Cell Biol* 10:6160-6171.

Timares L, Katiyar SK, Elmets CA (2008) DNA damage, apoptosis and langerhans cells--Activators of UV-induced immune tolerance. *Photochem Photobiol* 84:422-436.

Tinwell H, Stephens SC, Ashby J (1991) Arsenite as the probable active species in the human carcinogenicity of arsenic: mouse micronucleus assays on Na and K arsenite, orpiment, and Fowler's solution. *Environ Health Perspect* 95:205-210.

Tokar EJ, Benbrahim-Tallaa L, Ward JM, Lunn R, Sams RL, 2nd, Waalkes MP (2010) Cancer in experimental animals exposed to arsenic and arsenic compounds. *Crit Rev Toxicol* 40:912-927.

Tokar EJ, Diwan BA, Ward JM, Delker DA, Waalkes MP (2011) Carcinogenic effects of "whole-life" exposure to inorganic arsenic in CD1 mice. *Toxicol Sci* 119:73-83.

Tornaletti S (2009) DNA repair in mammalian cells: Transcription-coupled DNA repair: directing your effort where it's most needed. *Cell Mol Life Sci* 66:1010-1020.

Vink AA, Roza L (2001) Biological consequences of cyclobutane pyrimidine dimers. *J Photochem Photobiol B* 65:101-104.

Vodenicharov MD, Ghodgaonkar MM, Halappanavar SS, Shah RG, Shah GM (2005) Mechanism of early biphasic activation of poly(ADP-ribose) polymerase-1 in response to ultraviolet B radiation. *J Cell Sci* 118:589-599.

Vodenicharov MD, Sallmann FR, Satoh MS, Poirier GG (2000) Base excision repair is efficient in cells lacking poly(ADP-ribose) polymerase 1. *Nucleic Acids Res* 28:3887-3896.

Volker M, Mone MJ, Karmakar P, van Hoffen A, Schul W, Vermeulen W, *et al.* (2001) Sequential assembly of the nucleotide excision repair factors in vivo. *Mol Cell* 8:213-224.

von Thaler AK, Kamenisch Y, Berneburg M (2010) The role of ultraviolet radiation in melanomagenesis. *Exp Dermatol* 19:81-88.

Wakasugi M, Kawashima A, Morioka H, Linn S, Sancar A, Mori T, *et al.* (2002) DDB accumulates at DNA damage sites immediately after UV irradiation and directly stimulates nucleotide excision repair. *J Biol Chem* 277:1637-1640.

Walter I, Schwerdtle T, Thuy C, Parsons JL, Dianov GL, Hartwig A (2007) Impact of arsenite and its methylated metabolites on PARP-1 activity, PARP-1 gene expression and poly(ADP-ribosyl)ation in cultured human cells. *DNA Repair (Amst)* 6:61-70.

Wang QE, Zhu Q, Wani G, El-Mahdy MA, Li J, Wani AA (2005) DNA repair factor XPC is modified by SUMO-1 and ubiquitin following UV irradiation. *Nucleic Acids Res* 33:4023-4034.

Wang Y, Dawson VL, Dawson TM (2009) Poly(ADP-ribose) signals to mitochondrial AIF: a key event in parthanatos. *Exp Neurol* 218:193-202.

Wang Z, Dey S, Rosen BP, Rossman TG (1996) Efflux-mediated resistance to arsenicals in arsenic-resistant and -hypersensitive Chinese hamster cells. *Toxicol Appl Pharmacol* 137:112-119.

Wanibuchi H, Hori T, Meenakshi V, Ichihara T, Yamamoto S, Yano Y, *et al.* (1997) Promotion of rat hepatocarcinogenesis by dimethylarsinic acid: association with elevated ornithine decarboxylase activity and formation of 8-hydroxydeoxyguanosine in the liver. *Jpn J Cancer Res* 88:1149-1154.

Warner ML, Moore LE, Smith MT, Kalman DA, Fanning E, Smith AH (1994) Increased micronuclei in exfoliated bladder cells of individuals who chronically ingest arsenic-contaminated water in Nevada. *Cancer Epidemiol Biomarkers Prev* 3:583-590.

Watt FM, Lo Celso C, Silva-Vargas V (2006) Epidermal stem cells: an update. *Curr Opin Genet Dev* 16:518-524.

Whitehouse CJ, Taylor RM, Thistlethwaite A, Zhang H, Karimi-Busheri F, Lasko DD, *et al.* (2001) XRCC1 stimulates human polynucleotide kinase activity at damaged DNA termini and accelerates DNA single-strand break repair. *Cell* 104:107-117.

WHO (2004) Guidelines for Drinking Water Quality. Recommendations. *World Health Organization, Geneva* 1:306-308.

Wischermann K, Popp S, Moshir S, Scharfetter-Kochanek K, Wlaschek M, de Gruijl F, *et al.* (2008) UVA radiation causes DNA strand breaks, chromosomal aberrations and tumorigenic transformation in HaCaT skin keratinocytes. *Oncogene* 27:4269-4280.

Woodhouse BC, Dianov GL (2008) Poly ADP-ribose polymerase-1: an international molecule of mystery. *DNA Repair (Amst)* 7:1077-1086.

Wu X, Shell SM, Liu Y, Zou Y (2007) ATR-dependent checkpoint modulates XPA nuclear import in response to UV irradiation. *Oncogene* 26:757-764.

Yager JW, Wiencke JK (1997) Inhibition of poly(ADP-ribose) polymerase by arsenite. *Mutat Res* 386:345-351.

Yamamoto S, Wanibuchi H, Hori T, Yano Y, Matsui-Yuasa I, Otani S, *et al.* (1997) Possible carcinogenic potential of dimethylarsinic acid as assessed in rat in vivo models: a review. *Mutat Res* 386:353-361.

Yelamos J, Schreiber V, Dantzer F (2008) Toward specific functions of poly(ADP-ribose) polymerase-2. *Trends Mol Med* 14:169-178.

You YH, Lee DH, Yoon JH, Nakajima S, Yasui A, Pfeifer GP (2001) Cyclobutane pyrimidine dimers are responsible for the vast majority of mutations induced by UVB irradiation in mammalian cells. *J Biol Chem* 276:44688-44694.

Young AR, Potten CS, Nikaido O, Parsons PG, Boenders J, Ramsden JM, *et al.* (1998) Human melanocytes and keratinocytes exposed to UVB or UVA in vivo show comparable levels of thymine dimers. *J Invest Dermatol* 111:936-940.

Youssef KK, Van Keymeulen A, Lapouge G, Beck B, Michaux C, Achouri Y, *et al.* (2010) Identification of the cell lineage at the origin of basal cell carcinoma. *Nat Cell Biol* 12:299-305.

Yu HS, Liao WT, Chai CY (2006) Arsenic carcinogenesis in the skin. *J Biomed Sci* 13:657-666.

Zhang M, Qureshi AA, Guo Q, Han J (2011) Genetic variation in DNA repair pathway genes and melanoma risk. *DNA Repair (Amst)* 10:111-116.

Zhou X, Sun X, Cooper KL, Wang F, Liu KJ, Hudson LG (2011) Arsenite interacts selectively with zinc finger proteins containing C3H1 or C4 motifs. *J Biol Chem* 286:22855-22863.

Zhu G, Chang P, Lippard SJ (2010) Recognition of platinum-DNA damage by poly(ADP-ribose) polymerase-1. *Biochemistry* 49:6177-6183.